

Local Two-Sample Testing over Graphs and Point-Clouds by Random-Walk Distributions

Boris Landa^{1,*}, Rihao Qu^{2,4,5}, Joseph Chang³, and Yuval Kluger^{1,2,4}

¹Program in Applied Mathematics, Yale University

²Department of Pathology, Yale University School of Medicine

³Department of Statistics and Data Science, Yale University

⁴Interdepartmental Program in Computational Biology and Bioinformatics, Yale University

⁵Department of Immunology, Yale School of Medicine

*Corresponding author. Email: boris.landa@yale.edu

September 8, 2021

Abstract

Rejecting the null hypothesis in two-sample testing is a fundamental tool for scientific discovery. Yet, aside from concluding that two samples do not come from the same probability distribution, it is often of interest to characterize how the two distributions differ. Given samples from two densities f_1 and f_0 , we consider the task of localizing occurrences of the inequality $f_1 > f_0$. To avoid the challenges associated with high-dimensional space, we propose a general hypothesis testing framework where hypotheses are formulated adaptively to the data by conditioning on the combined sample from the two densities. We then investigate a special case of this framework where the notion of locality is captured by a random walk on a weighted graph constructed over this combined sample. We derive a tractable testing procedure for this case employing a type of scan statistic, and provide non-asymptotic lower bounds on the power and accuracy of our test to detect whether $f_1 > f_0$ in a local sense. Furthermore, we characterize the test's consistency according to a certain problem-hardness parameter, and show that our test achieves the minimax detection rate for this parameter. We conduct numerical experiments to validate our method, and demonstrate our approach on two real-world applications: detecting and localizing arsenic well contamination across the United States, and analyzing two-sample single-cell RNA sequencing data from melanoma patients.

1 Introduction

A prototypical situation native to two-sample testing is an experiment that produces two sets of observations, and the goal is to determine whether they were generated by the same underlying distribution. While standard two-sample tests can at most provide a negative answer, namely, to reject (with prescribed significance) the null hypothesis that the two distributions are identical, it is often of interest to provide more detailed information on the differences between the distributions. In particular, the difference between the distributions may be minute or nonexistent everywhere but in a few small regions of the sample space. In such a case it is of interest to identify these regions, and to describe the relation between the distributions in these regions (e.g., if one of the distributions is uniformly larger than the other). Indeed, local variants of two-sample testing are required in numerous scientific applications, such as single-cell RNA sequencing [62], astronomy [23], and climate analysis [46]. Many applications of interest, including the above, involve high-dimensional

data. We note, however, that density estimation in high dimension is prohibitive due to the curse of dimensionality. Hence, local analysis of the differences between two high-dimensional distributions is a particularly challenging task.

In this work, we consider the following setting. Let f_1 and f_0 be two probability density functions defined on a measurable space \mathcal{X} , and suppose that X is a random variable that is generated by sampling from f_1 with probability $p \in (0, 1)$ and sampling from f_0 with probability $1 - p$. In other words, given a *class* random variable $Z \sim \text{Bernoulli}(p)$, where p is the class prior, we have

$$(X \mid Z = 1) \sim f_1, \quad \text{and} \quad (X \mid Z = 0) \sim f_0. \quad (1)$$

We then take z_1, \dots, z_n and x_1, \dots, x_n as i.i.d. samples from the joint distribution of Z and X , where z_i as the class label of the sample x_i . Given the labels z_1, \dots, z_n and the samples x_1, \dots, x_n , the goal in standard two-sample testing to determine whether the densities $f_1(x)$ and $f_0(x)$ are identical, i.e., to attempt to reject the null hypothesis $f_1(x) = f_0(x)$ for all $x \in \mathcal{X}$, with prescribed significance. Here, we are interested in a refined local variant of this task, which is, loosely speaking, to determine whether $f_1(x) > f_0(x)$ in each of possibly many regions of interest in the sample space, noting that determining the other direction of the inequality, i.e., $f_1(x) < f_0(x)$, can be considered equivalently by interchanging the roles of f_1 and f_0 . We refer to this task as *local two-sample testing*, and propose a precise problem formulation and hypothesis testing framework in Section 2.1.

While two-sample testing has a long history and has been extensively studied in the context of high dimension, general-purpose variants for local two-sample testing have been considered only recently [32, 26, 25, 14, 12], mostly through the machinery of classification and regression. In particular, [32] proposed a general framework for this task using regression, where the idea is to regress the probabilities of the labels z_1, \dots, z_n conditioned on x_1, \dots, x_n , and to compute a pointwise statistic from the discrepancy between the class prior p and the output of the regression model at a given point x . Then, each such statistic is compared to its distribution under the (global) null hypothesis: $f_1(x) = f_0(x)$ for all $x \in \mathcal{X}$, using a permutation test combined with a multiple testing procedure. This methodology allows one to reject the global null and accept a pointwise alternatives of the form $f_0(x) \neq f_1(x)$ for a specific x , and hence acts a local two-sample test. The performance of the resulting local test in [32] was analyzed in terms of both the (global) type I error and the (local) type II error, for various regressions models, and under certain smoothness and structural assumptions on f_0 and f_1 .

A major limitation of the approach mentioned above is that even if the test rejects the global null hypothesis and accepts a pointwise alternative at x_i , we cannot conclude that $f_1(x_i) \neq f_0(x_i)$ with finite-sample probabilistic guarantees. Indeed, for a given finite sample, a null hypothesis of the form $f_0(x_i) = f_1(x_i)$ cannot be decisively rejected unless f_0 and f_1 are known to be sufficiently smooth, since under the pointwise null $f_0(x_i) = f_1(x_i)$, z_i is 1 with probability p and is 0 otherwise, regardless of the distributions of the other labels. Clearly, when the test rejects the global null hypothesis and accepts an alternative at x_i , the rejection relies on labels from a certain neighborhood of x_i . However, it is challenging to determine what that neighborhood is, as it depends implicitly on the regression model used and the unknown densities f_0 and f_1 , thereby limiting the interpretability of the test's outcome.

A different methodology that is closely related to local two-sample testing, and is able to address the above-mentioned limitation, is *scan statistics* [24], and particularly *spatial scan statistics* [34, 36, 21], where hypotheses are associated with explicit spatial neighborhoods. Spatial scan statistics is a widely-used methodology for detecting regions, usually in one or two dimensions, in which observed values of random variables suggest departure from a null hypothesis. For instance, suppose that each random variable is a count of disease cases in a town. Then, a typical procedure in spatial scan statistics is to compute statistics summarizing the total number of disease cases in certain predefined

geographic regions (each containing multiple towns), and to scan over the different regions and their summarizing statistics to identify regions of elevated illness [37, 35]. In the context of our setting, one can detect that $f_1(x) > f_0(x)$ in a certain region of \mathcal{X} if the corresponding local proportion of labels satisfying $z_i = 1$ (with x_i in that region) significantly exceeds the global proportion p . In most cases of spatial scan statistics, the geographic regions are defined by simple shapes in the ambient space, such as intervals in one dimension, and rectangles, circles, or ellipses in two dimensions, all of which vary in their location (e.g., center) and scale (size). The use of different scales is fundamental, since larger scales correspond to larger regions that include more random variables, allowing for more power to detect weak deviations from the null (as the number of random variables associated with a geographic region is analogous to the sample size observed locally).

Due to the curse of dimensionality, standard techniques in spatial scan statistics are restricted to low-dimensional Euclidean space. Indeed, covering the ambient space with simple predefined shapes (e.g., balls that vary in their location and scale) is prohibitive in high dimension, and the corresponding scan procedure becomes infeasible, both from a computational perspective and from that of multiple testing. Moreover, many real-world datasets are known to be intrinsically low-dimensional and admit a non-Euclidean geometry, i.e., reside on or near a low-dimensional Riemannian manifold embedded in the ambient space. Arguably, in such cases it is inappropriate to define the regions of interest according to the high-dimensional ambient space, as the underlying notion of locality can be fundamentally different. Therefore, in such cases the notion of locality should be inferred directly from the data, allowing for a data-driven approach to scientific discovery.

Aside from simple spatial domains, the methodology of scan statistics was also extended to graph domains [4, 3], which are widely-used in data analysis for representing high-dimensional datasets that are intrinsically low-dimensional. In the setup of graph scan statistics, a random variable is attached to each node in a graph, and the goal is to detect a community in the graph that behaves anomalously. In [3], it was proposed to define communities as arbitrary sub-graphs that admit certain connectivity constraints. In this setting, the null hypothesis is defined by having identically distributed random variables over the graph nodes (e.g., the variables are all normal with variance 1 and mean 0), while an alternative (the anomaly) is a piecewise constant model for the parameters of the random variables (e.g., the random variables are all normal with variance 1 and mean 0 outside the anomalous community, and some positive constant mean inside). Then, a statistic indicative of an anomaly for each community is computed (typically a generalized likelihood ratio), and the maximal statistic from all communities is compared to its distribution under the null. Since the number of communities defined via graph connectivity constraints is typically very large, scanning over all communities (or even a representative subset of them) is prohibitive, and various other approaches have been proposed; see [1, 49, 52, 51, 47, 50, 13, 11] and references therein for more details. Consequently, probabilistic guarantees in this line of work are generally limited to the inference task of determining whether at least one community in the network is anomalous, and do not address the localization of the anomalous communities.

In this work, we provide a general framework for local two-sample testing that is founded on the idea of conditioning on the given samples x_1, \dots, x_n . In particular, the hypotheses are formulated as inequalities concerning the values of the densities $f_0(x)$ and $f_1(x)$ evaluated only for $x = x_1, \dots, x_n$, rather than for all x in the ambient space. This idea allows us to avoid the curse of dimensionality by determining the subsets of the samples x_1, \dots, x_n that are employed for testing $f_1(x) > f_0(x)$ adaptively (e.g., via clustering or near-neighbour graphs), instead of using predefined regions in the ambient space. More generally, our framework allows for testing whether certain weighted averages of $\{f_1(x_i) - f_0(x_i)\}_{i=1}^n$ are strictly positive, where the weights come from a family that may depend on the samples x_1, \dots, x_n . The weights in the family should be chosen as to emphasize subsets of x_1, \dots, x_n according to a notion of locality (e.g., a measure of similarity between the

samples provided by a domain expert), and obviates the need for explicit model assumptions on the densities f_1 and f_0 . The main advantage of our approach is that it allows for interpretable local null hypotheses that are concerned with the differences $\{f_1(x_i) - f_0(x_i)\}_{i=1}^n$, and can be rejected with finite-sample probabilistic guarantees with the only assumption that the labels conditional on the samples are independent. When rejected, these null hypotheses provide neighborhoods in which $f_1 > f_0$.

As a useful special case of our framework, we leverage a weighted graph over the sample $\{x_1, \dots, x_n\}$ to capture the geometry of the data. In this setting, the random variables associated with the graph nodes are the labels z_1, \dots, z_n conditioned on the samples x_1, \dots, x_n , and the goal is to find neighborhoods in the graph where the local proportion of labels satisfying $z_i = 1$ is significantly larger than their global proportion p . We generalize the notion of a neighborhood of a data point to a probability distribution arising from a random walk started at this data point, and show that it provides a natural concept of location and scale (analogously to regions typically used in spatial scan statistics). Crucially, we show that this usage of a random walk allows for a computationally tractable testing procedure and favorable theoretical guarantees on the power and accuracy associated with detecting all the neighborhoods in which $f_1 > f_0$. We also establish the optimality of the detection rate for our proposed testing procedure in a minimax sense, and demonstrate our approach on both simulated and experimental data.

The main contributions of this work are summarized as follows:

1. **Framework.** We propose a general framework for local two-sample testing that avoids the curse of dimensionality and the need for explicit model assumptions on the densities f_0 and f_1 . The hypotheses in our framework are adapted to the data by conditioning on the observations x_1, \dots, x_n , and allow for finite-sample probabilistic guarantees in determining that $f_1 > f_0$ in a certain local sense.
2. **Testing procedure.** We derive a computationally-tractable testing procedure for determining whether $f_1 > f_0$ in neighborhoods defined according to a random walk over the sample. We identify that a symmetric and positive semidefinite transition probability matrix is particularly well suited for this task, as it admits many useful properties and allows all random walk distributions to be well approximated by a set with controlled cardinality.
3. **Analysis.** We analyze the performance of the testing procedure according to our hypothesis testing framework, and derive bounds on the power and the accuracy of the method to detect that $f_1 > f_0$ in a given neighborhood. We also show that our method achieves the minimax detection rate in terms of a certain problem hardness parameter among all methods that are locally consistent as $n \rightarrow \infty$ (a concept defined in our framework via an appropriate risk function).
4. **Examples.** We demonstrate the performance of our approach and the fit to our theory through numerical simulations, and show the practical usefulness of our method to extract novel scientific insights in real-world applications.

2 Problem formulation and main results

Throughout this work we assume, unless stated otherwise, that all quantities are conditioned on x_1, \dots, x_n by default. Therefore, the only source of randomness is in the labels z_1, \dots, z_n , and in particular, each label z_i is independently sampled from $(Z \mid X = x_i)$, where Z and X are as

described in Section 1. Specifically, according to Bayes' law, we have

$$(Z | X = x) = \begin{cases} 1, & \text{with probability } \frac{f_1(x)p}{f(x)}, \\ 0, & \text{with probability } \frac{f_0(x)(1-p)}{f(x)}, \end{cases} \quad (2)$$

where $f(x)$ is the marginal distribution of X , namely

$$f(x) = pf_1(x) + (1-p)f_0(x). \quad (3)$$

In other words, x_1, \dots, x_n are first sampled independently from their marginal distribution $f(x)$, after which they are fixed, and the labels z_1, \dots, z_n are sampled from independent but not identically distributed Bernoullis according to (2), which constitute the random variables in our setting. As motivated in the introduction, the conditioning on the samples x_1, \dots, x_n allows our hypothesis testing framework to be stated in terms of the samples, without having to consider the ambient space \mathcal{X} directly.

2.1 Problem formulation

2.1.1 Local two-sample testing by distributions over the sample

Given x_1, \dots, x_n , we encapsulate the idea of “regions of interest” in a family of discrete probability distributions \mathcal{F} over the sample $\{x_1, \dots, x_n\}$. Specifically, \mathcal{F} consists of a collection, possibly infinite, of nonnegative weight vectors of the form $\mathbf{w} = [w_1, \dots, w_n]$, each satisfying $\sum_{i=1}^n w_i = 1$. In addition, we assume that

Assumption 1. \mathcal{F} is deterministic given x_1, \dots, x_n .

That is, Assumption 1 requires that \mathcal{F} depend only on the samples x_1, \dots, x_n and *not* on the labels z_1, \dots, z_n . This assumption is crucial for formulating our hypothesis testing framework and for providing finite-sample probabilistic guarantees on a testing procedure that uses the distributions in \mathcal{F} . Loosely speaking, we consider each probability distribution $\mathbf{w} \in \mathcal{F}$ as describing a neighborhood of $\{x_1, \dots, x_n\}$ according to the samples x_i for which the corresponding value w_i is sufficiently large. To further clarify this point, consider the following two examples.

Example 1. Let $\mathcal{C}_1, \dots, \mathcal{C}_L$ be a clustering of x_1, \dots, x_n to L disjoint clusters (by, e.g., k -means, spectral clustering, etc.), where \mathcal{C}_ℓ is the set of indices of the samples in the ℓ 'th cluster. Then, a corresponding choice of \mathcal{F} is $\mathcal{F} = \{\mathbb{1}_{\mathcal{C}_1}/|\mathcal{C}_1|, \dots, \mathbb{1}_{\mathcal{C}_L}/|\mathcal{C}_L|\}$, where $\mathbb{1}_{\mathcal{C}_\ell}$ is the indicator vector over \mathcal{C}_ℓ , and $|\mathcal{C}_\ell|$ is the size of the ℓ 'th cluster.

The distributions in \mathcal{F} do not have to be uniform nor defined over disjoint subsets of $\{x_1, \dots, x_n\}$. As another example, \mathcal{F} can be defined via a nonnegative kernel such as the Gaussian kernel, assuming that a metric $D_{\mathcal{X}}(\cdot, \cdot)$ over \mathcal{X} is given, as follows.

Example 2. Suppose that $K \in \mathbb{R}^{n \times n}$ is given by $K_{i,j} = \exp\{-D_{\mathcal{X}}^2(x_i, x_j)/\sigma\}$, for some $\sigma > 0$. Then, one can take $\mathcal{F} = \{K_1/\sum_j K_{1,j}, \dots, K_n/\sum_j K_{n,j}\}$, where K_i is the i 'th row of K .

We remark that \mathcal{F} can be formed by combining the constructions from the above two examples using multiple kernels and clustering choices, thereby providing a rich multi-resolution description of the sample. For instance, one may use \mathcal{F} from Example 1 with different numbers of clusters L , together with \mathcal{F} from Example 2 using different values of σ , and take the union of all resulting

distributions. We propose a specific construction for \mathcal{F} that similarly allows for a multi-resolution description of the sample in Section 2.1.3.

Next, to define a measure of discrepancy between f_1 and f_0 , we employ the function

$$s(x) := \mathbb{E}[Z | X = x] - p = \Pr\{Z = 1 | X = x\} - p = p(1 - p) \frac{f_1(x) - f_0(x)}{f(x)}, \quad (4)$$

where $f(x)$ is from (3), and $s(x)$ is defined only for $x \in \mathcal{X}$ for which $f(x) > 0$. Evidently, $s(x)$ is bounded, and in particular $-p \leq s(x) \leq 1 - p$, where $s(x)$ attains its maximum $1 - p$ whenever $f_0(x) = 0$, and attains its minimum $-p$ whenever $f_1(x) = 0$. Therefore, the function $s(x)$ can be thought of as a normalized pointwise difference between f_1 and f_0 . We note that $s(x)$ was also used as the target of the regression model in [32] for the purpose of local two-sample testing.

Using \mathcal{F} and the function $s(x)$, we consider the following problem.

Problem 1. *Given z_1, \dots, z_n and \mathcal{F} , determine for which $\mathbf{w} \in \mathcal{F}$, if any, $\sum_{i=1}^n w_i s(x_i) > 0$.*

The motivation for using the quantity $\sum_{i=1}^n w_i s(x_i)$ in Problem 1 is as follows. Suppose for simplicity that \mathcal{X} is the Euclidean space \mathbb{R}^D , and let $\omega(x)$ be a nonnegative bounded function on \mathbb{R}^D . Since x_1, \dots, x_n were sampled independently from the marginal density $f(x)$, for sufficiently large n we have

$$\frac{1}{n} \sum_{i=1}^n \omega(x_i) s(x_i) \approx p(1 - p) \int_{\mathbb{R}^D} \omega(x) (f_1(x) - f_0(x)) dx. \quad (5)$$

The right-hand side in (5), up to a constant, is the weighted average of the difference between the densities $f_1(x)$ and $f_0(x)$ with respect to the “weight” function $\omega(x)$. Ideally, it is desirable to determine that the right-hand side in (5) is positive when $\omega(x)$ is either a localized function around some point $y \in \mathbb{R}^D$, e.g., the Gaussian kernel $\exp\{-\|y - x\|_2^2/\sigma\}$, or if $\omega(x)$ is the indicator function over some subset of \mathbb{R}^D . In the context of Problem 1, the quantity $\sum_{i=1}^n w_i s(x_i)$ can be thought of as a sample-based approximation to the right-hand side in (5) for a particular choice of $\omega(x)$ (up to the constant factor $np(1 - p)$). However, in this work we do not simply choose a predefined class of functions for $\omega(x)$ (and then take \mathcal{F} by sampling these functions at x_1, \dots, x_n), but allow \mathcal{F} to adapt to the given samples (as in Example 1).

Since $w_i \geq 0$, and since $s(x_i) > 0$ if and only if $f_1(x_i) > f_0(x_i)$, by finding \mathbf{w} that solves Problem 1 we guarantee that $f_1(x_i) > f_0(x_i)$ for at least one index i for which $w_i > 0$. That is, if $\Omega(\mathbf{w}) = \{x_i : i \in \{1, \dots, n\}, w_i > 0\}$, then any \mathbf{w} solving Problem 1 implies that $f_1(x) > f_0(x)$ somewhere in $\Omega(\mathbf{w})$. Consequently, solving Problem 1 is particularly advantageous when the distributions in \mathcal{F} are sparse, as it allows us to effectively localize the phenomenon $f_1(x) > f_0(x)$ to a restricted subset of $\{x_1, \dots, x_n\}$. More generally, finding \mathbf{w} that solves Problem 1 admits a useful interpretation even if \mathbf{w} is not sparse, but sufficiently localized in a certain subset of $\{x_1, \dots, x_n\}$. We further discuss the motivation behind Problem 1 and compare it to alternative formulations in Remark 1 below. In addition, we point out that we do not expect a method to detect *all* $\mathbf{w} \in \mathcal{F}$ for which $\sum_{i=1}^n w_i s(x_i) > 0$. Specifically, we allow a method to detect a distribution $\hat{\mathbf{w}}$ that is very close (in an appropriate metric) to \mathbf{w} that satisfies $\sum_{i=1}^n w_i s(x_i) > 0$, even if \mathbf{w} itself is not detected. This concept is incorporated in our hypothesis testing framework, and in particular, in the local risk function that we define in the next section.

Remark 1. *Let \mathcal{H} be a collection of subsets of $\{x_1, \dots, x_n\}$. One task that can come to mind is to determine for which subset $\Omega \in \mathcal{H}$ we have $f_1(x) > f_0(x)$ for all $x \in \Omega$. However, such a task does not lend itself to non-parametric finite-sample probabilistic guarantees, since as explained in the introduction one cannot determine with high significance that $f_1(x_i) > f_0(x_i)$ for any single*

x_i , let alone for all $x \in \Omega$ (without explicit assumptions on the densities f_1 and f_0). Instead, one could consider the relaxed task of determining for which $\Omega \in \mathcal{H}$ we have $f_1(x) > f_0(x)$ for at least one $x \in \Omega$. However, this task is not sufficiently informative, since if one finds Ω that solves this problem, than any other set Ω' that includes Ω is immediately also a solution, even if $f_1(x) > f_0(x)$ only in a tiny portion of Ω' . In contrast, Problem 1 does not suffer from such redundancy, since even in the simple case that \mathbf{w} and \mathbf{w}' are uniform distributions over Ω and Ω' , respectively, finding that \mathbf{w} solves Problem 1 does not imply that \mathbf{w}' also solves it. Whether or not \mathbf{w}' solves Problem 1 depends on how the values of $s(x)$ behave on average for all $x \in \Omega'$. Hence, determining that \mathbf{w}' solves Problem 1 is a stronger finding than simply $f_1(x) > f_0(x)$ for some $x \in \Omega'$.

2.1.2 Hypothesis testing framework

We next describe a hypothesis testing framework that formalizes Problem 1, and provide appropriate risk functions to assess the performance of a corresponding testing procedure, both in the global sense of detecting that there exists some $\mathbf{w} \in \mathcal{F}$ that solves Problem 1, and also in an appropriate local sense of determining which one it is.

Let $\mathcal{G} \subseteq \mathcal{F}$, and denote $\mathbf{s} = [s(x_1), \dots, s(x_n)]$. We define $H_0(\mathcal{G})$ as a parametrized null hypothesis according to

$$H_0(\mathcal{G}) : \langle \mathbf{w}, \mathbf{s} \rangle \leq 0, \quad \forall \mathbf{w} \in \mathcal{G}, \quad (6)$$

where $\langle \cdot, \cdot \rangle$ is the standard scalar product. We denote $H_0 = H_0(\mathcal{F})$, and refer to H_0 simply as the null hypothesis. Note that H_0 also includes the typical null hypothesis used in two-sample testing, where $s(x) = 0$ for all $x \in \mathcal{X}$, i.e., f_1 and f_0 are identical. Next, for $\mathbf{w} \in \mathcal{F}$ and $\gamma \geq 0$ we define $H_1(\mathbf{w}, \gamma)$ as a specific alternative to $H_0(\mathbf{w})$ via

$$H_1(\mathbf{w}, \gamma) : \langle \mathbf{w}, \mathbf{s} \rangle > \gamma \|\mathbf{w}\|_2. \quad (7)$$

Note that $H_1(\mathbf{w}, 0)$ implies that $\langle \mathbf{w}, \mathbf{s} \rangle > 0$ and is therefore the alternative to $H_0(\mathbf{w})$. The parameter γ in (7) factors into account both the magnitude of the local deviation between f_1 and f_0 and the effective size of \mathbf{w} , as defined by $\|\mathbf{w}\|_2$ (which is smaller for more spread-out distributions); see the following remark.

Remark 2. Suppose that \mathbf{w} is the uniform distribution over a subset of nodes $\Omega \subset \{x_1, \dots, x_n\}$ with $|\Omega| = m$, i.e.,

$$w_i = \begin{cases} 1/m, & x_i \in \Omega, \\ 0, & \text{otherwise.} \end{cases} \quad (8)$$

In this case we have $\|\mathbf{w}\|_2 = 1/\sqrt{m}$, and $H_1(\mathbf{w}, \gamma)$ implies that $\sqrt{m} \left(\frac{1}{m} \sum_{x_i \in \Omega} s(x_i) \right) > \gamma$. Therefore, under $H_1(\mathbf{w}, \gamma)$, the quantity γ^2 can be interpreted as a lower bound on the number of samples in the region Ω , multiplied by the squared average value of $s(x)$ in that region. Hence, γ reflects both the size of the region corresponding to \mathbf{w} , and the discrepancy between f_1 and f_0 in that region.

The reason that we include the quantity $\|\mathbf{w}\|_2$ in our alternative $H_1(\mathbf{w}, \gamma)$ is that $\langle \mathbf{w}, \mathbf{s} \rangle$ alone may be insufficient to describe the power of a test to detect that $\langle \mathbf{w}, \mathbf{s} \rangle > 0$. For example, if we consider the setting in Remark 2, knowing the quantity $\frac{1}{m} \sum_{x_i \in \Omega} s(x_i)$ is not enough to characterize the performance of a test (to detect that $\frac{1}{m} \sum_{x_i \in \Omega} s(x_i) > 0$ using the labels z_1, \dots, z_n), as another crucial quantity is $|\Omega| = m$, which is the number of labels that are actually relevant for this task (acting as an effective sample size). Clearly, it may be impossible to detect that $\frac{1}{m} \sum_{x_i \in \Omega} s(x_i) > 0$ with high probability from the labels $\{z_i : x_i \in \Omega\}$ if $|\Omega| = m$ is very small (e.g., $m = 1$), even if $\frac{1}{m} \sum_{x_i \in \Omega} s(x_i)$ is large.

Let H_1 be the alternative to H_0 , i.e., $H_1 = \cup_{\mathbf{w} \in \mathcal{F}} H_1(\mathbf{w}, 0)$, and consider a test $Q_{\mathbf{z}} \in \{0, 1\}$ whose input is the vector of labels $\mathbf{z} = [z_1, \dots, z_n]$, and output is 1 for H_1 and 0 for H_0 . We define the *global* risk of the test $Q_{\mathbf{z}}$, for a given $\gamma \geq 0$, as the sum of the worst-case type I and worst-case type II errors, that is

$$R_{\mathcal{F}}^{(n)}(Q_{\mathbf{z}}, \gamma) = \sup_{f_1, f_0 \in H_0} \Pr\{Q_{\mathbf{z}} = 1 \mid f_0, f_1\} + \sup_{\mathbf{w} \in \mathcal{F}} \sup_{f_1, f_0 \in H_1(\mathbf{w}, \gamma)} \Pr\{Q_{\mathbf{z}} = 0 \mid f_0, f_1\}. \quad (9)$$

According to (9) and our definition of the null H_0 , it is clear that the global risk $R_{\mathcal{F}}^{(n)}(Q_{\mathbf{z}}, \gamma)$ penalizes any test that incorrectly determines the sign of $\langle \mathbf{w}, \mathbf{s} \rangle$, which is a crucial property if our goal is to decide whether $f_1(x) > f_0(x)$ locally. However, the global risk only quantifies our ability to determine whether some alternative is true, and not which one it is.

According to Problem 1, our testing methodology is not expected to return just a binary value (for H_0 or H_1), hence we consider its output to be a family of distributions $\hat{\mathcal{G}}_{\mathbf{z}} \subseteq \mathcal{F}$, where each $\mathbf{w} \in \hat{\mathcal{G}}_{\mathbf{z}}$ represents an accepted alternative $H_1(\mathbf{w}, 0)$. From this point onward, we will refer to $\hat{\mathcal{G}}_{\mathbf{z}}$ as a *local* test. The binary test $Q_{\mathbf{z}}$ can then be defined directly via the local test $\hat{\mathcal{G}}_{\mathbf{z}}$ by taking $Q_{\mathbf{z}} = 0$ if $\hat{\mathcal{G}}_{\mathbf{z}}$ is an empty set, and $Q_{\mathbf{z}} = 1$ otherwise. Given a local test $\hat{\mathcal{G}}_{\mathbf{z}}$ and a parameter γ , we introduce the *local* risk $r_{\mathcal{F}}^{(n)}(\hat{\mathcal{G}}_{\mathbf{z}}, \gamma)$ as

$$r_{\mathcal{F}}^{(n)}(\hat{\mathcal{G}}_{\mathbf{z}}, \gamma) = \sup_{\hat{\mathcal{G}} \subseteq \mathcal{F}} \sup_{f_1, f_0 \in H_0(\hat{\mathcal{G}})} \Pr\{\hat{\mathcal{G}} \cap \mathcal{G} \neq \emptyset \mid f_0, f_1\} + \sup_{\mathbf{w} \in \mathcal{F}} \sup_{f_1, f_0 \in H_1(\mathbf{w}, \gamma)} \mathbb{E}[\inf_{\hat{\mathbf{w}} \in \hat{\mathcal{G}}_{\mathbf{z}}} \mathcal{E}_{\text{TV}}(\hat{\mathbf{w}}, \mathbf{w}) \mid f_0, f_1], \quad (10)$$

where $\mathcal{E}_{\text{TV}}(\hat{\mathbf{w}}, \mathbf{w}) = \frac{1}{2} \sum_{i=1}^n |\hat{w}_i - w_i|$ is the total variation distance between $\hat{\mathbf{w}}$ and \mathbf{w} , and we define $\inf_{\hat{\mathbf{w}} \in \hat{\mathcal{G}}_{\mathbf{z}}} \mathcal{E}_{\text{TV}}(\hat{\mathbf{w}}, \mathbf{w}) = 1$ if $\hat{\mathcal{G}}_{\mathbf{z}}$ is an empty set. In plain words, the first summand in (10) is the worst-case probability to accept a false alternative, and the second summand in (10) is the worst-case expected error (in total variation distance) between \mathbf{w} from a true alternative and its closest element in the output of the local test $\hat{\mathcal{G}}_{\mathbf{z}}$. The motivation behind (10) is as follows. By making the first term in (10) small, we guarantee that the local test is likely to output only distributions from true alternatives. By making the second term in (10) small, we guarantee that a distribution \mathbf{w} from a true alternative $H_1(\mathbf{w}, \gamma)$ is likely to be approximately detected (by finding a similar distribution $\hat{\mathbf{w}} \in \mathcal{F}$ in total variation distance).

Observe that according to (7), if $\gamma \leq \gamma'$ then $\{f_0, f_1 \in H_1(\mathbf{w}, \gamma')\} \subseteq \{f_0, f_1 \in H_1(\mathbf{w}, \gamma)\}$ for each $\mathbf{w} \in \mathcal{F}$. Consequently, the risks $R_{\mathcal{F}}^{(n)}(Q_{\mathbf{z}}, \gamma)$ and $r_{\mathcal{F}}^{(n)}(\hat{\mathcal{G}}_{\mathbf{z}}, \gamma)$ decrease as γ increases. In the case that γ is large enough so that the set $\{f_1, f_0 \in \cup_{\mathbf{w} \in \mathcal{F}} H_1(\mathbf{w}, \gamma)\}$ is empty, the second summands in both (9) and (10) are set to be zero, in which case taking $\hat{\mathcal{G}}_{\mathbf{z}} = \emptyset$ and $Q_{\mathbf{z}} = 0$ gives $R_{\mathcal{F}}^{(n)}(Q_{\mathbf{z}}, \gamma) = r_{\mathcal{F}}^{(n)}(\hat{\mathcal{G}}_{\mathbf{z}}, \gamma) = 0$. Therefore, the parameter γ can be viewed as a problem-hardness parameter, where the larger γ is, the easier the hypothesis testing problem is, both in terms of the global risk $R_{\mathcal{F}}^{(n)}(Q_{\mathbf{z}}, \gamma)$ and of the local risk $r_{\mathcal{F}}^{(n)}(\hat{\mathcal{G}}_{\mathbf{z}}, \gamma)$. In addition, we have the following relation between the global and local risks.

Lemma 1. *If $Q_{\mathbf{z}}$ is the test associated with $\hat{\mathcal{G}}_{\mathbf{z}}$ (i.e., $Q_{\mathbf{z}} = 0$ if $\hat{\mathcal{G}}_{\mathbf{z}}$ is empty and $Q_{\mathbf{z}} = 1$ otherwise), then for any family of distributions \mathcal{F} and $\gamma \geq 0$*

$$R_{\mathcal{F}}^{(n)}(Q_{\mathbf{z}}, \gamma) \leq r_{\mathcal{F}}^{(n)}(\hat{\mathcal{G}}_{\mathbf{z}}, \gamma). \quad (11)$$

The proof can be found Appendix C. Next, we define the notions of global and local consistencies.

Definition 1 (Local and global consistency). *A local test $\hat{\mathcal{G}}_{\mathbf{z}}$ is said to be locally consistent with respect to a sequence $\{\gamma_n\}$ if $\lim_{n \rightarrow \infty} r_{\mathcal{F}}^{(n)}(\hat{\mathcal{G}}_{\mathbf{z}}, \gamma_n) = 0$, and is said to be globally consistent if $\lim_{n \rightarrow \infty} R_{\mathcal{F}}^{(n)}(Q_{\mathbf{z}}, \gamma_n) = 0$, where $Q_{\mathbf{z}} = 0$ if $\hat{\mathcal{G}}_{\mathbf{z}}$ is empty and $Q_{\mathbf{z}} = 1$ otherwise.*

Since the global and local risks are both nonnegative, and according to Lemma 1, if a local test $\hat{\mathcal{G}}_{\mathbf{z}}$ is locally consistent, then it is also globally consistent. Hence, if $\hat{\mathcal{G}}_{\mathbf{z}}$ is not globally consistent, then it cannot possibly be locally consistent. Given a local test $\hat{\mathcal{G}}_{\mathbf{z}}$, it is of primary interest to determine for which sequences $\{\gamma_n\}_{n=1}^{\infty}$ it is globally and locally consistent. In particular, it is desirable to find a local test which is locally consistent for sequences $\{\gamma_n\}$ for which γ_n is as small as possible as $n \rightarrow \infty$.

One of strong suits of our hypothesis testing framework is that it does not require any structural assumptions or parametric models on the densities f_1 and f_0 , nor any assumptions on their smoothness in the ambient space \mathcal{X} . This is one of key advantages of conditioning on the observations x_1, \dots, x_n , as the only assumption required for rejecting $\langle \mathbf{w}, \mathbf{s} \rangle \leq 0$ (with prescribed significance) is that the sample-label pairs $(x_1, z_1), \dots, (x_n, z_n)$ are independent (which leads to the independence of the labels conditional on the samples). If $\langle \mathbf{w}, \mathbf{s} \rangle \leq 0$ is rejected for a specific \mathbf{w} , the large entries in \mathbf{w} indicate the samples that are most important in the rejection. This observation provides a useful tool for subsequent analysis, particularly if \mathbf{w} is sparse or approximately sparse, but also when \mathbf{w} represents a cluster in the data, since such clusters typically have meaningful interpretations through expert knowledge.

2.1.3 Local two-sample testing by random-walk distributions

The hypothesis testing framework detailed in the previous section allows one to evaluate the performance of a testing procedure with respect to a given family \mathcal{F} , but is not concerned with the question of how to choose \mathcal{F} . In general, the choice of \mathcal{F} should be guided by expert knowledge and by examining the standard tools and processing pipelines that are in current use for the type of data in question. In this section and for the rest of this work, we focus on a specific choice of \mathcal{F} that we believe to be particularly well suited for data residing on a low-dimensional manifold with interpretable latent parameters. Specifically, we propose and analyze a multi-resolution approach where \mathcal{F} is a family of random-walk distributions over a given weighted graph.

Suppose that G is a weighted graph whose vertices are $\{x_1, \dots, x_n\}$, and whose edges (and weights) are given by a nonnegative adjacency matrix $W \in \mathbb{R}^{n \times n}$ satisfying the following assumption.

Assumption 2. *W is symmetric, stochastic, positive semidefinite (PSD), and deterministic given x_1, \dots, x_n .*

For instance, if x_1, \dots, x_n reside in Euclidean space, then a matrix W satisfying Assumption 2 can be obtained by diagonally scaling [53, 33] the Gaussian kernel $\exp\{\|x_i - x_j\|_2^2 / \sigma\}$ to have row and column sums of 1, i.e., $W_{i,j} = d_i \exp\{\|x_i - x_j\|_2^2 / \sigma\} d_j$ for an appropriate choice of d_1, \dots, d_n [38, 44], where σ is a tunable “bandwidth” parameter. It is worthwhile to point out that this choice of W admits a useful interpretation in the context of manifold learning. Specifically, if x_1, \dots, x_n are sampled uniformly from a smooth low-dimensional Riemannian manifold embedded in Euclidean space, then the matrix $I - W$ provides a sample-based approximation to the Laplace-Beltrami operator on the manifold, and W^t (i.e., the t 'th matrix power of W) provides an approximation to the solution of the heat equation on the manifold at time σt [44, 17, 60]. These solutions describe the propagation of heat on the manifold as time progresses, with the initial condition being a point source. Consequently, for a given point on the manifold, the propagation of heat from that point characterizes local regions on the manifold that grow as time progresses, where the notion of locality is adapted to the geometry of the manifold; see Section 6.1 for a simple toy example that illustrates this concept.

Our approach in this work is not limited to a specific choice of W , and in Section 5 we propose a procedure for constructing W satisfying Assumption 2 from an arbitrary nonnegative matrix K provided by the user (and is deterministic given x_1, \dots, x_n). Intuitively, K should be an affinity matrix encoding the similarities between the points x_1, \dots, x_n , and preferably should be exactly or approximately sparse. If K is not readily available, it can be formed by standard approaches such as nearest-neighbour graphs and nonnegative kernels via a metric over \mathcal{X} (see for example [42, 41, 17, 8, 38] and references therein), which is typically provided by a domain expert.

According to Assumption 2, W is stochastic, i.e., $W_{i,j} \geq 0$ for all i, j , and $\sum_{j=1}^n W_{i,j} = 1$ for all i , hence W can serve as a transition probability matrix of a Markov chain over $\{x_1, \dots, x_n\}$, where $W_{i,j}$ is the probability to transition from x_i to x_j at each step. Consequently, for a random walk that started at x_i , the quantity $W_{i,j}^t$, which is the (i, j) 'th entry of the t 'th matrix power of W , is the probability to be at x_j after t steps. We then take into \mathcal{F} all distributions associated with the random walk, i.e., when starting at all possible vertices x_1, \dots, x_n , and for all possible time steps $t = 1, 2, \dots, \infty$. Specifically,

$$\mathcal{F} = \{W_i^t : 1 \leq i \leq n, t = 1, 2, \dots, \infty\}, \quad (12)$$

where $W_i^t \in \mathbb{R}^n$ stands for the i 'th row of W^t . Clearly, by Assumption 2 it follows that \mathcal{F} satisfies Assumption 1.

Since W_i^t is the distribution of the location of a random-walker that started at x_i after t steps, it describes neighborhoods around x_i at multiple scales. More precisely, since W is symmetric and stochastic, it is doubly stochastic, and it follows that the entropy of W_i^t (given by $-\sum_{j=1}^n W_{i,j}^t \log W_{i,j}^t$) is monotonically increasing in t (see e.g., [43]), meaning that W_i^t becomes more spread-out as t increases. Moreover, since W is PSD, the associated Markov chain is aperiodic, and W_i^t converges to a stationary distribution as $t \rightarrow \infty$, which is the uniform distribution over the connected component of G that contains x_i (see Proposition 2 in Section 3.1 for more details). Hence, the random walk distribution W_i^t admits a natural notion of location and scale, where i is the location parameter and t is the scale. Figure 1 illustrates a prototypical behavior of the random walk distributions W_i^t on a dataset resembling the shape of a Swiss roll. Notably, the propagation of the random walk is restricted to the graph structure – which captures the non-Euclidean geometry of the dataset.

The role of the scale parameter t in our setting is analogous to that of the window length in one-dimensional spatial scan statistics (see [59] and references therein), where a larger window length (i.e., larger scale) allows for better detection power given that everything else remains equal. Since one does not know apriori what is the smallest scale t at which a difference between f_1 and f_0 might be detected (with prescribed significance), it is desirable to consider all possible scales, hence our proposed choice of \mathcal{F} . We mention that the requirements in Assumption 2 that W is symmetric and PSD ensure that the random-walk is sufficiently well-behaved for our purposes; see Proposition 3 in Section 3.1. All properties of W appearing in Assumption 2 are required in the derivation and analysis of our testing procedure.

2.2 Method and main results

2.2.1 Testing procedure

We now describe the main ideas and ingredients in our testing procedure, whose derivation can be found in Section 3. In Section 3.2 we show that for any given $\mathbf{w} \in \mathcal{F}$, one can reject $H_0(\mathbf{w})$ in favor of $H_1(\mathbf{w}, 0)$ at significance level α if the statistic

$$\mathcal{S}(\mathbf{w}) = \frac{\langle \mathbf{w}, \mathbf{z} - p \rangle}{\|\mathbf{w}\|_2}, \quad (13)$$

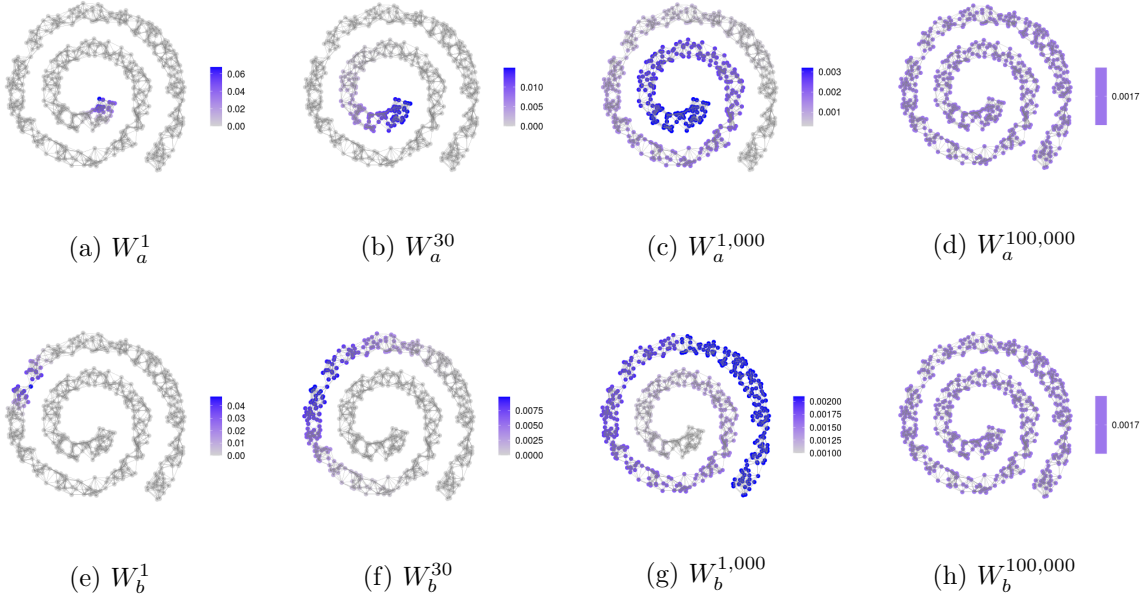


Figure 1: Random-walk distributions W_i^t with two distinct locations: $i = a$ (top row) and $i = b$ (bottom row), and scales $t = 1, 30, 1000, 100000$ (from left to right). The matrix W was formed according to Section 5 from a symmetric 10-NN graph (where x_i and x_j are connected if at least one of them belongs to the 10 nearest neighbours of the other). For $t = 1$, W_i^t encodes the immediate surroundings of x_i , and as t grows, W_i^t spreads further and further away from x_i until it converges to the uniform distribution over the connected component that contains x_i .

exceeds the threshold $\sqrt{0.5 \log(1/\alpha)}$, where $\mathbf{z} = [z_1, \dots, z_n]$. The numerator of (13) is simply an unbiased estimator of $\langle \mathbf{w}, \mathbf{s} \rangle$, and the purpose of the denominator is to normalize the variance of the statistic according to the effective size of \mathbf{w} ; see Section 3.2. If \mathbf{w} is a uniform distribution over a subset of nodes, then $\mathcal{S}(\mathbf{w})$ is also known as the *positive elevated-mean statistic* [47, 10], which often arises as a generalized likelihood ratio in certain simple parametric models. The prior p is assumed to be known throughout the derivation and analysis of our method in Section 3, and we describe how to adapt our approach to unknown p in Section 4.

Since the random-walk distribution \mathbf{w} for which $\mathcal{S}(\mathbf{w})$ is most likely to reject the null is unknown in advance, and since computing $\mathcal{S}(\mathbf{w})$ for all $\mathbf{w} \in \mathcal{F}$ is infeasible, we first define a finite set of distributions $\tilde{\mathcal{F}} \subset \mathcal{F}$ which represents \mathcal{F} in a suitable way, and then compute $\mathcal{S}(\mathbf{w})$ only for $\mathbf{w} \in \tilde{\mathcal{F}}$. A naive approach to choose $\tilde{\mathcal{F}}$ is to exploit the fact that the random walk distributions W_i^t converge to stationary distributions as $t \rightarrow \infty$. Namely, to scan over all integers t up to a sufficiently large time step that is related to the *mixing time* [39] of the Markov chain. However, such an approach is unsatisfactory on its own, since the convergence to the stationary distributions can be arbitrarily slow, depending on W (and specifically on the largest eigenvalue of W that is smaller than 1). Instead, in Section 3.2 we propose to form the set of distributions $\tilde{\mathcal{F}} \subset \mathcal{F}$ via a sequence of judiciously-chosen time steps $1 = t_1^{(i)} < t_2^{(i)} < \dots < t_{M_i}^{(i)}$ for each point x_i , and to take into $\tilde{\mathcal{F}}$ only the random-walk distributions $\{W_i^{t_j^{(i)}}\}_{i,j}$. In particular, we find these time steps by ensuring that the statistics $\{\mathcal{S}(\mathbf{w})\}_{\mathbf{w} \in \tilde{\mathcal{F}}}$ form an ϵ -net over $\{\mathcal{S}(\mathbf{w})\}_{\mathbf{w} \in \mathcal{F}}$ (i.e., each element in the latter set is approximated by some element in the former set to a prescribed accuracy) for arbitrary labels z_1, \dots, z_n , and for a prescribed accuracy parameter ϵ (which we show how to tune automatically in

Section 3.3). Furthermore, we show that $\tilde{\mathcal{F}}$ forms an ϵ -net over \mathcal{F} in total variation distance with accuracy $\epsilon/2$. Therefore, $\tilde{\mathcal{F}}$ is a favorable surrogate for \mathcal{F} if ϵ is sufficiently small. Crucially, we show that this choice of $\tilde{\mathcal{F}}$ leads to a computationally tractable testing procedure with favorable statistical guarantees, primarily due to the fact that the cardinality of $\tilde{\mathcal{F}}$ can be at most $\mathcal{O}(n^2 \log n)$ regardless of the matrix W ; see the next section for more details.

After evaluating the set of distributions $\tilde{\mathcal{F}} \subset \mathcal{F}$, our testing procedure is straightforward. We simply test $H_0(\mathbf{w})$ against $H_1(\mathbf{w}, 0)$ for each $w \in \tilde{\mathcal{F}}$ using $\mathcal{S}(\mathbf{w})$, while correcting for multiple testing via the Bonferroni procedure. Specifically, for a prescribed significance level $\alpha \in (0, 1)$, we reject all $H_0(\mathbf{w})$ with $\mathbf{w} \in \tilde{\mathcal{F}}$, for which

$$\mathcal{S}(\mathbf{w}) > \sqrt{0.5 \log\left(\sum_{i=1}^n M_i/\alpha\right)}, \quad (14)$$

where $\sum_{i=1}^n M_i = |\tilde{\mathcal{F}}|$ is the total number of random-walk time steps chosen for the ϵ -net. In the context of our hypothesis testing problem, our local test $\hat{\mathcal{G}}_{\mathbf{z}}$ includes all distributions $\mathbf{w} \in \tilde{\mathcal{F}}$ that satisfy (14), and $Q_{\mathbf{z}}$ is the corresponding test that is 1 if $\max_{\mathbf{w} \in \tilde{\mathcal{F}}} \mathcal{S}(\mathbf{w})$ exceeds the threshold $\sqrt{0.5 \log(\sum_{i=1}^n M_i/\alpha)}$, and 0 otherwise. While our testing methodology here is conservative, it avoids the need for costly permutation tests or asymptotic approximations, and most importantly, we show that our particular construction of $\tilde{\mathcal{F}}$ makes it optimal in a minimax sense in terms of the required sequences $\{\gamma_n\}_{n=1}^{\infty}$ to achieve local and global consistency (as defined in Section 2.1).

If we inspect the expression in (13), we see that if the quantity $\langle \mathbf{w}, \mathbf{z} \rangle$ is kept fixed, then the statistic $\mathcal{S}(\mathbf{w})$ attains larger values for smaller values of $\|\mathbf{w}\|_2$. By utilizing the properties of W from Assumption 2, it is not difficult to show that $\|W_i^t\|_2$ is monotonically decreasing with t (see Proposition 3 in Section 3.1). Therefore, it is generally easier to reject null hypotheses $H_0(W_i^t)$ that are associated with larger scales t . This fact emphasizes again the importance of scanning over multiple values of t . To further clarify this point, consider $t = 1$ and suppose that the affinity matrix W has only a few non-zeros in each row. Then, $\|W_i^1\|_2$ may not be small enough for (14) to hold, even if $\langle W_i^1, \mathbf{z} \rangle = 1$ (i.e., all labels in the vicinity of x_i are 1). On the other hand, (14) can be easily satisfied for sufficiently large t even if $\langle W_i^t, \mathbf{z} \rangle$ is only marginally larger than p , as long as the number of samples in the connected component that includes x_i is not too small (since W_i^t converges, as $t \rightarrow \infty$, to the uniform distribution over the connected component that includes x_i , in which case $1/\|W_i^t\|_2$ converges to the square-root of the number of nodes in that connected component).

In Figure 2 we exemplify our testing procedure on the Swiss roll type data from Figure 1, where we used $n = 2400$ samples with $p = 0.5$; see Figure 2a. The densities f_0 and f_1 are piece-wise constant and chosen such that $f_1 > f_0$, $f_1 < f_0$, and $f_1 = f_0$ on certain prescribed sections along the trajectory of the Swiss roll; see Figure 2b. To detect regions where $f_1 > f_0$, we applied our testing procedure with significance $\alpha = 0.05$ and obtained the random-walk distribution W_i^t that corresponds to the largest statistic (among $\mathcal{S}(W_i^t)$ for $t = t_1^{(i)}, \dots, t_{M_i}^{(i)}$ and $i = 1, \dots, n$) that passed the threshold (14); see Figure 2c. Similarly, we applied our testing procedure to the negated labels (i.e., when replacing ones with zeros and vice-versa) to detect where $f_1 < f_0$, which is equivalent to taking the smallest statistic from the testing procedure when applied to the original labels (since z_i is replaced with $1 - z_i$ and p is replaced with $1 - p$); see Figure 2d. While it is difficult to identify the regions where $f_1 > f_0$ and $f_1 < f_0$ from Figure 2a visually, our method is able to capture these regions through the random walk distributions that passed the threshold (13). Evidently, the distributions depicted in Figures 2c and 2d, which correspond to time steps $t = 111$ and $t = 172$, respectively, are largely consistent with Figure 2b. It is important to mention that due to the curved nature of the data, it is inappropriate to define a testing procedure that ignores the samples

x_1, \dots, x_n , e.g., to scan over balls in the ambient space that vary in their center and radii. In particular, such a scan would not be able to exploit all samples in the contiguous regions where $f_1 > f_0$ or $f_1 < f_0$, and may often mix between the samples in the two regions.

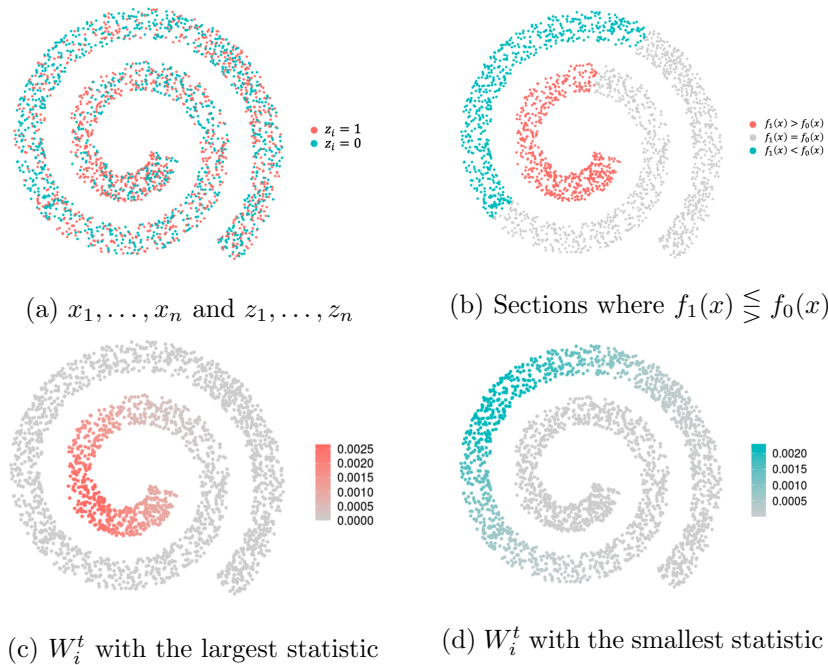


Figure 2: (a) Simulated Swiss roll data with $p = 0.5$ and $n = 2400$ samples colored by their labels. (b) Samples x_i for which $f_1(x_i) > f_0(x_i)$ (red), $f_1(x_i) < f_0(x_i)$ (blue), and $f_1(x_i) = f_0(x_i)$ (gray). (c) Random walk distribution W_i^t corresponding to the largest statistic in the scan. (d) Random walk distribution W_i^t corresponding to the smallest statistic in the scan.

For practical purposes, when (14) holds we not only accept $H_1(\mathbf{w}, 0)$, but also accept an alternative of the form $H_1(\mathbf{w}, \hat{\gamma})$ by specifying $\hat{\gamma} > 0$; see Section 3.2. Note that any accepted $H_1(\mathbf{w}, \hat{\gamma})$ also implies $H_1(\mathbf{w}, 0)$, hence it is sufficient to provide only the former. The purpose of specifying $\hat{\gamma}$ in an alternative $H_1(\mathbf{w}, \hat{\gamma})$ is that it provides a lower bound on $\langle \mathbf{w}, \mathbf{s} \rangle$ (see (7)), which is a local measure of discrepancy between f_1 and f_0 describing effect size rather than significance.

Clearly, our approach requires the class prior probability p and a matrix W satisfying assumption 2. In Section 4 we use the full probabilistic model in Section 1 (i.e., without conditioning on x_1, \dots, x_n) and describe how to modify our test to cope with unknown p by estimating a confidence interval for binomial proportion (where the binomial variable is $\sum_{i=1}^n z_i$). In Section 5 we describe how to construct W satisfying Assumption 2 from an arbitrary nonnegative matrix K (which is deterministic given x_1, \dots, x_n). Specifically, we use the geometric-mean for symmetrization and apply diagonal scaling for making the matrix doubly stochastic. We show that this procedure finds the nonnegative, symmetric, and stochastic matrix closest to K in KL-divergence. After symmetrization and diagonal scaling, we square the resulting matrix to make it PSD, which is a non-restrictive step equivalent to taking only the even time steps in the previously-resulting random walk.

For the reader's convenience, we summarize our testing procedure in Algorithm 1. We Analyze the computational complexity of Algorithm 1 in Appendix A.

Algorithm 1 Local two-sample testing by random-walk distributions

Input: Binary labels $\mathbf{z} = [z_1, \dots, z_n]$, nonnegative affinity matrix $K \in \mathbb{R}^{n \times n}$ (which is deterministic given x_1, \dots, x_n), and significance level $\alpha \in (0, 1)$.

- 1: Construct W using (48) and (50) in Section 5.
 - 2: Find the connected components $\mathcal{C}_1, \dots, \mathcal{C}_L \subset \{1, \dots, n\}$ of the graph described by W .
 - 3: Evaluate the eigen-decomposition of each principal submatrix $W^{(\ell)} = [W_{i,j}]_{i \in \mathcal{C}_\ell, j \in \mathcal{C}_\ell}$, $\ell = 1, \dots, L$.
 - 4: Choose $\varepsilon \in (0, 1)$ by minimizing $h(\varepsilon)$ from (40), or according to Table 2 in Appendix B.
 - 5: Compute the time steps $t_1^{(i)}, \dots, t_{M_i}^{(i)}$ for each $i = 1, \dots, n$ using Algorithm 2.
 - 6: If the class prior $p \in (0, 1)$ is unknown, set it as the upper bound from the Clopper-Pearson method applied to $\sum_{i=1}^n z_i$ with coverage $1 - \alpha/2$ (see Section 4), and subsequently replace α with $\alpha/2$.
 - 7: **for all** $i \in \{1, \dots, n\}$ and $j \in \{1, \dots, M_i\}$ **do**
 - 8: Compute: $\hat{\gamma}_{i,j} = \mathcal{S}(W_i^{t_j^{(i)}}) - \sqrt{0.5 \log(\sum_{k=1}^n M_k / \alpha)}$.
 - 9: **end for**
 - 10: For each pair (i, j) with $\hat{\gamma}_{i,j} > 0$ reject $H_0(W_i^{t_j^{(i)}})$ and accept $H_1(W_i^{t_j^{(i)}}, \hat{\gamma}_{i,j})$.
-

2.2.2 Analysis and theoretical guarantees

In Sections 3.3 and 3.4 we analyze our testing procedure assuming the prior p is known. The main results are as follows, which for simplicity are presented here assuming the graph G is connected (while the results in Sections 3.3 consider an arbitrary number of connected components in G). In Lemma 7 in Section 3.3 we show that

$$M_i \leq \min \left\{ \left\lceil \frac{\log(n/\varepsilon)}{\log((\lambda_{<1})^{-1})} \right\rceil, \left\lceil \frac{\log(n)}{\log(1 + \varepsilon^2/n)} \right\rceil \right\}, \quad (15)$$

where M_i is the number of chosen time steps $t_1^{(i)}, \dots, t_{M_i}^{(i)}$ (for the ε -net) for each index i , and $\lambda_{<1}$ is the largest eigenvalue of W which is strictly smaller than 1. Of particular interest is the fact that the quantity $\log(n)/\log(1 + \varepsilon^2/n)$ in (15) is independent of W and its spectrum, meaning that the cardinality of our constructed ε -net cannot be too large even when the convergence to a stationary distribution of the random walk is arbitrarily slow. As far as we know, this is a new result on the random walk distributions associated with a PSD transition probability matrix, and may be of independent interest. Furthermore, (15) implies that $|\tilde{\mathcal{F}}| = \mathcal{O}(n^2 \log n)$ (see the discussion following Lemma 7 in Section 3.3), hence the scan over $\tilde{\mathcal{F}}$ is always computationally feasible, even in the worst-case scenario where $\lambda_{<1}$ is arbitrarily close to 1.

In Theorem 8 and equation (42) in Section 3.3, we show that the power of $Q_{\mathbf{z}}$ (our binary test) to detect an alternative $H_1(\mathbf{w}, \gamma)$ is at least

$$1 - \exp \left[-2(\gamma - \hat{h}_{n,\alpha,\lambda_{<1}}(\varepsilon))^2 \right], \quad (16)$$

where ε is the accuracy of the ε -net, and $\hat{h}_{n,\alpha,\lambda_{<1}}(\varepsilon)$ is given in (42) in Section 3.3. In addition, we also show that the accuracy of our local test $\hat{\mathcal{G}}_{\mathbf{z}}$ can be quantified according to

$$\sup_{f_1, f_0 \in H_1(\mathbf{w}, \gamma)} \mathbb{E} \left[\inf_{\hat{\mathbf{w}} \in \hat{\mathcal{G}}_{\mathbf{z}}} \mathcal{E}_{\text{TV}}(\hat{\mathbf{w}}, \mathbf{w}) \mid f_1, f_0 \right] \leq \varepsilon \cdot \min \left\{ \frac{1-p}{2\gamma}, \frac{1}{2} \right\} + \exp \left[-2(\gamma - \hat{h}_{n,\alpha,\lambda_{<1}}(\varepsilon))^2 \right]. \quad (17)$$

Recall that the error in the left-hand side of (17) appears in the second summand of the local risk (10), and is the worst-case discrepancy (in expected total variation distance) between \mathbf{w} from a

true alternative $H_1(\mathbf{w}, 0)$ and its closest element in $\hat{\mathcal{G}}_{\mathbf{z}}$. Evidently, if the lower bound in (16) on the power of the test $Q_{\mathbf{z}}$ is large, then the error in (17) is small (provided that ε is sufficiently small). Therefore, it is desirable to minimize $\hat{h}_{n,\alpha,\lambda_{<1}}(\varepsilon)$ over ε . We refer the reader to tables 1 and 2 in Appendix B for the minimized values of $\hat{h}_{n,\alpha,\lambda_{<1}}(\varepsilon)$ and the corresponding best ε , respectively, for a wide range of the parameters n , $\lambda_{<1}$, and α (covering most practical situations). It is worthwhile to point out that the minimized values of $\hat{h}_{n,\alpha,\lambda_{<1}}(\varepsilon)$ are confined to the interval (2.6, 4.7) for the considered parameters, which is useful for extracting interpretable non-asymptotic guarantees on the power of the test $Q_{\mathbf{z}}$ and the accuracy of the local test $\hat{\mathcal{G}}_{\mathbf{z}}$.

By characterizing $\hat{h}_{n,\alpha,\lambda_{<1}}(\varepsilon)$ asymptotically, we provide in Theorem 9 in Section 3.3 sufficient conditions for the local consistency of our test. In particular, we show that our test is locally consistent (taking the significance α as $1/\log n$) if

$$\liminf_{n \rightarrow \infty} \frac{\gamma_n}{\sqrt{\log n}} > C, \quad (18)$$

where C can always be taken as 1, or it can be taken between $\sqrt{0.5}$ and 1 depending on the behavior of $\lambda_{<1}$ with n . In particular, we can take $C = \sqrt{0.5}$ if $\lambda_{<1}$ is bounded away from 1 for all n , in which case our test is locally consistent if γ_n is asymptotically larger than $\sqrt{0.5 \log n}$. Otherwise, our test is always locally consistent if γ_n is asymptotically larger than $\sqrt{\log n}$, regardless of W . Recall that if a local test is locally consistent, then it is also globally consistent. In Theorem 10 in Section 3.4 we complement our consistency guarantees by showing that if

$$\limsup_{n \rightarrow \infty} \frac{\gamma_n}{\sqrt{\log n}} < \frac{1-p}{\sqrt{\log(p^{-1})}}, \quad (19)$$

then there exists no single local test that can be globally consistent (and hence locally consistent) universally for all matrices W satisfying Assumption 2. This result, together with our local consistency guarantees, implies that our local test achieves the minimax detection rate in terms of γ_n (of a single test for all matrices W), which is $\sqrt{\log n}$, for attaining either global or local consistency. See Figure 3 for a summary our consistency guarantees.

2.2.3 Examples

In Section 6.1 we demonstrate our approach on a synthetic example where $p = 0.5$, f_0 and f_1 are restricted to a closed curve in the Euclidean space, and the Gaussian kernel is used to form K . We then showcase our ability to accurately detect the region of the curve where $f_1 > f_0$, and corroborate our theoretical results concerning the power of our test. In Sections 6.2 and 6.3 we apply our method to two real-world datasets, the first concerns Arsenic well contamination across the United States, and the second is single-cell RNA sequencing data from melanoma patients before and after immunotherapy treatment. We analyze each of these datasets using Algorithm 1, and demonstrate how to extract useful insights from the alternatives that are accepted by our method.

3 Method derivation and analysis

3.1 Preliminaries

Let G be a weighted graph over $\{x_1, \dots, x_n\}$ with adjacency matrix W satisfying Assumption 2, where $W_{i,j} \neq 0$ if and only if x_i and x_j are connected. Suppose that G has exactly L connected components, where the vertex indices of the ℓ 'th connected component are given by $\mathcal{C}_\ell \subset \{1, \dots, n\}$,

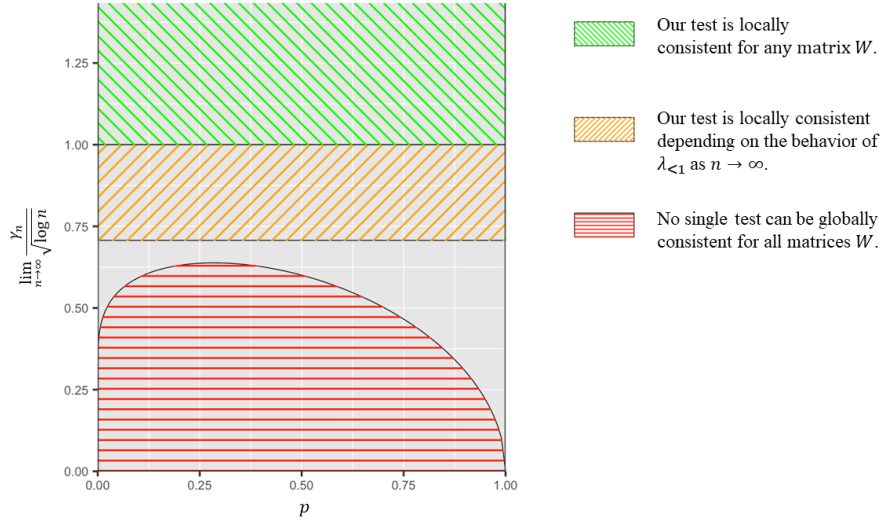


Figure 3: Summary of our consistency guarantees. If $\lim_{n \rightarrow \infty} \gamma_n / \sqrt{\log n} < (1-p) / \sqrt{\log(p^{-1})}$, then no local test can be globally (and locally) consistent for all matrices W satisfying Assumption 2; see Theorem 10 in Section 3.4. If $\lim_{n \rightarrow \infty} \gamma_n / \sqrt{\log n} \in (\sqrt{0.5}, 1)$, then the local (and global) consistency of our test depends on the convergence rate of $\lambda_{<1}$ to 1 as $n \rightarrow \infty$; see Theorem 9 in Section 3.3. If $\lim_{n \rightarrow \infty} \gamma_n / \sqrt{\log n} > 1$, then our test is locally (and globally) consistent for all matrices W satisfying Assumption 2

with size $n_\ell := |\mathcal{C}_\ell|$. We define $W^{(\ell)}$ to be the principal submatrix of W that corresponds to \mathcal{C}_ℓ , namely $W^{(\ell)} := [W]_{i \in \mathcal{C}_\ell, j \in \mathcal{C}_\ell}$, where $[W]_\Omega$ is the restriction of W to its entries in the subset Ω .

The next proposition provides several trivial spectral properties of W .

Proposition 2 (Spectral properties of W). *We have the following:*

1. W admits an eigen-decomposition with real-valued and nonnegative eigenvalues $\{\lambda_1^{(\ell)}, \dots, \lambda_{n_\ell}^{(\ell)}\}_{\ell=1}^L$ and corresponding orthonormal eigenvectors $\{\psi_1^{(\ell)}, \dots, \psi_{n_\ell}^{(\ell)}\}_{\ell=1}^L$.
2. For each $\ell = 1, \dots, L$, the values $\lambda_1^{(\ell)}, \dots, \lambda_{n_\ell}^{(\ell)}$ and the vectors $[\psi_1^{(\ell)}[j]]_{j \in \mathcal{C}_\ell}, \dots, [\psi_{n_\ell}^{(\ell)}[j]]_{j \in \mathcal{C}_\ell} \in \mathbb{R}^{n_\ell}$ are the eigenvalues and eigenvectors, respectively, of the principal submatrix $W^{(\ell)}$. Additionally, for each $\ell = 1, \dots, L$ we have $\psi_k^{(\ell)}[j] = 0$ for all $j \notin \mathcal{C}_\ell$ and all k .
3. For each $\ell = 1, \dots, L$, we have $1 = \lambda_1^{(\ell)} > \lambda_2^{(\ell)} \geq \lambda_3^{(\ell)} \geq \dots \geq \lambda_{n_\ell}^{(\ell)} \geq 0$, and $\psi_1^{(\ell)}[j] = 1/\sqrt{n_\ell}$ for all $j \in \mathcal{C}_\ell$.

Proof. Property 1 follows from the fact that W is symmetric and PSD, while property 2 follows from the fact that the rows and columns of W can be permuted (symmetrically) into a block-diagonal form with $\{W^{(\ell)}\}_{\ell=1}^L$ on its main diagonal. Last, property 3 follows from the fact that for each $\ell = 1, \dots, L$, $W^{(\ell)}$ is nonnegative, irreducible, and doubly stochastic (see chapter 8 in [30]). \square

Using the spectral properties of W described in Proposition 2, the following proposition establishes key properties of the random-walk distributions $\{W_i^t\}_{i,t}$, fundamental to the results and their proofs presented throughout Section 3 and the appendices.

Proposition 3 (Properties of the random-walk distributions W_i^t). *The following holds for all $i = 1, \dots, n$:*

1. $\|W_i^t\|_2$ is monotonically decreasing in t , i.e., $\|W_i^\tau\|_2 \leq \|W_i^t\|_2$ for all positive integers $\tau \geq t$.
2. For all positive integers $t' \leq t \leq \tau \leq \tau'$, we have $\|W_i^t - W_i^\tau\|_2^2 \leq \|W_i^{t'}\|_2^2 - \|W_i^{\tau'}\|_2^2$.
3. If $i \in \mathcal{C}_\ell$, then $W_{i,j}^t = 0$ for all $j \notin \mathcal{C}_\ell$ and integers $t > 0$, and $1/n_\ell \leq \|W_i^t\|_2^2 \leq 1/n_\ell + (\lambda_2^{(\ell)})^{2t}$.

The proof appears in Appendix D, and is based on the eigen-decomposition of W^t and Proposition 2.

3.2 Procedure for local two-sample testing over the family \mathcal{F}

As mentioned in the beginning of Section 2.1, we assume throughout this section that x_1, \dots, x_n are given, and all quantities are conditioned on x_1, \dots, x_n by default. Consequently, \mathcal{F} is deterministic according to Assumption 1, and each label z_i is independently sampled from $(Z \mid X = x_i)$, see (2). Throughout Section 3 we also assume that the class prior p is known, and we refer the reader to Section 4 for an adaptation of our approach to the setting where p is unknown.

Let us define

$$Y = Z - p, \quad y_i = z_i - p, \quad i = 1, \dots, n, \quad (20)$$

and denote $\mathbf{y} = [y_1, \dots, y_n]$. Using (4), we have that

$$\mathbb{E}[Y \mid X = x] = s(x). \quad (21)$$

Notice that y_1, \dots, y_n from (20) are independent (since z_1, \dots, z_n are independent), and bounded. Hence, when conditioned on x_1, \dots, x_n , the variables $\{w_i y_i\}_{i=1}^n$ are also independent and bounded (since \mathcal{F} is deterministic according to Assumption 1). Consequently, we have the following lemma, which is based on Hoeffding's inequality [28] for sums of independent and bounded random variables.

Lemma 4. *For any fixed $\alpha \in (0, 1)$ and $\mathbf{w} \in \mathcal{F}$, we have that*

$$\Pr \left\{ \frac{\langle \mathbf{w}, \mathbf{y} \rangle}{\|\mathbf{w}\|_2} > \frac{\langle \mathbf{w}, \mathbf{s} \rangle}{\|\mathbf{w}\|_2} + \sqrt{0.5 \log(1/\alpha)} \right\} \leq \alpha, \quad (22)$$

$$\Pr \left\{ \frac{\langle \mathbf{w}, \mathbf{y} \rangle}{\|\mathbf{w}\|_2} < \frac{\langle \mathbf{w}, \mathbf{s} \rangle}{\|\mathbf{w}\|_2} - \sqrt{0.5 \log(1/\alpha)} \right\} \leq \alpha. \quad (23)$$

The proof can be found in Appendix E. Recall that under the specific null $H_0(\mathbf{w})$ we have that $\langle \mathbf{w}, \mathbf{s} \rangle \leq 0$. Therefore, given $\alpha \in (0, 1)$ and a specific $\mathbf{w} \in \mathcal{F}$, if we wish to test $H_0(\mathbf{w})$ against $H_1(\mathbf{w}, 0)$ we can reject $H_0(\mathbf{w})$ at significance level α if

$$\mathcal{S}(\mathbf{w}) := \frac{\langle \mathbf{w}, \mathbf{y} \rangle}{\|\mathbf{w}\|_2} > \sqrt{0.5 \log(1/\alpha)}. \quad (24)$$

It is important to note that the above test is invariant to the choice of \mathcal{F} , and holds for any \mathbf{w} which is a deterministic probability distribution over $\{x_1, \dots, x_n\}$.

Evidently, the test (24) is useful only for testing $H_0(\mathbf{w})$ against $H_1(\mathbf{w}, 0)$ for a predefined $\mathbf{w} \in \mathcal{F}$. To test H_0 against H_1 , it is natural to consider the scan statistic $\sup_{\mathbf{w} \in \mathcal{F}} \mathcal{S}(\mathbf{w})$ which extends $\mathcal{S}(\mathbf{w})$ by searching over all $\mathbf{w} \in \mathcal{F}$. Notably, $\sup_{\mathbf{w} \in \mathcal{F}} \mathcal{S}(\mathbf{w})$ scans over an infinite number of time steps

t for each W_i^t , hence it is desirable to approximate $\sup_{\mathbf{w} \in \mathcal{F}} \mathcal{S}(\mathbf{w})$ by computing $\mathcal{S}(\mathbf{w})$ only for \mathbf{w} in a finite subset of \mathcal{F} . Specifically, for each index i , we approximate $\mathcal{S}(W_i^t)$ by replacing W_i^t with one of M_i possible distributions $W_i^{t_1}, \dots, W_i^{t_{M_i}}$ corresponding to carefully-chosen time steps $1 = t_1^{(i)} < t_2^{(i)} < \dots < t_{M_i}^{(i)}$, whose evaluation we describe next.

Given a prescribed accuracy parameter $\varepsilon \in (0, 1)$, we define

$$T_\ell = \left\lceil \frac{\log(n_\ell/\varepsilon)}{\log((\lambda_2^{(\ell)})^{-1})} \right\rceil, \quad \ell = 1, \dots, L, \quad (25)$$

recalling that $\lambda_2^{(\ell)}$ is the second-largest eigenvalue of $W^{(\ell)} = [W_{i,j}]_{i \in \mathcal{C}_\ell, j \in \mathcal{C}_\ell}$ (see Proposition 2), and n_ℓ is the size of the ℓ 'th connected component of G (i.e., $n_\ell = |\mathcal{C}_\ell|$). If $\lambda_2^{(\ell)} = 0$, we define $T_\ell = 1$ (which is the limit of (25) as $\lambda_2^{(\ell)} \rightarrow 0$). Note that $\lambda_2^{(\ell)} < 1$ according to Proposition 2, hence $\log((\lambda_2^{(\ell)})^{-1}) > 0$. Now, for each $i = 1, \dots, n$, we start by taking $t_{M_i}^{(i)} = T_\ell$, and proceed by finding the time steps $t_{M_i-1}^{(i)} > t_{M_i-2}^{(i)} > \dots > t_1^{(i)} = 1$ recursively, going backwards towards smaller values of t , by taking $t_{j-1}^{(i)}$ as the smallest integer $t \in [1, t_j^{(i)} - 1]$ that satisfies

$$\|W_i^{t+1}\|_2^2 \leq \|W_i^{t_j^{(i)}}\|_2^2 (1 + \varepsilon^2/n_\ell). \quad (26)$$

This procedure is summarized in Algorithm 2. Note that the time steps $t_1^{(i)}, \dots, t_{M_i}^{(i)}$ (and their number $- M_i$) may vary for each index i . In Section 3.3 we show that choosing the points $\{t_1^{(i)}, \dots, t_{M_i}^{(i)}\}_{i=1}^n$ according to Algorithm 2 guarantees that the set $\{\mathcal{S}(\mathbf{w}) : \mathbf{w} \in \tilde{\mathcal{F}}\}$ forms an ε -net over $\{\mathcal{S}(\mathbf{w}) : \mathbf{w} \in \mathcal{F}\}$ with controlled accuracy ε (for arbitrary labels z_1, \dots, z_n).

Algorithm 2 Evaluating $\{t_1^{(i)}, \dots, t_{M_i}^{(i)}\}_{i=1}^n$

- 1: **for all** $\ell \in \{1, \dots, L\}$ and $i \in \mathcal{C}_\ell$ **do**
 - 2: Initialize: $\tau_1^{(i)} = T_\ell$ from (25), $k = 1$.
 - 3: **while** $\tau_k^{(i)} \neq 1$ **do**:
 - 4: Take $\tau_{k+1}^{(i)}$ as the smallest integer $t \in [1, \tau_k^{(i)} - 1]$ such that $\|W_i^{t+1}\|_2^2 \leq \|W_i^{\tau_k^{(i)}}\|_2^2 (1 + \varepsilon^2/n_\ell)$.
 - 5: Update: $k \leftarrow k + 1$.
 - 6: **end while**
 - 7: Set $M_i = k$.
 - 8: **end for**
 - 9: Return $t_j^{(i)} = \tau_{M_i-j+1}^{(i)}$ for all $j = 1, \dots, M_i$ and $i = 1, \dots, n$.
-

Given $\{t_1^{(i)}, \dots, t_{M_i}^{(i)}\}_{i=1}^n$, we define $\tilde{\mathcal{F}}$ as the set

$$\tilde{\mathcal{F}} = \{W_i^t : 1 \leq i \leq n, t = t_1^{(i)}, \dots, t_{M_i}^{(i)}\}. \quad (27)$$

Since the cardinality of $\tilde{\mathcal{F}}$ is $\sum_{i=1}^n M_i$, using Lemma 4 and applying the union bound over the set $\tilde{\mathcal{F}}$ (while replacing α with $\alpha/\sum_{i=1}^n M_i$), we get that

$$\Pr \left\{ \bigcup_{\mathbf{w} \in \tilde{\mathcal{F}}} \left\{ \frac{\langle \mathbf{w}, \mathbf{y} \rangle}{\|\mathbf{w}\|_2} > \sqrt{0.5 \log \left(\sum_{i=1}^n M_i / \alpha \right) + \frac{\langle \mathbf{w}, \mathbf{s} \rangle}{\|\mathbf{w}\|_2}} \right\} \right\} \leq \alpha. \quad (28)$$

Therefore, we define our local test $\hat{\mathcal{G}}_{\mathbf{z}}$ as

$$\hat{\mathcal{G}}_{\mathbf{z}} = \left\{ \mathbf{w} \in \tilde{\mathcal{F}} : \mathcal{S}(\mathbf{w}) > \sqrt{0.5 \log\left(\sum_{i=1}^n M_i/\alpha\right)} \right\}, \quad (29)$$

which according to (28) (see also (65) in Appendix C) guarantees that

$$\sup_{f_0, f_1 \in H_0} \Pr\{Q_{\mathbf{z}} = 1 \mid f_0, f_1\} \leq \sup_{\mathcal{G} \subseteq \mathcal{F}} \sup_{f_0, f_1 \in H_0(\mathcal{G})} \Pr\{\hat{\mathcal{G}}_{\mathbf{z}} \cap \mathcal{G} \neq \emptyset \mid f_0, f_1\} \leq \alpha, \quad (30)$$

where $Q_{\mathbf{z}} = 0$ if $\hat{\mathcal{G}}_{\mathbf{z}}$ is empty and $Q_{\mathbf{z}} = 1$ otherwise, recalling that $H_0 = H_0(\mathcal{F})$. Note that in this case $Q_{\mathbf{z}}$ is the test that rejects H_0 and accepts H_1 if the scan statistic $\max_{\mathbf{w} \in \tilde{\mathcal{F}}} \mathcal{S}(\mathbf{w})$ exceeds the threshold $\sqrt{0.5 \log(\sum_{i=1}^n M_i/\alpha)}$. Since each $\mathbf{w} \in \hat{\mathcal{G}}_{\mathbf{z}}$ describes a rejected null hypothesis $H_0(\mathbf{w})$, our approach here is equivalent to applying the test in (24) to all $\mathbf{w} \in \tilde{\mathcal{F}}$ while correcting for multiple testing via the Bonferroni procedure (to control the family-wise error rate in the strong sense). While our overall approach here is conservative, we show in Sections 3.3 and 3.4 that for our particular choice of $\tilde{\mathcal{F}}$ this approach is in fact nearly optimal in a minimax sense in terms of the sequences $\{\gamma_n\}$ that guarantee global and local consistency. We mention that one may use a procedure other than Bonferroni's for controlling the family-wise error rate in the strong sense, such as Holm's [29] or Hochberg's [27]. The advantage of using Bonferroni, aside from its simplicity, is that the null hypotheses that are rejected by our method are in line with a certain quantity that we provide for describing effect size, as discussed next.

For practical purposes, aside from providing distributions \mathbf{w} from rejected $H_0(\mathbf{w})$, when analyzing a two-sample dataset it is useful to have a quantitative measure of discrepancy between f_1 and f_0 for each accepted alternative $H_1(\mathbf{w}, 0)$, which can speak of effect size rather than significance. To this end, observe that according to (28), if we reject $H_0(\mathbf{w})$ at significance α , we also reject the hypothesis $\langle \mathbf{w}, \mathbf{s} \rangle < \hat{\gamma} \|\mathbf{w}\|_2$ at significance α , where

$$\hat{\gamma} = \mathcal{S}(\mathbf{w}) - \sqrt{0.5 \log\left(\sum_{i=1}^n M_i/\alpha\right)}, \quad (31)$$

which is equivalent to accepting the alternative $H_1(\mathbf{w}, \hat{\gamma})$. Importantly, each accepted alternative $H_1(\mathbf{w}, \hat{\gamma})$ provides a lower bound on $\langle \mathbf{w}, \mathbf{s} \rangle$ through (7), which acts as a local measure of discrepancy between f_1 and f_0 .

3.3 Analysis and consistency guarantees

As mentioned in Section 3.2, the purpose of Algorithm 2 is to provide an ϵ -net over $\{\mathcal{S}(\mathbf{w}) : \mathbf{w} \in \mathcal{F}\}$, in the sense that each statistic $\mathcal{S}(W_i^t)$ can be approximated by $\mathcal{S}(W_i^{t_j^{(i)}})$, for some j , to a prescribed accuracy ϵ . Specifically, we define an approximation scheme as follows. Given the points $\{t_1^{(i)}, \dots, t_{M_i}^{(i)}\}_{i=1}^n$ from Algorithm 2, we approximate $\mathcal{S}(W_i^t)$ by $\mathcal{S}(W_i^{\pi(t)})$, where π is the map

$$\pi(t) := \begin{cases} 1, & t = 1, \\ t_{j+1}^{(i)}, & t_j^{(i)} < t \leq t_{j+1}^{(i)}, \quad 1 \leq j \leq M_i - 1, \\ t_{M_i}^{(i)}, & t > t_{M_i}^{(i)}. \end{cases} \quad (32)$$

We then have the following result.

Lemma 5 (ϵ -net properties). Fix $0 < \epsilon < 1$, and let $\{t_1^{(i)}, \dots, t_{M_i}^{(i)}\}_{i=1}^n$ be the output of Algorithm 2. Then,

$$\left| \mathcal{S}(W_i^t) - \mathcal{S}(W_i^{\pi(t)}) \right| \leq \epsilon, \quad (33)$$

and

$$\mathcal{E}_{\text{TV}}(W_i^t, W_i^{\pi(t)}) \leq \frac{\epsilon \|W_i^t\|_2}{2}, \quad (34)$$

for all $i = 1, \dots, n$ and $t = 1, 2, \dots, \infty$.

The proof can be found in Appendix F. Lemma 5 establishes that $\{\mathcal{S}(\mathbf{w})\}_{\mathbf{w} \in \tilde{\mathcal{F}}}$ is an ϵ -net over $\{\mathcal{S}(\mathbf{w})\}_{\mathbf{w} \in \mathcal{F}}$ with controlled accuracy ϵ . Hence, if we take ϵ small enough, we lose very little information by not computing all possible statistics $\{\mathcal{S}(\mathbf{W})\}_{\mathbf{W} \in \mathcal{F}}$. Additionally, since $\|W_i^t\|_2 \leq 1$ for all i and t , Lemma 5 also establishes that $\tilde{\mathcal{F}}$ is an ϵ -net over \mathcal{F} in total variation distance with accuracy $\epsilon/2$. Therefore, for sufficiently small ϵ , not only that $\mathcal{S}(W_i^{\pi(t)})$ is large if $\mathcal{S}(W_i^t)$ is large, but also $W_i^{\pi(t)}$ is close to W_i^t in total variation distance. For these arguments to be useful, we need to show that $\mathcal{S}(W_i^{\pi(t)})$ is large under the alternative $H_1(W_i^t, \gamma)$ (if γ is large enough). This is the subject of the following corollary of Lemmas 4 and 5.

Corollary 6. Fix $0 < \epsilon < 1$ and $0 < \tilde{\alpha} < 1$, and let $\{t_1^{(i)}, \dots, t_{M_i}^{(i)}\}_{i=1}^n$ be from Algorithm 2. Then, under $H_1(W_i^t, \gamma)$, with probability at least $1 - \tilde{\alpha}$ we have

$$\mathcal{S}(W_i^{\pi(t)}) > \gamma - \epsilon - \sqrt{0.5 \log(1/\tilde{\alpha})}, \quad (35)$$

for all $i = 1, \dots, n$ and $t = 1, 2, \dots, \infty$.

Proof. Under $H_1(W_i^t, \gamma)$, we know that $\langle W_i^t, \mathbf{s} \rangle / \|W_i^t\|_2 > \gamma$. Therefore, employing Lemma 5 and the probabilistic lower bound (23), we can write

$$\mathcal{S}(W_i^{\pi(t)}) \geq \mathcal{S}(W_i^t) - \epsilon \geq \frac{\langle W_i^t, \mathbf{s} \rangle}{\|W_i^t\|_2} - \epsilon - \sqrt{0.5 \log(1/\tilde{\alpha})} > \gamma - \epsilon - \sqrt{0.5 \log(1/\tilde{\alpha})}, \quad (36)$$

with probability at least $1 - \tilde{\alpha}$. □

Recall that according to our definition of $\hat{\mathcal{G}}_{\mathbf{z}}$ in (29), we accept all alternatives $H_1(\mathbf{w}, 0)$ for which $\mathcal{S}(\mathbf{w}) > \sqrt{0.5 \log(\sum_{i=1}^n M_i / \alpha)}$, where $\mathbf{w} \in \tilde{\mathcal{F}}$ and M_i is number of chosen time steps in the ϵ -net for each index i . Consequently, Corollary 6 implies that under $H_1(W_i^t, \gamma)$, we accept the alternative $H_1(W_i^{\pi(t)}, 0)$ with probability at least $1 - \tilde{\alpha}$ if $\gamma - \epsilon - \sqrt{0.5 \log(1/\tilde{\alpha})} > \sqrt{0.5 \log(\sum_{i=1}^n M_i / \alpha)}$. This enables us to obtain the power of the test $Q_{\mathbf{z}}$ against any alternative $H_1(W_i^t, \gamma)$ in terms of the quantity $\sum_{i=1}^n M_i = |\tilde{\mathcal{F}}|$. To make this quantity more meaningful, we have the following result concerning M_i .

Lemma 7 (Number of ϵ -net nodes). Fix $0 < \epsilon < 1$, and let $\{t_1^{(i)}, \dots, t_{M_i}^{(i)}\}_{i=1}^n$ be the output of Algorithm 2. Then,

$$M_i \leq \min \left\{ T_\ell, \left\lceil \frac{\log(n_\ell)}{\log(1 + \epsilon^2/n_\ell)} \right\rceil \right\}, \quad i \in \mathcal{C}_\ell, \quad \ell = 1, \dots, L, \quad (37)$$

where T_ℓ is from (25).

The proof can be found in Appendix G, and is based on the recurrence relation (in j) $\|W_i^{t_j^{(i)}}\|_2^2 > \|W_i^{t_{j-1}^{(i)}}\|_2^2(1 + \frac{\varepsilon^2}{n_\ell})$, which follows immediately from step 4 in Algorithm 2. It is noteworthy that T_ℓ (defined in (25)) can be arbitrarily large if $\lambda_2^{(\ell)}$ approaches 1. Nevertheless, and perhaps somewhat surprisingly, Lemma 7 asserts that M_i admits a universal bound independent of $W^{(\ell)}$ and its spectrum. Fixing ε , it is of interest to briefly discuss the asymptotic behavior of M_i and the size of $\tilde{\mathcal{F}}$ as $n \rightarrow \infty$. According to the definition of T_ℓ , if $\lambda_2^{(\ell)}$ is bounded away from 1 as $n \rightarrow \infty$, then Lemma 7 asserts that $M_i = \mathcal{O}(\log n_\ell) = \mathcal{O}(\log n)$, in which case $|\tilde{\mathcal{F}}| = \sum_{i=1}^n M_i = \mathcal{O}(n \log n)$. On the other hand, even if $\lambda_2^{(\ell)}$ approaches 1 arbitrarily fast as $n \rightarrow \infty$, we can use

$$\left\lceil \frac{\log(n_\ell)}{\log(1 + \varepsilon^2/n_\ell)} \right\rceil \leq \left\lceil \frac{\log(n)}{\log(1 + \varepsilon^2/n)} \right\rceil \underset{n \rightarrow \infty}{\sim} \frac{n \log n}{\varepsilon^2}. \quad (38)$$

Therefore, for a fixed ε we always have that $M_i = \mathcal{O}(n \log n)$, and consequently $|\tilde{\mathcal{F}}| = \mathcal{O}(n^2 \log n)$, regardless of W and its spectrum.

Employing Corollary 6 and Lemma 7, we can now provide a lower bound on the power of the test $Q_{\mathbf{z}}$ against any alternative $H_1(\mathbf{w}, \gamma)$, and also an upper bound on the error $\sup_{f_0, f_1 \in H_1(\mathbf{w}, \gamma)} \mathbb{E}[\inf_{\hat{\mathbf{w}} \in \hat{\mathcal{G}}_{\mathbf{z}}} \mathcal{E}_{\text{TV}}(\hat{\mathbf{w}}, \mathbf{w}) \mid f_0, f_1]$, in terms of the quantities appearing in (37). This is the subject of the next theorem.

Theorem 8 (Power and accuracy). *Fix $0 < \varepsilon < 1$, $0 < \alpha < 1$, and let $\{t_1^{(i)}, \dots, t_{M_i}^{(i)}\}_{i=1}^n$ be the output of Algorithm 2. Let $\hat{\mathcal{G}}_{\mathbf{z}}$ be as in (29) and suppose that $Q_{\mathbf{z}}$ is the test that outputs 1 if $\hat{\mathcal{G}}_{\mathbf{z}}$ is empty, and 0 otherwise. Then, the power of the test $Q_{\mathbf{z}}$ over any alternative $H_1(\mathbf{w}, \gamma)$, with $\mathbf{w} \in \mathcal{F}$, is at least*

$$1 - \exp[-2(\gamma - h(\varepsilon))^2], \quad (39)$$

for all $\gamma > h(\varepsilon)$, where

$$h(\varepsilon) = \varepsilon + \sqrt{0.5 \log \left(\sum_{\ell=1}^L \frac{n_\ell}{\alpha} \min \left\{ \left\lceil \frac{\log(n_\ell/\varepsilon)}{\log([\lambda_2^{(\ell)}]^{-1})} \right\rceil, \left\lceil \frac{\log(n_\ell)}{\log(1 + \varepsilon^2/n_\ell)} \right\rceil \right\} \right)}. \quad (40)$$

Furthermore, for all $\mathbf{w} \in \mathcal{F}$ and $\gamma > h(\varepsilon)$ we have

$$\sup_{f_1, f_0 \in H_1(\mathbf{w}, \gamma)} \mathbb{E}[\inf_{\hat{\mathbf{w}} \in \hat{\mathcal{G}}_{\mathbf{z}}} \mathcal{E}_{\text{TV}}(\hat{\mathbf{w}}, \mathbf{w}) \mid f_1, f_0] \leq \varepsilon \cdot \min \left\{ \frac{1-p}{2\gamma}, \frac{1}{2} \right\} + \exp[-2(\gamma - h(\varepsilon))^2]. \quad (41)$$

The proof can be found in Appendix H. Naturally, to maximize the power of the test against any alternative $H_1(\mathbf{w}, \gamma)$ (for a fixed significance α) it is desirable to make $h(\varepsilon)$ as small as possible. Therefore, the parameter $\varepsilon \in (0, 1)$ should be chosen by minimizing the right-hand side of (40), which can be accomplished numerically given α , $\{n_\ell\}_{\ell=1}^L$, and $\{\lambda_2^{(\ell)}\}_{\ell=1}^L$. To somewhat simplify this minimization and related subsequent analysis, notice that

$$h(\varepsilon) \leq \hat{h}_{n, \alpha, \lambda_{<1}}(\varepsilon) := \varepsilon + \sqrt{0.5 \log \left(\frac{n}{\alpha} \min \left\{ \left\lceil \frac{\log(n/\varepsilon)}{\log(\lambda_{<1}^{-1})} \right\rceil, \left\lceil \frac{\log(n)}{\log(1 + \varepsilon^2/n)} \right\rceil \right\} \right)}, \quad (42)$$

which only depends only on n , ε , and $\lambda_{<1} := \max_\ell \lambda_2^{(\ell)}$, which is the largest eigenvalue of W which is strictly smaller than 1 (or equivalently, the $(L+1)$ 'th largest eigenvalue of W). Clearly, the results in Theorem 8 also hold if we replace $h(\varepsilon)$ with its upper bound $\hat{h}_{n, \alpha, \lambda_{<1}}(\varepsilon)$. We refer the reader to Tables 1 and 2 in Appendix B, where we list the values of ε and the corresponding

values of $\hat{h}_{n,\alpha,\lambda_{<1}}(\varepsilon)$ that minimize $\hat{h}_{n,\alpha,\lambda_{<1}}(\varepsilon)$ (via a grid search) for the array of parameters $n = 10^3, 10^4, 10^5, 10^6$, $\alpha = 10^{-1}, 10^{-2}, 10^{-3}$, and $\lambda_{<1} = 0.9, 0.99, 0.999, 1 - 10^{-4}, 1 - 10^{-5}, 1 - 10^{-6}, 1 - 10^{-9}, 1 - 10^{-12}, 1 - 10^{-16}$. Notably, for all of the above-mentioned values of n , α , and $\lambda_{<1}$, the minimized values of $\hat{h}_{n,\alpha,\lambda_{<1}}(\varepsilon)$ are confined to the interval (2.6, 4.7). Furthermore, when $\lambda_{<1} < 1 - 10^{-5}$ the bound in (42) is dominated by $\log(n/\varepsilon)/\log(\lambda_{<1}^{-1})$ and the corresponding best values of ε are around 0.005. On the other hand, when $\lambda_{<1} > 1 - 10^{-5}$ the bound in (42) becomes dominated by $\log(n)/\log(1 + \varepsilon^2/n)$ and the corresponding best values of ε are around 0.1.

In essence, Theorem 8 provides a guarantee on the power of the test $Q_{\mathbf{z}}$ against any alternative $H_1(\mathbf{w}, \gamma)$ for $\gamma > h(\varepsilon)$. Since the test $Q_{\mathbf{z}}$ controls the type I error at level α (see (30)), Theorem 8 immediately provides an upper bound on the global Risk $R_{\mathcal{F}}^{(n)}(Q_{\mathbf{z}}, \gamma)$ from (9). Similarly, equation (41) in Theorem 8 provides an upper bound on the second summand of the local risk $r_{\mathcal{F}}^{(n)}(\hat{\mathcal{G}}_{\mathbf{z}}, \gamma)$ from (10), whereas the first summand in (10) is upper bounded by α (see (30)). By analyzing the resulting upper bound on $r_{\mathcal{F}}^{(n)}(\hat{\mathcal{G}}_{\mathbf{z}}, \gamma)$ asymptotically (as $n \rightarrow \infty$), we get the following theorem characterizing the local consistency of $\hat{\mathcal{G}}_{\mathbf{z}}$ from (29) (recalling the definitions of global and local consistencies in Section 2.1.2).

Theorem 9 (Local consistency guarantees). *Fix $\varepsilon \in (0, 1)$, take $\alpha = 1/\log n$, and let $\hat{\mathcal{G}}_{\mathbf{z}}$ be the local test described in (29). Additionally, let $\{\gamma_n\}$ be a sequence, and define*

$$c = \liminf_{n \rightarrow \infty} \frac{\gamma_n}{\sqrt{\log n}}. \quad (43)$$

Then, $\hat{\mathcal{G}}_{\mathbf{z}}$ is locally consistent w.r.t. $\{\gamma_n\}$ if one of the following holds:

1. $c > 1$.
2. $c > \sqrt{0.5}$ and $\lambda_{<1}$ is bounded away from 1 for all n .
3. $c > \sqrt{0.5 + \delta}$ for some $\delta \in (0, 0.5)$, and $\lim_{n \rightarrow \infty} (1 - \lambda_{<1})n^\delta > 0$.

The proof can be found in Appendix I. Fundamentally, part 1 of Theorem 9 states that $\hat{\mathcal{G}}_{\mathbf{z}}$ is locally consistent, i.e., $r_{\mathcal{F}}^{(n)}(\hat{\mathcal{G}}_{\mathbf{z}}, \gamma_n) \rightarrow 0$ as $n \rightarrow \infty$, as long as γ_n grows asymptotically faster than $\sqrt{\log n}$ (even if by a factor slightly larger than 1) for any matrix W satisfying Assumption 2. Parts 2 and 3 improve upon the required growth of γ_n from part 1 (by a constant factor) if $\lambda_{<1}$ is either bounded away from 1, or it converges to 1 no faster than $1/n^\delta$ for some $0 < \delta < 0.5$. As discussed in Section 2.1, local consistency implies global consistency, hence $\hat{\mathcal{G}}_{\mathbf{z}}$ is globally consistent under the same conditions as in Theorem 9.

3.4 Problem impossibility and minimax detection rate

Let \mathcal{W} be the space of all matrices satisfying assumption 2. In order to complement the consistency guarantees provided in Theorem 9, we consider the minimax global risk

$$\tilde{R}^{(n)}(\gamma) = \min_{Q_{\mathbf{z}}} \sup_{W \in \mathcal{W}} R_{\mathcal{F}}^{(n)}(Q_{\mathbf{z}}, \gamma), \quad (44)$$

where the minimization in (44) is over all deterministic tests $Q_{\mathbf{z}} : \{0, 1\}^n \rightarrow \{0, 1\}$. In particular, our aim here is to provide necessary conditions on $\{\gamma_n\}$ so that $\lim_{n \rightarrow \infty} \tilde{R}^{(n)}(\gamma_n) = 0$ can hold. Such conditions on $\{\gamma_n\}$ are necessary for any single local test to be globally consistent universally for all matrices $W \in \mathcal{W}$. In turn, such conditions are also necessary for any local test to be locally consistent universally for all matrices $W \in \mathcal{W}$ (by the virtue of Lemma 1). Towards that end, we have the following theorem.

Theorem 10. *If $\{\gamma_n\}$ is a sequence that satisfies*

$$\limsup_{n \rightarrow \infty} \frac{\gamma_n}{\sqrt{\log n}} < \frac{1-p}{\sqrt{\log(p^{-1})}}, \quad (45)$$

then $\lim_{n \rightarrow \infty} \tilde{R}^{(n)}(\gamma_n) \geq 1$.

The proof of Theorem 10 can be found in Appendix J, and is based on analyzing the setting where the graph G has approximately $n/\log n$ connected components of size proportional to $\log n$. Essentially, Theorem 10 states that no local test can be globally consistent universally for all matrices $W \in \mathcal{W}$ (satisfying Assumption 2) if γ_n is asymptotically smaller than $\sqrt{((1-p)^2/\log(p^{-1})) \log n}$. Therefore, the same conclusion holds for local consistency. On the other hand, from Theorem 9 we know that $\hat{\mathcal{G}}_{\mathbf{z}}$ from (29) is locally consistent (and hence globally consistent) universally for all $W \in \mathcal{W}$ if γ_n is asymptotically larger than $\sqrt{\log n}$. Combining Theorems 9 and 10 implies that γ_n has to grow with rate at least $\sqrt{\log n}$ (disregarding constants) for any single $\hat{\mathcal{G}}_{\mathbf{z}}$ to be locally or globally consistent for all $W \in \mathcal{W}$. We therefore conclude that our local test $\hat{\mathcal{G}}_{\mathbf{z}}$ achieves the minimax detection rate of γ_n both globally and locally.

4 Adapting to unknown prior p

Next, we treat the case where the prior p is unknown, and must be inferred from the labels z_1, \dots, z_n . To this end, we return to the full probabilistic model described in the introduction, where both z_1, \dots, z_n and x_1, \dots, x_n are random, sampled independently from the joint distribution of Z and X . In other words, we do not condition on x_1, \dots, x_n , which was required in Sections 2.1 and 3 for the hypothesis testing framework to be well defined (by making W and \mathcal{F} non random).

In the full probabilistic model discussed here, the labels z_1, \dots, z_n are sampled independently from $\text{Bernoulli}(p)$, and therefore $\sum_{i=1}^n z_i \sim \text{Binomial}(n, p)$. Estimating confidence intervals for a binomial proportion p is a problem with a long history and extensive literature (see for example [58, 9] and the references therein). One popular approach is the Clopper–Pearson method [16], which is based on inverting a Binomial test. The Clopper–Pearson method is an *exact* method, meaning that for a prescribed $\alpha \in (0, 1)$, the one-sided Clopper–Pearson method outputs an upper bound \hat{p}_+ such that $p \leq \hat{p}_+$ with probability at least $1 - \alpha$, a probability referred to as the *coverage*.

In order to modify our method from Section 3.2 to account for unknown p , we require an upper bound for p . We have the following proposition, which is an analogue of (28) when using an estimated upper bound for p instead of p directly. We emphasize that the claim “with probability” in the next proposition is interpreted in the sense of sampling z_1, \dots, z_n and x_1, \dots, x_n from the joint distribution of Z and X .

Proposition 11. *Suppose that $p \leq \hat{p}_+$ with probability at least $1 - \alpha/2$. Then, with probability at least $1 - \alpha$*

$$\hat{\mathcal{S}}(\mathbf{w}) := \frac{\langle \mathbf{w}, \mathbf{z} - \hat{p}_+ \rangle}{\|\mathbf{w}\|_2} \leq \sqrt{0.5 \log(2 \sum_{i=1}^n M_i/\alpha) + \frac{\langle \mathbf{w}, \mathbf{s} \rangle}{\|\mathbf{w}\|_2}}, \quad \forall \mathbf{w} \in \tilde{\mathcal{F}}. \quad (46)$$

Proof. Observe that Lemma 4 and subsequently the probabilistic bound in (28) (obtained from Lemma 4 using the union bound) hold conditionally on any x_1, \dots, x_n . Therefore, even though W , \mathcal{F} , and $\{t_j^{(i)}\}_{i,j}$ are random variables in the setting of this section, Lemma 4 and (28) also hold

unconditionally of x_1, \dots, x_n . Hence, using the probabilistic bound (28) with $\alpha/2$ instead of α , and together with the union bound, we have with probability at least $1 - \alpha$

$$\frac{\langle \mathbf{w}, \mathbf{z} - \hat{p}_+ \rangle}{\|\mathbf{w}\|_2} = \frac{\langle \mathbf{w}, \mathbf{y} + p - \hat{p}_+ \rangle}{\|\mathbf{w}\|_2} \leq \frac{\langle \mathbf{w}, \mathbf{y} \rangle}{\|\mathbf{w}\|_2} \leq \sqrt{0.5 \log(2 \sum_{i=1}^n M_i/\alpha)} + \frac{\langle \mathbf{w}, \mathbf{s} \rangle}{\|\mathbf{w}\|_2}, \quad (47)$$

where we used the fact that $p - \hat{p}_+ \leq 0$ with probability at least $1 - \alpha/2$. \square

Evidently, \hat{p}_+ from the (one-sided) Clopper–Pearson method can be used in conjunction with Proposition 11. Employing Proposition 11, we can use the method described in Section 3.2 if we replace $\mathcal{S}(\mathbf{w})$ with $\hat{\mathcal{S}}(\mathbf{w})$ from (46) and replace α with $\alpha/2$, respectively. This modification can be found in Step 6 of Algorithm 1 in Section 2.2. We remark that when using \hat{p}_+ (which is an estimated upper bound for p) rather than knowing p (as in Section 3.2) the significance level α should be interpreted in the sense of the full probabilistic model described in Section 1.

5 Construction of W

Our statistical framework is based on a matrix W that satisfies Assumption 2. To construct such a matrix, we require a graph (either directed or undirected) over $\{x_1, \dots, x_n\}$ that encodes the similarities between x_1, \dots, x_n . We assume that this graph is represented by a nonnegative affinity matrix $K \in \mathbb{R}^{n \times n}$, which is a deterministic function of x_1, \dots, x_n . If an unweighted graph over $\{x_1, \dots, x_n\}$ is provided, we simply take $K_{i,j}$ to be 1 if x_i is connected to x_j and 0 otherwise.

Given a nonnegative matrix K , we define the matrices $\widetilde{W}, \widetilde{K} \in \mathbb{R}^{n \times n}$ via

$$\widetilde{W}_{i,j} = d_i \widetilde{K}_{i,j} d_j, \quad \widetilde{K}_{i,j} = \sqrt{K_{i,j} K_{j,i}}, \quad (48)$$

where $d_1, \dots, d_n > 0$ are the diagonal scaling factors of a doubly stochastic normalization of \widetilde{K} , i.e., d_1, \dots, d_n are such that the sums of all rows and all columns of \widetilde{W} are 1 [53, 31]. Such scaling factors exist if the matrix \widetilde{K} has full-support [18], a property related to the zero-pattern of \widetilde{K} . Importantly, d_1, \dots, d_n always exist if \widetilde{K} is strictly positive, or if it is zero only on its main diagonal (see [38]). Otherwise, the typical situation where d_1, \dots, d_n would not exist is if some rows/columns of \widetilde{K} are too sparse, a problem that can be circumvented by discarding these rows and columns. When they exist, the scaling factors d_1, \dots, d_n can be computed by the classical Sinkhorn-Knopp iterations [54], or by more recent algorithms employing convex optimization [2].

Clearly, \widetilde{W} from (48) is nonnegative, symmetric, and stochastic. While there are countless ways to construct a matrix with these properties from K , \widetilde{W} from (48) admits the favorable property that it is the closest symmetric and stochastic matrix to K in KL-divergence. Specifically, we have the following proposition.

Proposition 12. *Suppose that there exist $d_1, \dots, d_n > 0$ such that \widetilde{W} from (48) is stochastic. Then, \widetilde{W} is also the solution to*

$$\underset{H \in \mathbb{R}_+^{n \times n}}{\text{Minimize}} \quad \sum_{i=1}^n D_{KL}(H_i \parallel K_i) \quad \text{Subject to} \quad H \mathbf{1}_n = \mathbf{1}_n, \quad H = H^T, \quad (49)$$

where H_i and K_i are the i 'th rows of H and K respectively, $\mathbf{1}_n$ is a column vector of n ones, and $D_{KL}(H_i \parallel K_i) = \sum_{j=1}^n H_{i,j} \log(H_{i,j}/K_{i,j})$ is the Kullback–Leibler divergence from K_i to H_i .

We note that the result described in Proposition 12 is already known for the special that K is symmetric (and hence $\widetilde{K} = K$), see Proposition 2 in [61]. Therefore, the contribution of Proposition 12 is to describe the appropriate form of symmetrization (i.e., the formula for \widetilde{K}) in the context of finding the closest symmetric and doubly stochastic matrix to an arbitrary nonnegative matrix K (under KL-divergence loss). The proof of Proposition 12 can be found in Appendix K, and follows from the Lagrangian of (49). Note that the KL-divergence is typically used for measuring discrepancies between probability distributions, whereas $\{K_i\}$ are not proper probability distributions. Nevertheless, it is easy to verify that replacing K_i in (49) with its normalized variant $K_i / \sum_{j=1}^n K_{i,j}$ leads to an equivalent optimization problem (using the fact that $\sum_{j=1}^n W_{i,j} = 1$ for all $i = 1, \dots, n$).

Finally, in order to obtain W satisfying Assumption 2 from \widetilde{W} (in case K is not PSD), we take

$$W = \widetilde{W}^2, \quad (50)$$

which further ensures that W is PSD while retaining the properties held by \widetilde{W} of non-negativity, symmetry, and stochasticity. Note that the random-walk arising from W is equivalent to the one arising from \widetilde{W} when restricting the latter to even time steps. Therefore, (50) can also be interpreted as bypassing unstable periodic behavior of the random walk associated with \widetilde{W} if it describes a bipartite graph.

6 Examples

6.1 Simulation: data sampled from a closed curve

In our first example, we simulated data points sampled uniformly from a smooth closed curve, over which $f_1(x) > f_0(x)$ in a certain localized region. We then analyzed the performance of the test described in Section 3.2. In particular, we investigated the power of the test with respect to the effective size of the deviating region (where $f_1(x) > f_0(x)$) and the magnitude of the difference between f_1 and f_0 .

6.1.1 The setup

In this example, the points $x_1, \dots, x_n \in \mathbb{R}^2$ were sampled from the unit circle \mathbb{S}_1 , i.e.,

$$x_i[1] = \cos(\theta_i), \quad x_i[2] = \sin(\theta_i), \quad (51)$$

for $i = 1, \dots, n$. The angles $\theta_1, \dots, \theta_n \in [-\pi, \pi)$ are i.i.d, each sampled from $f_1(\theta)$ or $f_0(\theta)$ with probability $p = 0.5$, where

$$f_1(\theta) = \begin{cases} \frac{1 + b \cos(\omega\theta)}{2\pi}, & |\theta| < \frac{3\pi}{2\omega}, \\ \frac{1}{2\pi}, & \text{Otherwise} \end{cases}, \quad f_0(\theta) = \begin{cases} \frac{1 - b \cos(\omega\theta)}{2\pi}, & |\theta| < \frac{3\pi}{2\omega}, \\ \frac{1}{2\pi}, & \text{Otherwise.} \end{cases} \quad (52)$$

We have that

$$\begin{aligned} f(\theta) &= pf_1(\theta) + (1-p)f_0(\theta) = \frac{1}{2\pi}, \\ s(\theta) &= p(1-p) \frac{f_1(\theta) - f_0(\theta)}{f(\theta)} = \begin{cases} 2p(1-p)b \cos(\omega\theta), & |\theta| < \frac{3\pi}{2\omega}, \\ 0, & \text{Otherwise.} \end{cases} \end{aligned} \quad (53)$$

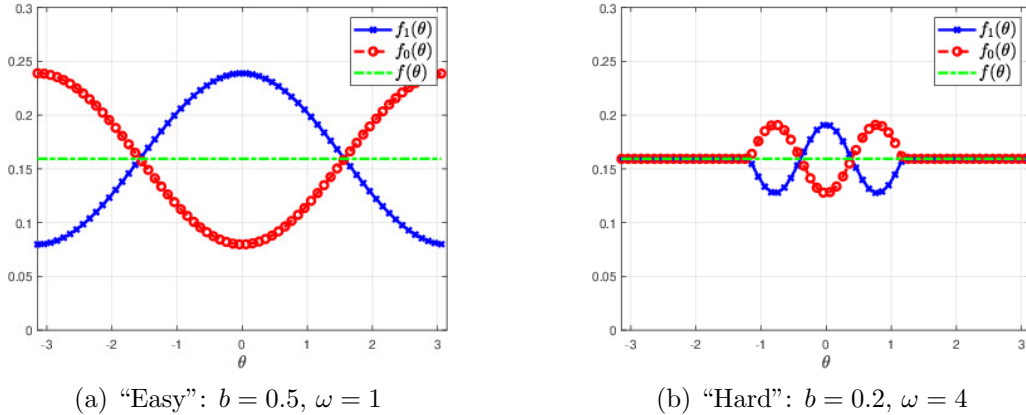


Figure 4: The distributions f_1 , f_0 , and f corresponding to the unit circle example described in (51)–(53). In this example $f(\theta)$ is the uniform distribution, and $f_1(\theta) > f_0(\theta)$ around $\theta = 0$ in a region determined by ω , while the magnitude of $f_1(\theta) - f_0(\theta)$ is determined by b .

It is evident from (53) that the points $x_1 \dots, x_n$ are sampled uniformly from the unit circle. Observe that $f_1(\theta) > f_0(\theta)$ only in a single contiguous region around $\theta = 0$, whose size depends on the parameter ω (smaller values of ω correspond to larger regions where $f_1(\theta) > f_0(\theta)$, and vice-versa). Additionally, the parameter $b \in [0, 1]$ controls the magnitude of the difference between f_1 and f_0 , where $b = 0$ results in the null hypothesis H_0 , since $f_1(\theta) = f_0(\theta)$. Figure 4 illustrates the distributions $f_1(\theta)$, $f_0(\theta)$, and $f(\theta)$, for two scenarios where $(b, \omega) = (0.5, 1)$ (figure (a)) and $(b, \omega) = (0.2, 4)$ (figure (b)). The former corresponds to an “easy” scenario where the magnitude of $f_1 - f_0$ is relatively large, and $f_1(\theta) > f_0(\theta)$ on a large portion of $[-\pi, \pi)$, whereas the latter corresponds to a “hard” scenario where the magnitude of $f_1 - f_0$ is much smaller, and $f_1(\theta) > f_0(\theta)$ only in a restricted part of $[-\pi, \pi)$.

After generating the points x_1, \dots, x_n together with the labels z_1, \dots, z_n , we formed an affinity matrix K using the Gaussian kernel

$$K_{i,j} = \exp(-\|x_i - x_j\|_2^2 / \sigma), \quad (54)$$

and followed with the construction of W according to (48) and (50) in Section 5, using $\sigma = 0.01$. Since x_1, \dots, x_n are sampled uniformly from a smooth Riemannian manifold without boundary, as $n \rightarrow \infty$ and $\sigma \rightarrow 0$ the matrix W^t is expected to converge pointwise to the heat kernel on the manifold [44]. Since our manifold is a smooth closed curve, the heat kernel is approximately the Gaussian kernel with respect to the geodesic distance. Therefore, for a suitable range of parameters σ , n , and t , we use the approximation

$$W_{i,j}^t \approx C_i G_{2\sigma t}(\theta_i, \theta_j), \quad G_\tau(\theta, \varphi) := \exp\{-(\text{mod}\{\theta - \varphi, 2\pi\})^2 / \tau\}. \quad (55)$$

where C_i is a normalization constant (accommodating for the fact that $\sum_{j=1}^n W_{i,j}^t = 1$). Figure 5 compares between W_1^t and the right-hand side of (55) for several values of t , where we used $\theta_1 = 0$ and sampled $\theta_2, \dots, \theta_n$, with $n = 5000$, independently and uniformly from $[0, 2\pi)$. Indeed, Figure 5 suggests that the approximation (55) is highly accurate.

6.1.2 Results

In Figure 6a we illustrate a typical array of points x_1, \dots, x_n and their labels z_1, \dots, z_n , sampled according to (51)–(53), for $n = 5000$, $b = 0.3$, and $\omega = 2$. We added a small amount of noise to

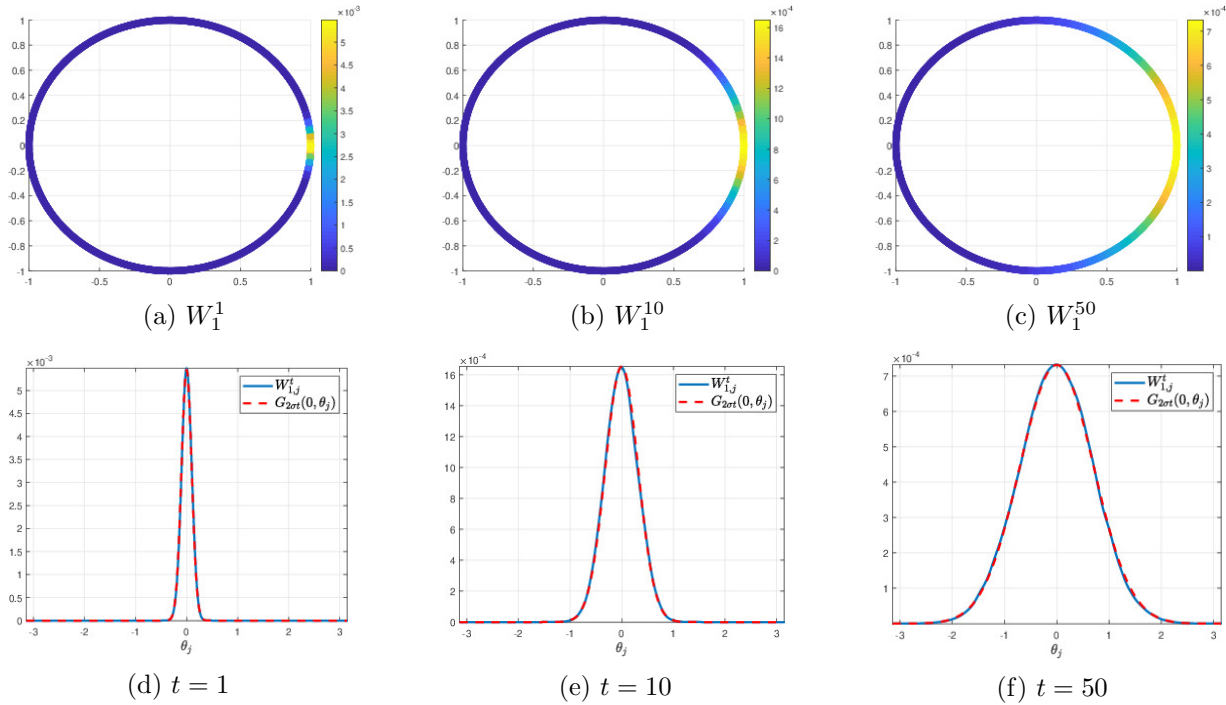


Figure 5: The random-walk distributions W_1^t (with $\theta_1 = 0$), $t = \{1, 10, 50\}$, versus their approximations in (55), for $n = 5000$ and $\sigma = 0.01$

the coordinates of x_1, \dots, x_n for improved visibility of the labels. Although somewhat difficult to determine by the naked eye, there is a slightly larger number of blue points than red in the vicinity of $\theta = 0$, matching the fact that $f_1(\theta) > f_0(\theta)$ in that region. We next applied Algorithm 1 to the labels z_1, \dots, z_n and the matrix K , with $\alpha = 0.05$ and treating $p = 0.5$ as known. We then found the indices (i^*, j^*) that correspond to the largest statistic among $\{\mathcal{S}(W_{i,j}^{t(i)})\}_{i,j}$, and denoted $t^* = t_{j^*}^{(i^*)}$. Figure (6b) colors the values of $W_{i^*}^{t^*}$ over the points x_1, \dots, x_n , and Figure (6c) compares between f_1, f_0 and $W_{i^*}^{t^*}$ (which was normalized appropriately for better visualization). Indeed, $W_{i^*}^{t^*}$ captures the region where $f_1(x) > f_0(x)$ over the points x_1, \dots, x_n , as $W_{i^*}^{t^*}$ is localized around $\theta = 0$, and is extremely small for $|\theta| > \pi/4$ (the region where $f_1(\theta) \leq f_0(\theta)$).

According to Theorem 8, our test has positive power to detect any alternative $H_1(\mathbf{w}, \gamma)$ for which $\gamma > h(\varepsilon)$. Consequently, to analyze the performance of our test in this setting and compare with numerical findings, we need to characterize γ from (7). Note that we can take

$$\gamma = \max_{1 \leq i \leq n} \sup_{t=1, \dots, \infty} \frac{\langle W_i^t, \mathbf{s} \rangle}{\|W_i^t\|_2}. \quad (56)$$

In Appendix L, we analyze (56) using (55) in the regime of large n and small σ , and show that

$$\gamma \approx (8/\pi e)^{1/4} b p (1-p) \sqrt{n/\omega}. \quad (57)$$

Therefore, employing Theorem 8, we expect our test $Q_{\mathbf{z}}$ to reject the null with probability at least ρ if

$$\gamma \approx (8/\pi e)^{1/4} b p (1-p) \sqrt{n/\omega} > h(\varepsilon) + \sqrt{0.5 \log(1/(1-\rho))}. \quad (58)$$

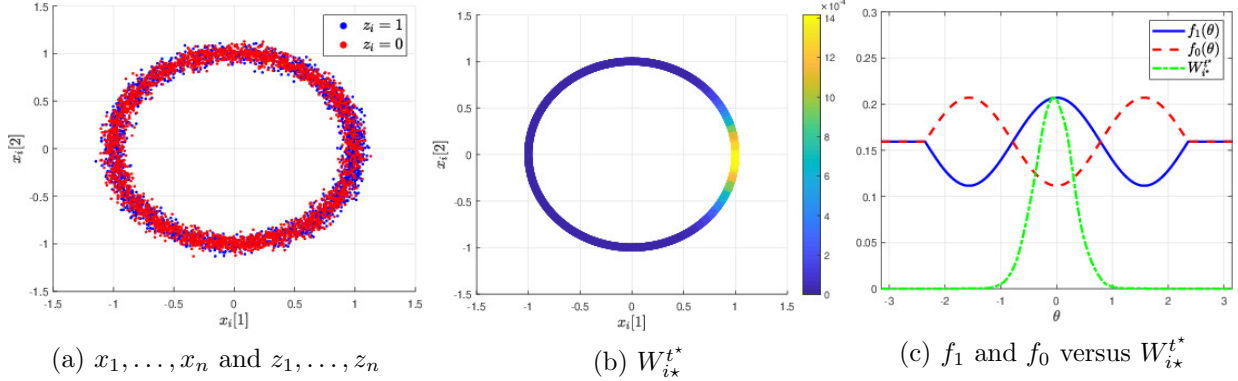


Figure 6: Figure (a) illustrates a typical array of points and labels sampled according to (51)–(53) (with noise added for visualization purposes), for $n = 5000$, $b = 0.3$, and $\omega = 2$. Figures (b) and (c) show the distribution W_{i*}^{t*} corresponding to the largest statistic $\mathcal{S}(W_{i*}^{t*})$ obtained from our method, using K from (54) with $\sigma = 0.01$, $\alpha = 0.05$, and $p = 0.5$.

The above condition can be written equivalently as a condition on b or on ω , according to

$$b \gtrsim \frac{h(\varepsilon) + \sqrt{0.5 \log(1/(1-\rho))}}{(8/\pi e)^{1/4} p(1-p) \sqrt{n/\omega}}, \quad \text{or} \quad \omega \lesssim \frac{nb^2 p^2 (1-p)^2 \sqrt{8/\pi e}}{(h(\varepsilon) + \sqrt{0.5 \log(1/(1-\rho))})^2}. \quad (59)$$

In Figure 7a we show the probability of rejecting H_0 , as estimated from 20 randomized trials over a grid of values of n and b , using $\alpha = 0.05$, $\varepsilon = 0.005$, and $\omega = 1$. In Figure 7a we also plot the curve corresponding to the condition on b in (59) for power at least $\rho = 0.9$. Analogously to Figure 7a, in Figure 7b we show the probability of rejecting H_0 over a grid of values of n and ω , using the same α , ε , and number of trials as for Figure 7a, while fixing $b = 0.5$. In Figure 7b we also plot the curve corresponding to the condition on ω in (59) for power at least $\rho = 0.9$. As expected, from Figures 7a and 7b we see that detecting $f_1(x) > f_0(x)$ locally becomes easier as b increases or ω decreases. Even for small values of b or large values of ω , detection of $f_1(x) > f_0(x)$ is eventually possible for sufficiently large n , since $\gamma \propto \sqrt{n} > \sqrt{\log n}$. It can be observed from both Figures 7a and 7b, that the theoretical curves corresponding to the conditions on b or ω in (59) agree very well with the simulation results.

6.2 Detection and localization of arsenic well contamination

To exemplify our method on a relatively simple low-dimensional real-world application, we analyzed arsenic concentration levels in 20,043 domestic wells across the conterminous United States, where the goal is to detect regions of significant arsenic contamination. Even though the underlying geographic data here is low-dimensional, the purpose of this example is to illustrate that our random walk based approach is able to adapt to the particular spatial arrangement of the wells, which is highly nonuniform, without the need to predefine shapes for scanning the whole geographic region, as in classical spatial scan statistics. We used data collected between 1973 and 2001, retrieved from the USGS National Water Information System [22]. We assigned a label of 1 to all wells with arsenic concentration exceeding the U.S. Environmental Protection Agency’s maximum allowed contamination level of $10\mu\text{g}/\text{L}$, which makes about 10% of all measured wells. Throughout this example, we set the significance level at $\alpha = 0.01$, and formed K from a symmetric 5-nearest-neighbour graph between the wells (using geographic location). That is, $K_{i,j} = K_{j,i} = 1$ if well x_i is

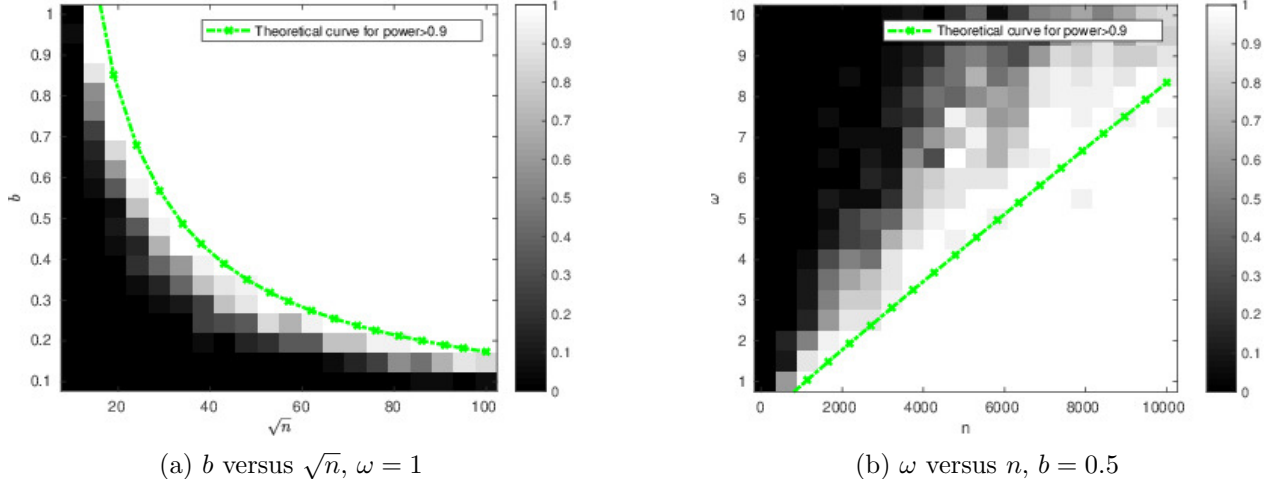


Figure 7: Empirical probability to accept H_1 from 20 trials, as a function of b , ω , and n , using $\alpha = 0.05$, $\varepsilon = 0.005$, and $\sigma = 0.01$. The green curve appearing in figure (a) corresponds to the condition on b from (59), while the green curve appearing in figure (b) corresponds to the condition on ω also from (59), where $\rho = 0.9$ (which is a lower bound on the power).

one of the 5 nearest wells to x_j (excluding itself) or vice versa, and $K_{i,j} = K_{j,i} = 0$ otherwise. This graph construction was chosen primarily due to its simplicity, and the number of nearest neighbours was chosen small so to make K sparse (and to consider only the immediate surroundings of each well). We remark that one may apply our testing methodology to several different graphs, and combine the results by correcting for multiple testing. We then formed W as described in Section 5, where we repeatedly removed the sparsest rows/columns of \tilde{W} until it could be diagonally-scaled (to be doubly stochastic). We ended up with 19,569 wells in 229 different connected components in the graph G (described by W). Most of the connected components were small (123 components with at most 20 wells), and 25 of them had at least 100 wells, where the largest connected component contained 3,730 wells. An upper bound on the prior p was found to be around 0.12 (using the Clopper-Pearson method, see step 6 in Algorithm 1).

Overall, Algorithm 1 yielded roughly 10^7 random-walk distributions that rejected the null, i.e., distributions $\mathbf{w} \in \tilde{\mathcal{F}}$ for which $\langle \mathbf{w}, \mathbf{s} \rangle > 0$ (with significance 0.01). These distributions correspond to random-walks that started at 2,262 different wells in 7 connected components (out of 229).

In Figure 8 we display the values of the random-walk distribution $W_i^{t_j^{(i)}}$ with the pair (i, j) that corresponds to the largest statistic $\mathcal{S}(W_i^{t_j^{(i)}})$ from the scan. It is notable that this distribution is quite spread-out, highlighting mainly two communities of wells in Nevada, but also other regions in Oregon, Idaho, and Washington. The distribution depicted in Figure 8 is associated with a walk time $t_j^{(i)} = 256$, and provides the lower bound $\langle W_i^{t_j^{(i)}}, \mathbf{s} \rangle > 0.26$ (computed from $\hat{\gamma}_{i,j} \|W_i^{t_j^{(i)}}\|_2$, see step 7 in Algorithm 1 and equation (7)). In Figure 9 we depict the distribution $W_i^{t_j^{(i)}}$ with the pair (i, j) that provides the largest lower bound on $\langle \mathbf{w}, \mathbf{s} \rangle$ among $\mathbf{w} \in \tilde{\mathcal{F}}$, which is $\langle W_i^{t_j^{(i)}}, \mathbf{s} \rangle > 0.4$ for $t_j^{(i)} = 24$. Recall that $\langle \mathbf{w}, \mathbf{s} \rangle \leq 1 - p \approx 0.9$ for any distribution \mathbf{w} , and hence a lower bound of 0.4 speaks of a substantial local difference between f_1 and f_0 . The distribution in Figure 9 is clearly much more localized than the distribution in Figure 8. Interestingly, this distribution takes its largest value in the city of Fallon, Nevada, which is known for its high arsenic concentration in

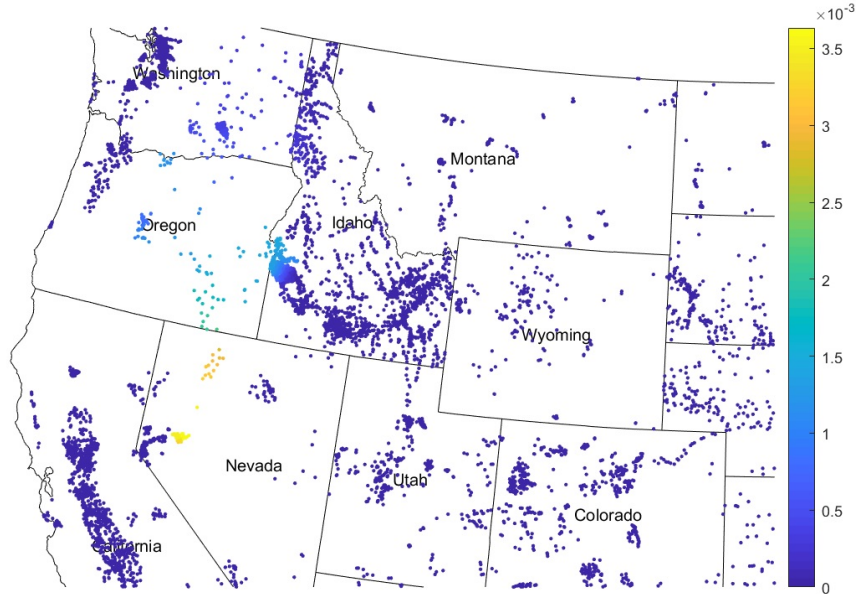


Figure 8: Values of the distribution $W_i^{t_j^{(i)}}$ for the pair (i, j) that corresponds to the largest statistic $\mathcal{S}(W_i^{t_j^{(i)}})$. This distribution is associated with the lower bound $\langle W_i^{t_j^{(i)}}, \mathbf{s} \rangle > \hat{\gamma}_{i,j} \|W_i^{t_j^{(i)}}\|_2 = 0.26$.

ground water, and has been the subject of several related studies [19, 55]. Our method can therefore be used to detect communities with significantly high arsenic contamination, allowing to further investigate the origins of the arsenic contamination or its effect on population health.

In Figure 10 we highlight all wells x_i for which $\langle W_i^t, \mathbf{s} \rangle > 0$ for at least one value of walk time $t \in \{t_j^{(i)}\}_{j=1}^{M_i}$. Notably, almost all such wells are located in the west, specifically in Arizona, Nevada, California, Oregon, Idaho, Washington, and Montana. This is largely consistent with specialized literature on the subject (see for example [20, 5]), which observed that most severe arsenic contaminations are found in the west of the USA. It is important to mention that the random-walk distributions corresponding to the locations depicted in Figure 10 can potentially be very spread-out (depending on the walk time that rejected the null), and may describe a region of the size of a state or even a few states. Furthermore, even if a distribution W_i^t rejected the null with high significance, the quantity $\langle W_i^t, \mathbf{s} \rangle$ could be very small, making the result less substantial. To complement the picture, in Figure 11 we highlight all wells x_i for which the scan found $\langle W_i^t, \mathbf{s} \rangle > 0.05$ for at least one value of walk time $t \in \{t_j^{(i)}\}_{j=1}^{M_i}$. Figure 11 highlights substantially less wells compared to Figure 10, and perhaps paints a more meaningful picture that is based on effect size rather than significance. To better understand the regions in which $f_1 > f_0$, it is important to explore the actual distributions W_i^t that rejected the null for each index i , possibly focusing on the ones that rejected the null with the smallest walk time, or the ones that provide the largest lower bounds on $\langle W_i^t, \mathbf{s} \rangle$.

6.3 Scientific discovery in single cell RNA sequencing data

In our third example, we applied our method to a published single cell RNA sequencing dataset of immune cells from melanoma patients [48]. Single-cell RNA sequencing (scRNA-seq) [57, 40], is an experimental procedure where large and heterogeneous samples of cells are characterized by their gene signatures. The gene signature of each cell, referred to as a gene expression profile, is a high-

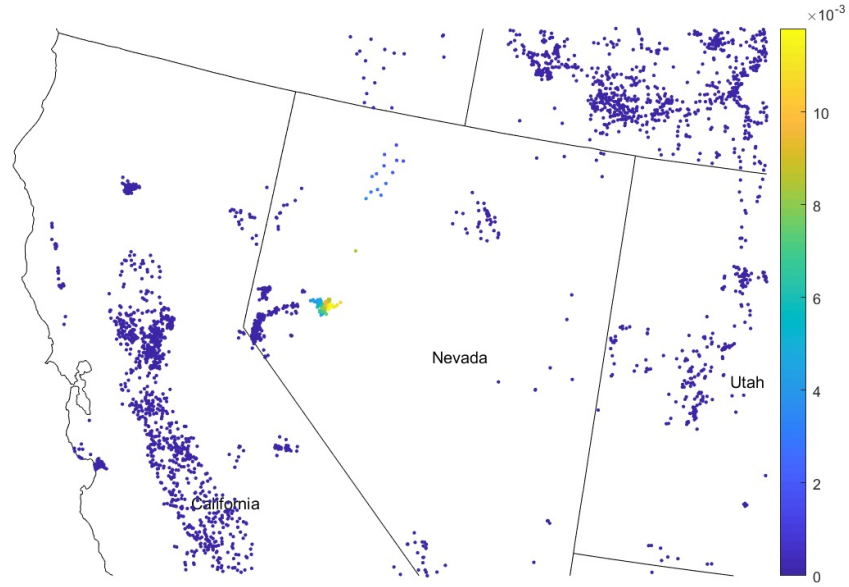


Figure 9: Values of the distribution $W_i^{t_j^{(i)}}$ for the pair (i, j) that corresponds to the largest lower bound $\langle W_i^{t_j^{(i)}}, \mathbf{s} \rangle > \hat{\gamma}_{i,j} \|W_i^{t_j^{(i)}}\|_2 = 0.4$. The largest values of $W_i^{t_j^{(i)}}$ are highly concentrated in the city of Fallon, Nevada.

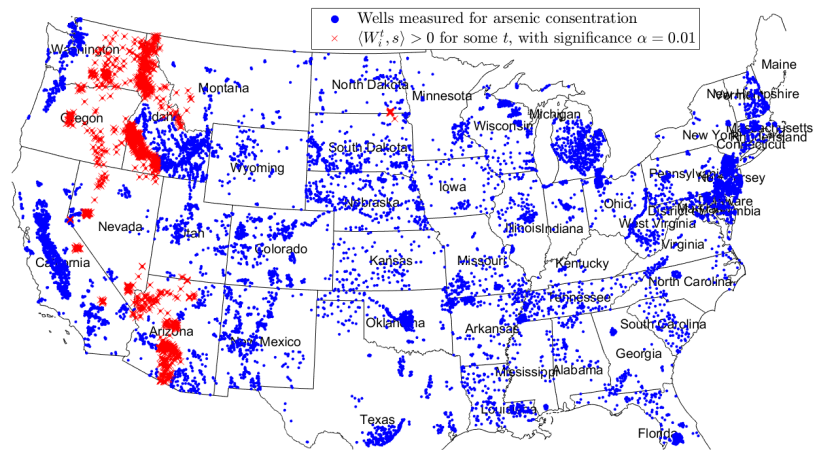


Figure 10: Wells x_i for which it was detected that $\langle W_i^t, \mathbf{s} \rangle > 0$ with significance $\alpha = 0.01$ for some walk time $t \in \{t_j^{(i)}\}_{j=1}^{M_i}$, versus all wells in which arsenic level was measured.

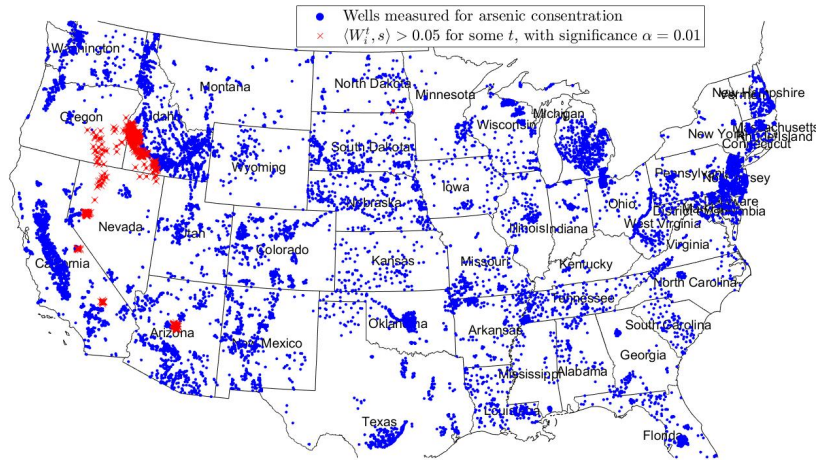


Figure 11: Wells x_i for which it was detected that $\langle W_i^t, s \rangle > 0.05$ with significance $\alpha = 0.01$ for some walk time $t \in \{t_j^{(i)}\}_{j=1}^{M_i}$, versus all wells in which arsenic level was measured.

dimensional vector in the gene feature-space. In many scRNA-seq experiments, cell populations from two distinct conditions/states are compared. For example, such cell populations can be sampled from a patient before or after treatment. A fundamental question then is whether there is a difference between the densities of the cell populations (in the gene signature space) before and after the treatment, and if so, in which cell sub-populations in particular [48]. Such cell sub-populations can be further investigated for unique functionality or characteristics, thereby providing novel scientific insights.

In the study carried out by Sade-Feldman et al. [48], they collected 16,291 cells from multiple melanoma patients that were treated with immunotherapy, where the expression levels of 55,737 genes were quantified for each cell. Therefore, the data is represented as matrix of size $55,737 \times 16,291$, whose (i, j) 'th entry represents the expression level of gene i in cell j . The authors of [48] identified 11 distinct cell-types in this data, which was based on whether specific genes of interest were highly expressed. In addition, the patients that showed positive response to the therapy in the post-treatment assessment were labelled as *responders*, while the others were labelled as *non-responders*. Thus, the cells from all patients were pooled into two sets - a set of cells from all responders (5,564 cells in total) with each one labelled as “R”, and a set of cells from all non-responders (10,727 cells in total), with each one labelled as “NR”.

We downloaded the preprocessed data matrix from the NCBI Gene Expression Omnibus [6] and used the R package Seurat [56] to process the data. Following the preprocessing pipeline described in [48], we generated a low-rank representation of the data (a matrix of size $30 \times 16,291$). In Figure 12 we visualize the resulting representation of the cells using UMAP [45], which is a popular dimensionality reduction technique for scRNA-seq data [7, 15], and color the cells according to their labels (Figure 12a) and types (Figure 12b). For simplicity, we retained the same notation for the cell types as in [48] by indexing 11 cell types from G1 to G11. Sade-Feldman et al. [48] examined for which cell type there is a significant discrepancy between the frequencies of “R” cells and “NR” cells. They found two cell types (G1, G10) in which the frequency of “R” cells is larger than of

“NR” cells. Additionally, they found four cell types (G3, G4, G6, G11) in which the frequency of “NR” cells is larger than of “R” cells. Evidently, in the approach by [48], the comparison between the densities of “R” and “NR” cells is conducted only at the cell type level. Distinctly, our goal here is to identify specific regions within the cell types where the density of the “R” cells is significantly larger than of the “NR” cells, or vice versa.

Based on the low-rank representation of the data as described above, we first calculated pairwise Euclidean distance among all cells and then formed the affinity matrix K based on the Gaussian kernel (see equation (54)), selecting the bandwidth σ to be equal to the 0.01% quantile of the distribution of all pairwise distances. The main diagonal of K was zeroed out (as suggested in [38] for improved robustness to heteroskedastic noise) and W was constructed as described in Section 5.

We initially set out to find neighborhoods of the sample where the density of “NR” cells is larger than that of “R” cells. Towards that end, we labelled the “NR” cells by 1, i.e., $z_i = 1$ for the “NR” cells and $z_i = 0$ for the “R” cells. Then we applied Algorithm 1 to the matrix W and the labels z_1, \dots, z_n , setting the significance level at $\alpha = 0.01$. An upper bound on the prior p was estimated to be around 0.67 using the Clopper-Pearson method (see step 6 in Algorithm 1). Finally, we found 328,260 distributions that rejected the null hypothesis, which were generated by random-walks starting from 6,261 cells. We labelled the 4,553 cells that satisfy $\langle W_i^t, \mathbf{s} \rangle > 0.05$ for at least one value of walk time $t \in \{t_j^{(i)}\}_{j=1}^{M_i}$ as “NR-enriched”.

Next, we turned to find neighborhoods of the sample where the density of “R” cells is larger than that of the “NR”. Towards that end, we repeated the same procedure as before but assigned labels of 1 to the “R” cells, i.e., $z_i = 1$ for the “R” cells and $z_i = 0$ for the “NR” cells. This resulted in 85,240 distributions corresponding to 5,986 cells passing the test (with an upper bound on the prior p around 0.35). Similarly, we labelled the 3,390 cells with $\langle W_i^t, \mathbf{s} \rangle > 0.05$ for at least one value of walk time $t \in \{t_j^{(i)}\}_{j=1}^{M_i}$ as “R-enriched”. The two groups of cells “R-enriched” and “NR-enriched” are highlighted in Figure 13.

Interestingly, within each of the four cell types G3, G4, G6, G11 that were found in [48] to have larger frequency of “NR” cells, our method also detected a corresponding subset of “NR-enriched” cells. Furthermore, the detected “NR-enriched” cells form contiguous structures within the original cell types, perhaps indicative of special cell sub-types. In addition, we also identified roughly 24.42% of the G9 cells (Exhausted/HS CD8+ T-cells) as “NR-enriched”, whereas G9 was not reported to have a significant difference in frequencies of “R” and “NR” cells in [48]. This new finding suggests that a subset of the G9 cells is more likely to be found in non-responders (i.e., patients who failed to respond to immunotherapy), and reveals the advantage of our approach over those that are based on predefined cell types.

7 Acknowledgements

We would like to thank Stefan Steinerberger, Ronald Coifman, Boaz Nadler, Vladimir Rokhlin, Sahand Negahban, and Dan Kluger for useful discussions and suggestions. This work was supported by the National Institutes of Health [R01GM131642, UM1DA051410, P50CA121974 and R61DA047037].

Appendix A Implementation details and computational complexity

We now discuss the implementation of the different steps of Algorithm 1, and analyze their computational complexities. We begin with step 1. Evaluating \tilde{K} directly according to (48) requires

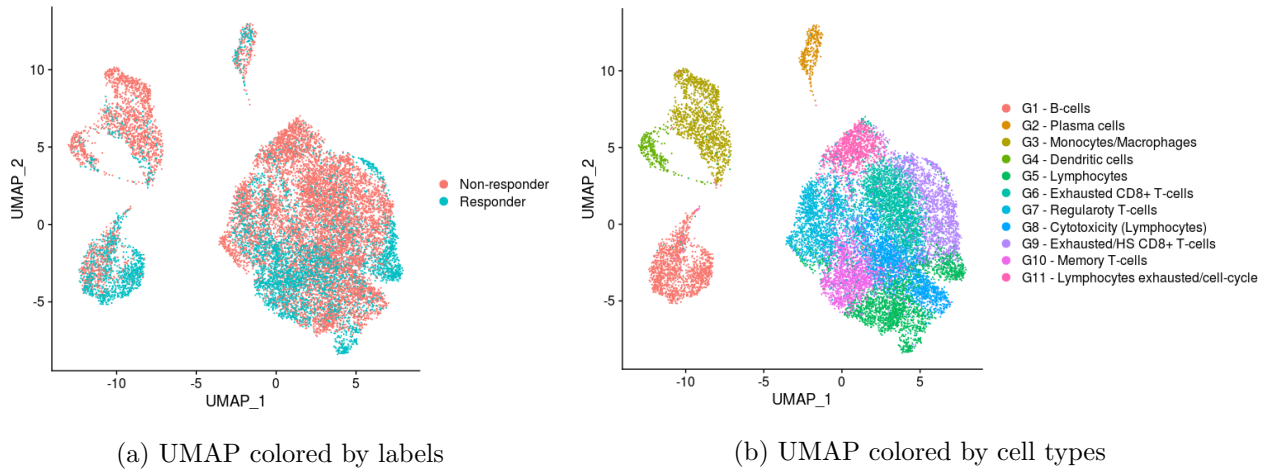


Figure 12: UMAP embedding of cells. Cells are colored according to their labels of “R” (responders to immunotherapy) or “NR” (non-responders to immunotherapy), and by the pre-annotated cell types from [48]

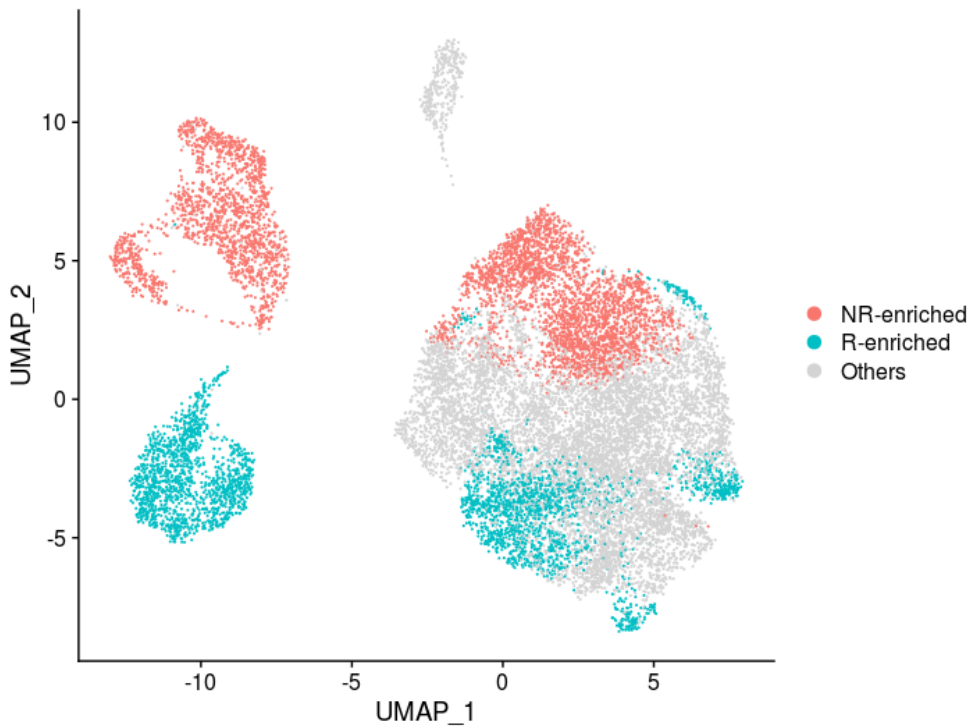


Figure 13: Cells x_i for which it was detected that $\langle W_i^t, \mathbf{s} \rangle > 0.05$ for at least one value of walk time $t \in \{t_j^{(i)}\}_{j=1}^{M_i}$ using significance level $\alpha = 0.01$. Red points are labelled as “NR-enriched”, and correspond to the setting where $z_i = 1$ for “NR” cells, and $z_i = 0$ for “R” cells. On the other hand, blue points are labeled as “R-enriched”, and correspond to the setting where $z_i = 1$ for “R” cells, and $z_i = 0$ for “NR” cells.

$\mathcal{O}(n^2)$ operations. Computing \widetilde{W} using the Sinkhorn-Knopp algorithm [54] costs $\mathcal{O}(n^2)$ operations for each iteration, and requires $\mathcal{O}(1/\log(\lambda_{<1}^{-1}))$ iterations if \widetilde{K} is fully indecomposable [33]. Hence, the overall computational complexity of evaluating \widetilde{W} is $\mathcal{O}(n^2/\log(\lambda_{<1}^{-1})) = \mathcal{O}(n^2/(1-\lambda_{<1}))$. Then, computing W according to (50) by direct squaring requires $\mathcal{O}(n^3)$ operations. Next, in step 2, the connected components of W can be obtained using standard Breadth-first or Depth-first searches (BFS or DFS), with computational complexity of $\mathcal{O}(n^2)$. The computational complexity of computing the eigen-decompositions of $\{W^{(\ell)}\}_{\ell=1}^L$ in step 3 is $\sum_{\ell=1}^L \mathcal{O}(n_\ell^3) = \mathcal{O}(n^3)$. Continuing, the minimization of (42) in step 4 can be approximated by a grid search over $\varepsilon \in (0, 1)$, with a resulting computational complexity of $\mathcal{O}(1)$ (since this minimization is independent of n).

We proceed by analyzing the computational complexity of Algorithm 2 (appearing in step 5 of Algorithm 1). Using the orthogonality of the eigenvectors of W , we can write

$$\|W_i^t\|_2^2 = \sum_{k=1}^{n_\ell} (\lambda_k^{(\ell)})^{2t} (\psi_k^{(\ell)}[i])^2, \quad (60)$$

which costs $\mathcal{O}(n_\ell)$ operations to compute for each $i \in \mathcal{C}_\ell$ and t (given the eigen-decomposition of $W^{(\ell)}$). Since $\|W_i^t\|_2^2$ is monotonically decreasing in t (see Proposition 3), step 4 in Algorithm 2 can be implemented using the bisection method. Therefore, step 4 in Algorithm 2 require $\mathcal{O}(n_\ell \log(T_\ell))$ operations (using the fact that $t_j^{(i)} \leq T_\ell$). Since the inner while loop in Algorithm 2 runs for $M_i - 1$ iterations, the computational complexity of Algorithm 2 is

$$\mathcal{O} \left(\sum_{\ell=1}^L \sum_{i \in \mathcal{C}_\ell} M_i n_\ell \log(T_\ell) \right) = \mathcal{O} \left(n^2 \cdot \max_{i=1, \dots, n} M_i \cdot \max_{\ell=1, \dots, L} \log(T_\ell) \right), \quad (61)$$

where we used the fact that $\sum_{\ell=1}^L n_\ell = n$. Therefore, if $\lambda_{<1}$ is bounded away from 1 as $n \rightarrow \infty$, then the computational complexity of Algorithm 2 is essentially $\mathcal{O}(n^2 \cdot \log n \cdot \log \log n)$, which is smaller than $\mathcal{O}(n^3)$. Otherwise, the computational complexity of Algorithm 2 depends on the convergence rate of $\lambda_{<1}$ to 1, and can be determined on a case-by-case basis using Lemma 7. If we assume that $1 - \lambda_{<1} \underset{n \rightarrow \infty}{\sim} n^{-r}$ for some $r > 0$, then the computational complexity of Algorithm 2 is $\mathcal{O}(n^3 \cdot (\log n)^2)$. Next, step 6 in Algorithm 1 requires $\mathcal{O}(n)$ operations to compute $\sum_{i=1}^n z_i$, and $\mathcal{O}(1)$ operations for the Clopper-Pearson method.

Last, we put our focus on analyzing the computational complexity of step 7 of Algorithm 1. The computationally-dominant part of this step is evaluating

$$\frac{\langle W_i^{t_j^{(i)}}, \mathbf{z} - p \rangle}{\|W_i^{t_j^{(i)}}\|_2}, \quad (62)$$

for all $i = 1, \dots, n$ and $j = 1, \dots, M_i$. Note that Algorithm 2 already evaluates the quantities $\|W_i^{t_j^{(i)}}\|_2$ for all i and j (using (60)), hence we only need to compute the numerator of (62). Similarly to the computation of $\|W_i^{t_j^{(i)}}\|_2$ in (60), this can be accomplished efficiently using the eigen-decomposition of W , as we can write

$$\langle W_i^{t_j^{(i)}}, \mathbf{z} - p \rangle = \sum_{k=1}^{n_\ell} \psi_k^{(\ell)}[i] (\lambda_k^{(\ell)})^{t_j^{(i)}} \langle \psi_k^{(\ell)}, \mathbf{z} - p \rangle, \quad (63)$$

for any $i \in \mathcal{C}_\ell$ and $j \in \{1, \dots, M_i\}$. Consequently, we first compute $\langle \psi_k^{(\ell)}, \mathbf{z} - p \rangle$ for all $k = 1, \dots, n_\ell$ and $\ell = 1, \dots, L$, which requires $\mathcal{O}(\sum_{\ell=1}^L n_\ell^2) = \mathcal{O}(n^2)$ operations. Then, we compute

$\{(W_i^{t_j^{(i)}}), \mathbf{z} - p)\}_{j=1}^{M_i}$ using (63), which requires $\mathcal{O}(n_\ell M_i)$ operations for each $i \in \mathcal{C}_\ell$. Overall, the computational complexity of step 6 in Algorithm 1 is therefore

$$\mathcal{O}(n^2) + \mathcal{O}\left(\sum_{\ell=1}^L \sum_{i \in \mathcal{C}_\ell} n_\ell M_i\right) = \mathcal{O}(n^2 \cdot \max_{i=1, \dots, n} M_i), \quad (64)$$

which is clearly lesser than the computational complexity of step 5, given by (61).

Overall, if $1 - \lambda_{<1} = \mathcal{O}(1/n)$ then the computational complexity of Algorithm 1 is dominated by the Sinkhorn-Knopp algorithm for computing \widetilde{W} , which is $\mathcal{O}(n^2/(1 - \lambda_{<1}))$. Otherwise, the computational complexity of Algorithm 1 is dominated by Algorithm 2, whose computational complexity in this case is at most $\mathcal{O}(n^3(\log n)^2)$. Therefore, the computational complexity of Algorithm 1 is $\mathcal{O}(n^3(\log n)^2)$ if $1 - \lambda_{<1} = \Omega(1/n)$.

Appendix B Tables for ε and $\hat{h}_{n, \alpha, \lambda_{<1}}(\varepsilon)$

α	n	$1 - \lambda_{<1}$								
		0.1	0.01	10^{-3}	10^{-4}	10^{-5}	10^{-6}	10^{-9}	10^{-12}	10^{-16}
0.1	10^3	2.647	2.860	3.056	3.239	3.413	3.455	3.455	3.455	3.455
	10^4	2.872	3.070	3.253	3.425	3.590	3.747	3.806	3.806	3.806
	10^5	3.078	3.264	3.436	3.600	3.757	3.907	4.121	4.121	4.121
	10^6	3.270	3.445	3.609	3.765	3.915	4.059	4.409	4.409	4.409
0.01	10^3	2.856	3.056	3.239	3.413	3.578	3.625	3.625	3.625	3.625
	10^4	3.066	3.252	3.425	3.590	3.747	3.898	3.959	3.959	3.959
	10^5	3.260	3.436	3.600	3.757	3.907	4.052	4.262	4.262	4.262
	10^6	3.442	3.608	3.765	3.915	4.059	4.199	4.541	4.541	4.541
10^{-3}	10^3	3.052	3.239	3.413	3.578	3.735	3.786	3.786	3.786	3.786
	10^4	3.249	3.425	3.590	3.747	3.898	4.043	4.107	4.107	4.107
	10^5	3.432	3.600	3.757	3.907	4.052	4.192	4.399	4.399	4.399
	10^6	3.605	3.765	3.915	4.059	4.199	4.334	4.670	4.670	4.670

Table 1: Values of $\min_\varepsilon \hat{h}_{n, \alpha, \lambda_{<1}}(\varepsilon)$ (recall that $\hat{h}_{n, \alpha, \lambda_{<1}}(\varepsilon) \geq h(\varepsilon)$), where $\hat{h}_{n, \alpha, \lambda_{<1}}(\varepsilon)$ is from (42).

α	\mathbf{n}	$1 - \lambda_{<1}$								
		0.1	0.01	10^{-3}	10^{-4}	10^{-5}	10^{-6}	10^{-9}	10^{-12}	10^{-16}
0.1	10^3	0.0083	0.0073	0.0069	0.0065	0.0061	0.1514	0.1514	0.1514	0.1514
	10^4	0.0060	0.0056	0.0053	0.0051	0.0048	0.0046	0.1362	0.1362	0.1362
	10^5	0.0048	0.0045	0.0043	0.0041	0.0039	0.0038	0.1252	0.1252	0.1252
	10^6	0.0038	0.0037	0.0036	0.0034	0.0033	0.0032	0.1165	0.1165	0.1165
0.01	10^3	0.0075	0.0067	0.0065	0.0061	0.0058	0.1437	0.1437	0.1437	0.1437
	10^4	0.0054	0.0053	0.0052	0.0048	0.0046	0.0044	0.1306	0.1306	0.1306
	10^5	0.0043	0.0043	0.0041	0.0039	0.0038	0.0036	0.1207	0.1207	0.1207
	10^6	0.0038	0.0036	0.0034	0.0033	0.0032	0.0030	0.1129	0.1129	0.1129
10^{-3}	10^3	0.0068	0.0067	0.0061	0.0058	0.0055	0.1370	0.1370	0.1370	0.1370
	10^4	0.0054	0.0050	0.0048	0.0046	0.0044	0.0042	0.1256	0.1256	0.1256
	10^5	0.0043	0.0041	0.0039	0.0038	0.0036	0.0035	0.1168	0.1168	0.1168
	10^6	0.0034	0.0033	0.0032	0.0032	0.0030	0.0029	0.1097	0.1097	0.1097

Table 2: Values of ε that minimize $\hat{h}_{n,\alpha,\lambda_{<1}}(\varepsilon)$ from (42).

Appendix C Proof of Lemma 1

First, we note that $Q_{\mathbf{z}} = 1$ if and only if $\hat{\mathcal{G}}_{\mathbf{z}} \cap \mathcal{F} \neq \emptyset$. Therefore, we can write

$$\sup_{f_1, f_0 \in H_0} \Pr\{Q_{\mathbf{z}} = 1 \mid f_0, f_1\} = \sup_{f_1, f_0 \in H_0(\mathcal{F})} \Pr\{\hat{\mathcal{G}}_{\mathbf{z}} \cap \mathcal{F} \neq \emptyset \mid f_0, f_1\} \leq \sup_{\mathcal{G} \subseteq \mathcal{F}} \sup_{f_1, f_0 \in H_0(\mathcal{G})} \Pr\{\hat{\mathcal{G}}_{\mathbf{z}} \cap \mathcal{G} \neq \emptyset \mid f_0, f_1\}. \quad (65)$$

Second, recall that by definition $\inf_{\hat{\mathbf{w}} \in \hat{\mathcal{G}}_{\mathbf{z}}} \mathcal{E}_{\text{TV}}(\hat{\mathbf{w}}, \mathbf{w}) = 1$ if $\hat{\mathcal{G}}_{\mathbf{z}}$ is an empty set, which holds if $Q_{\mathbf{z}} = 0$. Hence,

$$\begin{aligned} \sup_{\mathbf{w} \in \mathcal{F}} \sup_{f_1, f_0 \in H_1(\mathbf{w}, \gamma)} \mathbb{E}[\inf_{\hat{\mathbf{w}} \in \hat{\mathcal{G}}_{\mathbf{z}}} \mathcal{E}_{\text{TV}}(\hat{\mathbf{w}}, \mathbf{w}) \mid f_0, f_1] &\geq \sup_{\mathbf{w} \in \mathcal{F}} \sup_{f_1, f_0 \in H_1(\mathbf{w}, \gamma)} \Pr\{\inf_{\hat{\mathbf{w}} \in \hat{\mathcal{G}}_{\mathbf{z}}} \mathcal{E}_{\text{TV}}(\hat{\mathbf{w}}, \mathbf{w}) = 1 \mid f_0, f_1\} \cdot 1 \\ &\geq \sup_{\mathbf{w} \in \mathcal{F}} \sup_{f_1, f_0 \in H_1(\mathbf{w}, \gamma)} \Pr\{Q_{\mathbf{z}} = 0 \mid f_0, f_1\}. \end{aligned} \quad (66)$$

Appendix D Proof of Proposition 3

We start with the eigen-decomposition of W^t , which is given by

$$W_{i,j}^t = \sum_{k=1}^{n_\ell} \psi_k^{(\ell)}[i] (\lambda_k^{(\ell)})^t \psi_k^{(\ell)}[j], \quad (67)$$

and using the orthonormality of the eigenvectors of W we have

$$\|W_i^t\|_2^2 = \sum_{k=1}^{n_\ell} (\psi_k^{(\ell)}[i])^2 (\lambda_k^{(\ell)})^{2t}. \quad (68)$$

Property 1 in Proposition 3 follows directly from (68), which is monotonically decreasing in t since $0 \leq \lambda_k^{(\ell)} \leq 1$ for all k and ℓ . To prove property 2, we use (67), the orthonormality of the eigenvectors,

and fact that $(\lambda_k^{(\ell)})^t \geq (\lambda_k^{(\ell)})^\tau$ for $t \leq \tau$, which gives

$$\begin{aligned} \|W_i^t - W_i^\tau\|_2^2 &= \sum_{k=1}^{n_\ell} (\psi_k^{(\ell)}[i])^2 \left((\lambda_k^{(\ell)})^t - (\lambda_k^{(\ell)})^\tau \right)^2 = \sum_{k=1}^{n_\ell} (\psi_k^{(\ell)}[i])^2 \left((\lambda_k^{(\ell)})^{2t} + (\lambda_k^{(\ell)})^{2\tau} - 2(\lambda_k^{(\ell)})^t (\lambda_k^{(\ell)})^\tau \right) \\ &\leq \sum_{k=1}^{n_\ell} (\psi_k^{(\ell)}[i])^2 \left((\lambda_k^{(\ell)})^{2t} - (\lambda_k^{(\ell)})^{2\tau} \right) = \|W_i^t\|_2^2 - \|W_i^\tau\|_2^2 \leq \|W_i^t\|_2^2 - \|W_i^{\tau'}\|_2^2, \end{aligned} \quad (69)$$

where we also used property 1 from Proposition 3 in the last inequality. The first part of property 3 follows immediately from the eigen-decomposition of W^t and property 2 from Proposition 2. To prove the second part of property 3, we use (68) and Proposition 2 to write

$$\begin{aligned} \frac{1}{n_\ell} &= (\psi_1^{(\ell)}[i])^2 = (\psi_1^{(\ell)}[i])^2 (\lambda_1^{(\ell)})^{2t} \leq \sum_{k=1}^{n_\ell} (\psi_k^{(\ell)}[i])^2 (\lambda_k^{(\ell)})^{2t} \leq (\psi_1^{(\ell)}[i])^2 (\lambda_1^{(\ell)})^{2t} + (\lambda_2^{(\ell)})^{2t} \sum_{k=2}^{n_\ell} (\psi_k^{(\ell)}[i])^2 \\ &\leq \frac{1}{n_\ell} + (\lambda_2^{(\ell)})^{2t}. \end{aligned} \quad (70)$$

Appendix E Proof of Lemma 4

Proof. We first state Hoeffding's inequality for sums of bounded and independent random variables.

Theorem 13 (Hoeffding [28]). *Let u_1, \dots, u_n be independent random variables satisfying $u_i \in [a_i, b_i]$. Then,*

$$\Pr \left\{ \sum_{i=1}^n u_i - \mathbb{E} \left[\sum_{i=1}^n u_i \right] > t \right\} \leq \exp \left(-\frac{2t^2}{\sum_{i=1}^n (b_i - a_i)^2} \right), \quad (71)$$

$$\Pr \left\{ \sum_{i=1}^n u_i - \mathbb{E} \left[\sum_{i=1}^n u_i \right] < -t \right\} \leq \exp \left(-\frac{2t^2}{\sum_{i=1}^n (b_i - a_i)^2} \right). \quad (72)$$

Assuming all quantities are conditioned on x_1, \dots, x_n , using (21) we have

$$\mathbb{E} \left[\sum_{i=1}^n w_i y_i \right] = \sum_{i=1}^n w_i \mathbb{E}[y_i] = \sum_{i=1}^n w_i s_i. \quad (73)$$

Defining $u_i = w_i y_i$, we have that $u_i \in [-pw_i, (1-p)w_i]$, and Hoeffding's inequality asserts that

$$\Pr \left\{ \sum_{i=1}^n w_i y_i - \sum_{i=1}^n w_i s_i > t \right\} = \Pr \left\{ \sum_{i=1}^n w_i y_i - \mathbb{E} \left[\sum_{i=1}^n w_i y_i \right] > t \right\} \leq \exp \left(-\frac{2t^2}{\sum_{i=1}^n w_i^2} \right). \quad (74)$$

Taking $t = \|\mathbf{w}\|_2 \sqrt{0.5 \log(1/\alpha)}$ gives

$$\Pr \left\{ \sum_{i=1}^n w_i y_i - \sum_{i=1}^n w_i s_i > \|\mathbf{w}\|_2 \sqrt{0.5 \log(1/\alpha)} \right\} \leq \alpha, \quad (75)$$

which establishes (22). The proof of (23) is analogous to the proof of (22) when using (72) instead of (71), and we omit it for the sake of brevity. \square

Appendix F Proof of Lemma 5

F.1 Proof of (34)

According to the definition of T_ℓ from (25), and applying property 3 in Proposition 3, we have

$$\|W_i^{T_\ell}\|_2^2 \leq \frac{1}{n_\ell} + (\lambda_2^{(\ell)})^{2T_\ell} \leq \frac{1}{n_\ell} + \exp\left(\log(\lambda_2^{(\ell)}) \frac{2 \log(n_\ell/\varepsilon)}{\log((\lambda_2^{(\ell)})^{-1})}\right) = \frac{1}{n_\ell} + \frac{\varepsilon^2}{n_\ell^2}. \quad (76)$$

Consequently, by properties 2 and 3 in Proposition 3, we have for all $i \in \mathcal{C}_\ell$ and $t \geq T_\ell$

$$\mathcal{E}_{\text{TV}}(W_i^t, W_i^{\pi(t)}) = \frac{1}{2} \|W_i^t - W_i^{T_\ell}\|_1 \leq \frac{\sqrt{n_\ell}}{2} \|W_i^t - W_i^{T_\ell}\|_2 \leq \frac{1}{2} \sqrt{n_\ell \left(\|W_i^{T_\ell}\|_2^2 - \|W_i^t\|_2^2 \right)} \leq \frac{\varepsilon}{2\sqrt{n_\ell}} \leq \frac{\varepsilon \|W_i^t\|_2}{2}, \quad (77)$$

where we used (76) and the fact that $\|W_i^t\|_2^2 \geq 1/n_\ell$ for $i \in \mathcal{C}_\ell$ in the last two inequalities. Last, if $t_{j-1}^{(i)} < t \leq t_j^{(i)} < T_\ell$ for some j and ℓ , then according to (26) and properties 2 and 3 in Proposition 3, we can write

$$\begin{aligned} \mathcal{E}_{\text{TV}}(W_i^t, W_i^{\pi(t)}) &= \frac{1}{2} \|W_i^t - W_i^{t_j^{(i)}}\|_1 \leq \frac{\sqrt{n_\ell}}{2} \|W_i^t - W_i^{t_{j+1}^{(i)}}\|_2 \leq \frac{1}{2} \sqrt{n_\ell \left(\|W_i^{t_{j-1}^{(i)}+1}\|_2^2 - \|W_i^{t_j^{(i)}}\|_2^2 \right)} \\ &\leq \frac{\varepsilon}{2} \|W_i^{t_j^{(i)}}\|_2 \leq \frac{\varepsilon}{2} \|W_i^t\|_2. \end{aligned} \quad (78)$$

F.2 Proof of (33)

Recall that for $i \in \mathcal{C}_\ell$ we have $W_{i,j}^t = 0$ for all $j \notin \mathcal{C}_\ell$ and positive integers t (see Proposition 3). Therefore, using the fact that $-1 \leq 1-p \leq y_i \leq p \leq 1$ together with the Cauchy-Shwarz inequality, we can write

$$\begin{aligned} \left| \mathcal{S}(W_i^t) - \mathcal{S}(W_i^{\pi(t)}) \right| &= \left| \frac{\langle W_i^t, \mathbf{y} \rangle}{\|W_i^t\|_2} - \frac{\langle W_i^{\pi(t)}, \mathbf{y} \rangle}{\|W_i^{\pi(t)}\|_2} \right| = \left| \left\langle \frac{W_i^t}{\|W_i^t\|_2} - \frac{W_i^{\pi(t)}}{\|W_i^{\pi(t)}\|_2}, \mathbf{y} \right\rangle \right| \\ &= \left| \left\langle \frac{W_i^t}{\|W_i^t\|_2} - \frac{W_i^{\pi(t)}}{\|W_i^{\pi(t)}\|_2}, \mathbb{1}_{\mathcal{C}_\ell} \odot \mathbf{y} \right\rangle \right| \leq \left\| \frac{W_i^t}{\|W_i^t\|_2} - \frac{W_i^{\pi(t)}}{\|W_i^{\pi(t)}\|_2} \right\|_2 \|\mathbb{1}_{\mathcal{C}_\ell} \odot \mathbf{y}\|_2 \leq \sqrt{n_\ell} \left\| \frac{W_i^t}{\|W_i^t\|_2} - \frac{W_i^{\pi(t)}}{\|W_i^{\pi(t)}\|_2} \right\|_2, \end{aligned} \quad (79)$$

where $\mathbb{1}_{\mathcal{C}_\ell}$ is the indicator vector on \mathcal{C}_ℓ , and \odot is the Hadamard (element-wise) product.

Next, we establish the following lemma.

Lemma 14. *Let $u, v \in \mathbb{R}^n$ be such that $\|u\|_2 = 1$ and $\|v\|_2 \geq 1$. Then,*

$$\left\| u - \frac{v}{\|v\|_2} \right\|_2 \leq \|u - v\|_2. \quad (80)$$

Proof. Define $v_p = v/\|v\|_2$, and $v_\perp = av$ where a is the scalar that minimizes $\|u - av\|_2$. That is, v_\perp is the projection of u onto v , and hence $\langle v_\perp, u - v_\perp \rangle = 0$. In particular, we have that $a = \langle u, v \rangle / \|v\|_2^2$. Overall, we have that $\|v\|_2 \geq 1$, $\|v_p\|_2 = 1$, and $\|v_\perp\|_2 \leq 1$, where the last inequality is due to

$$\|v_\perp\|_2 = \frac{|\langle u, v \rangle| \|v\|_2}{\|v\|_2^2} = \frac{|\langle u, v \rangle|}{\|v\|_2} \leq \frac{\|u\|_2 \|v\|_2}{\|v\|_2} = 1, \quad (81)$$

using the Cauchy-Schwarz inequality and the fact that $\|u\|_2 = 1$. Since v, v_p, v_\perp are just different scalings of v , it follows that $\|v - v_\perp\|_2 \geq \|v_p - v_\perp\|_2$. Therefore, we can write

$$\|u - v_p\|_2^2 = \|u - v_\perp\|_2^2 + \|v_\perp - v_p\|_2^2 \leq \|u - v_\perp\|_2^2 + \|v - v_\perp\|_2^2 = \|u - v\|_2^2, \quad (82)$$

where we used the fact $\langle u - v_\perp, v \rangle = 0$ (and thus also $\langle u - v_\perp, v_\perp - v_p \rangle = \langle u - v_\perp, v - v_\perp \rangle = 0$). \square

The following is a corollary of Lemma 14 which is useful for our purposes.

Corollary 15. *Let $u, v \in \mathbb{R}^n$. Then*

$$\left\| \frac{u}{\|u\|_2} - \frac{v}{\|v\|_2} \right\|_2 \leq \frac{\|u - v\|_2}{\min\{\|u\|_2, \|v\|_2\}}. \quad (83)$$

Proof. If $\|u\|_2 \leq \|v\|_2$ we define $\tilde{u} = u/\|u\|_2$, $\tilde{v} = v/\|u\|_2$. Then we have $\|\tilde{u}\|_2 = 1$ and $\|\tilde{v}\|_2 \geq 1$, and by Lemma 14

$$\left\| \frac{u}{\|u\|_2} - \frac{v}{\|v\|_2} \right\|_2 = \left\| \tilde{u} - \frac{\tilde{v}}{\|\tilde{v}\|_2} \right\|_2 \leq \|\tilde{u} - \tilde{v}\|_2 = \frac{\|u - v\|_2}{\|u\|_2}. \quad (84)$$

If on the other hand $\|u\|_2 \geq \|v\|_2$, we define $\tilde{u} = v/\|v\|_2$, $\tilde{v} = u/\|v\|_2$, and the proof follows from applying Lemma 14 as in (84). \square

Now, let us write

$$\begin{aligned} & \max_{1 \leq i \leq n} \sup_{t=1, \dots, \infty} \left\| \frac{W_i^t}{\|W_i^t\|_2} - \frac{W_i^{\pi(t)}}{\|W_i^{\pi(t)}\|_2} \right\|_2 \\ &= \max_{1 \leq i \leq n} \max \left\{ \max_{1 \leq t \leq t_{M_i}^{(i)}} \left\| \frac{W_i^t}{\|W_i^t\|_2} - \frac{W_i^{\pi(t)}}{\|W_i^{\pi(t)}\|_2} \right\|_2, \sup_{t > t_{M_i}^{(i)}} \left\| \frac{W_i^t}{\|W_i^t\|_2} - \frac{W_i^{\pi(t)}}{\|W_i^{\pi(t)}\|_2} \right\|_2 \right\}. \end{aligned} \quad (85)$$

Since $\|W_i^t\|_2 \leq \|W_i^{t_{M_i}^{(i)}}\|_2$ for all $t > t_{M_i}^{(i)} = T_\ell$ (by Proposition 3 property 1), using Corollary 15 we have

$$\begin{aligned} & \sup_{t > t_{M_i}^{(i)}} \left\| \frac{W_i^t}{\|W_i^t\|_2} - \frac{W_i^{\pi(t)}}{\|W_i^{\pi(t)}\|_2} \right\|_2 = \sup_{t > T_\ell} \left\| \frac{W_i^t}{\|W_i^t\|_2} - \frac{W_i^{T_\ell}}{\|W_i^{T_\ell}\|_2} \right\|_2 \leq \sup_{t > T_\ell} \frac{\|W_i^t - W_i^{T_\ell}\|_2}{\|W_i^t\|_2} \\ & \leq \sup_{t > T_\ell} \sqrt{n_\ell} \|W_i^t - W_i^{T_\ell}\|_2 \leq \sup_{t > T_\ell} \sqrt{n_\ell \left(\|W_i^{T_\ell}\|_2^2 - \|W_i^t\|_2^2 \right)} \leq \frac{\varepsilon}{\sqrt{n_\ell}}, \end{aligned} \quad (86)$$

where we also used (32), property 3 in Proposition 3, and (77).

Next, if $M_i > 1$, using the fact that $t_1^{(i)} = 1$ and (32), we have

$$\begin{aligned} & \max_{1 \leq t \leq t_{M_i}^{(i)}} \left\| \frac{W_i^t}{\|W_i^t\|_2} - \frac{W_i^{\pi(t)}}{\|W_i^{\pi(t)}\|_2} \right\|_2 = \max_{2 \leq j \leq M_i} \max_{t_{j-1}^{(i)} < t \leq t_j^{(i)}} \left\| \frac{W_i^t}{\|W_i^t\|_2} - \frac{W_i^{\pi(t)}}{\|W_i^{\pi(t)}\|_2} \right\|_2 \\ & = \max_{2 \leq j \leq M_i} \max_{t_{j-1}^{(i)} < t \leq t_j^{(i)}} \left\| \frac{W_i^t}{\|W_i^t\|_2} - \frac{W_i^{t_j^{(i)}}}{\|W_i^{t_j^{(i)}}\|_2} \right\|_2. \end{aligned} \quad (87)$$

Note that if $M_i = 1$, then the left-most term in the above expression is 0. Since $\|W_i^t\|_2 \geq \|W_i^{t_j^{(i)}}\|_2$ for all integer $t \in (t_{j-1}^{(i)}, t_j^{(i)}]$ (according to property 1 in Proposition 3), applying Corollary 15 to (87) gives

$$\begin{aligned} & \max_{1 \leq t \leq t_{M_i}^{(i)}} \left\| \frac{W_i^t}{\|W_i^t\|_2} - \frac{W_i^{\pi(t)}}{\|W_i^{\pi(t)}\|_2} \right\|_2 \leq \max_{2 \leq j \leq M_i} \max_{t_{j-1}^{(i)} < t \leq t_j^{(i)}} \frac{\|W_i^t - W_i^{t_j^{(i)}}\|_2}{\|W_i^{t_j^{(i)}}\|_2} \\ & = \max_{2 \leq j \leq M_i} \max_{t_{j-1}^{(i)} + 1 \leq t \leq t_j^{(i)}} \frac{\|W_i^t - W_i^{t_j^{(i)}}\|_2}{\|W_i^{t_j^{(i)}}\|_2} \leq \max_{2 \leq j \leq M_i} \sqrt{\frac{\|W_i^{t_{j-1}^{(i)}+1}\|_2^2 - \|W_i^{t_j^{(i)}}\|_2^2}{\|W_i^{t_j^{(i)}}\|_2^2}} \leq \frac{\varepsilon}{\sqrt{n_\ell}}, \end{aligned} \quad (88)$$

where we also made use of property 2 from Proposition 3 and (26)) in the last two inequalities. Substituting (88) and (86) into (85), for $i \in \mathcal{C}_\ell$, gives

$$\sup_{t=1, \dots, \infty} \left\| \frac{W_i^t}{\|W_i^t\|_2} - \frac{W_i^{\pi(t)}}{\|W_i^{\pi(t)}\|_2} \right\|_2 \leq \frac{\varepsilon}{\sqrt{n_\ell}}, \quad (89)$$

which together with (79) provides the required result.

Appendix G Proof of Lemma 7

According to Algorithm 2, $\{t_j^{(i)}\}_{j=1}^{M_i}$ must be distinct positive integers, and therefore $M_i \leq t_{M_i}^{(i)} = T_\ell$ for all $i \in \mathcal{C}_\ell$. Next, recall that $t_{j-1}^{(i)}$ is the smallest integer $t \in [1, t_j^{(i)} - 1]$ such that (26) holds. Hence, since $\|W_i^t\|_2$ is monotonically decreasing in t , it is evident that either $t_{j-1}^{(i)} = t_1^{(i)} = 1$, or

$$\|W_i^{t_{j-1}^{(i)}}\|_2^2 > \|W_i^{t_j^{(i)}}\|_2^2 \left(1 + \frac{\varepsilon^2}{n_\ell}\right). \quad (90)$$

Equation (90) is a recurrence relation in the index j , and expanding it for $j = M_i, M_i - 1, \dots, 2$ gives

$$1 \geq \|W_i^{t_1^{(i)}}\|_2^2 > \|W_i^{t_{M_i}^{(i)}}\|_2^2 \left(1 + \frac{\varepsilon^2}{n_\ell}\right)^{M_i-1} \geq \frac{1}{n_\ell} \left(1 + \frac{\varepsilon^2}{n_\ell}\right)^{M_i-1}, \quad (91)$$

where we used property 3 in Proposition 3. Therefore, we have

$$M_i < 1 + \frac{\log(n_\ell)}{\log(1 + \varepsilon^2/n_\ell)}. \quad (92)$$

Since M_i is an integer, the above inequality actually implies

$$M_i \leq \left\lceil \frac{\log(n_\ell)}{\log(1 + \varepsilon^2/n_\ell)} \right\rceil. \quad (93)$$

Appendix H Proof of Theorem 8

Let $\tilde{\alpha} \in (0, 1)$, suppose that $\gamma \geq h(\varepsilon) + \sqrt{0.5 \log(1/\tilde{\alpha})}$ where $h(\varepsilon)$ is from (40), and denote $\mathbf{w} = W_i^t$. Then, according to Corollary 6, (40), and Lemma 7, with probability at least $1 - \tilde{\alpha}$ we have

$$\mathcal{S}(W_i^{\pi(t)}) > \gamma - \varepsilon - \sqrt{0.5 \log(1/\tilde{\alpha})} \geq h(\varepsilon) - \varepsilon \geq \sqrt{0.5 \log\left(\sum_{i=1}^n M_i/\alpha\right)}. \quad (94)$$

Therefore, if $\gamma \geq h(\varepsilon) + \sqrt{0.5 \log(1/\tilde{\alpha})}$, according to (29) we have that

$$\sup_{f_1, f_0 \in H_1(\mathbf{w}, \gamma)} \Pr\{Q_{\mathbf{z}} = 1 \mid f_0, f_1\} \geq \sup_{f_1, f_0 \in H_1(\mathbf{w}, \gamma)} \Pr\{W_i^{\pi(t)} \in \hat{\mathcal{G}}_{\mathbf{z}} \mid f_0, f_1\} \geq 1 - \tilde{\alpha}. \quad (95)$$

Clearly, if $\gamma > h(\varepsilon)$, the smallest $\tilde{\alpha}$ that satisfies $\gamma \geq h(\varepsilon) + \sqrt{0.5 \log(1/\tilde{\alpha})}$ is obtained by choosing $\tilde{\alpha}$ according to $\sqrt{0.5 \log(1/\tilde{\alpha})} = \gamma - h(\varepsilon)$. Manipulating this expression to extract $\tilde{\alpha}$ gives $\tilde{\alpha} = \exp[-2(\gamma - h(\varepsilon))^2]$, which together with (95) implies (39). To prove (41), we can write for all $f_1, f_0 \in H_1(W_i^t, \gamma)$

$$\begin{aligned} & \mathbb{E}[\inf_{\hat{\mathbf{w}} \in \hat{\mathcal{G}}_{\mathbf{z}}} \mathcal{E}_{\text{TV}}(\hat{\mathbf{w}}, W_i^t) \mid f_0, f_1] \\ & \leq \mathcal{E}_{\text{TV}}(W_i^{\pi(t)}, W_i^t) \cdot \Pr\{W_i^{\pi(t)} \in \hat{\mathcal{G}}_{\mathbf{z}} \mid f_0, f_1\} + 1 \cdot \Pr\{W_i^{\pi(t)} \notin \hat{\mathcal{G}}_{\mathbf{z}} \mid f_0, f_1\}, \end{aligned} \quad (96)$$

where we use the fact that the total variation distance is upper bounded by 1. Applying Lemma 5 (and particularly (34)) to bound $\mathcal{E}_{\text{TV}}(W_i^{\pi(t)}, W_i^t)$, and using (95) with $\tilde{\alpha} = \exp[-2(\gamma - h(\varepsilon))^2]$, gives

$$\sup_{f_1, f_0 \in H_1(W_i^t, \gamma)} \mathbb{E}[\inf_{\hat{\mathbf{w}} \in \hat{\mathcal{G}}_{\mathbf{z}}} \mathcal{E}_{\text{TV}}(\hat{\mathbf{w}}, W_i^t) \mid f_0, f_1] \leq \frac{\varepsilon \|W_i^t\|_2}{2} + \exp[-2(\gamma - h(\varepsilon))^2]. \quad (97)$$

Observe that by the definition of $H_1(\mathbf{w}, \gamma)$ in (7), the alternative $H_1(W_i^t, \gamma)$ implies that $\|W_i^t\|_2 \leq \langle W_i^t, \mathbf{s} \rangle / \gamma \leq (1 - p) / \gamma$. Applying this observation to (97), together with the fact that $\|W_i^t\|_2 \leq 1$, gives (41).

Appendix I Proof of Theorem 9

Taking $\alpha = 1/\log n$, and since ε is kept constant, we have

$$\limsup_{n \rightarrow \infty} \frac{\hat{h}_{n, \alpha, \lambda_{<1}}(\varepsilon)}{\sqrt{\log n}} = \limsup_{n \rightarrow \infty} \sqrt{\frac{0.5 \log \left(n \log n \cdot \min \left\{ \left\lceil \frac{\log(n/\varepsilon)}{\log(\lambda_{<1}^{-1})} \right\rceil, \left\lceil \frac{\log(n)}{\log(1+\varepsilon^2/n)} \right\rceil \right\} \right)}{\log n}}, \quad (98)$$

where $\hat{h}_{n, \alpha, \lambda_{<1}}$ is from (42). We begin by proving part 1 of Theorem 9. Notice that we can write

$$\begin{aligned} & \limsup_{n \rightarrow \infty} \sqrt{\frac{0.5 \log \left(n \log n \cdot \min \left\{ \left\lceil \frac{\log(n/\varepsilon)}{\log(\lambda_{<1}^{-1})} \right\rceil, \left\lceil \frac{\log(n)}{\log(1+\varepsilon^2/n)} \right\rceil \right\} \right)}{\log n}} \leq \lim_{n \rightarrow \infty} \sqrt{\frac{0.5 \log \left(n \log n \cdot \left\lceil \frac{\log(n)}{\log(1+\varepsilon^2/n)} \right\rceil \right)}{\log n}} \\ & = \lim_{n \rightarrow \infty} \sqrt{\frac{0.5 \log \left(\frac{n^2 (\log n)^2}{\varepsilon^2} \right)}{\log n}} = \lim_{n \rightarrow \infty} \sqrt{\frac{\log n + \log(\log n) - \log \varepsilon}{\log n}} = 1, \end{aligned} \quad (99)$$

where we used (38). Therefore, if $\liminf_{n \rightarrow \infty} \gamma_n / \sqrt{\log n} > 1$, then $\gamma_n > \hat{h}_{n, \alpha, \lambda_{<1}}(\varepsilon) \geq h(\varepsilon)$ for sufficiently large n . Furthermore, we have that $\gamma_n - \hat{h}_{n, \alpha, \lambda_{<1}}(\varepsilon) \xrightarrow[n \rightarrow \infty]{} \infty$, since

$$\liminf_{n \rightarrow \infty} \frac{\gamma_n - \hat{h}_{n, \alpha, \lambda_{<1}}(\varepsilon)}{\sqrt{\log n}} \geq \liminf_{n \rightarrow \infty} \frac{\gamma_n}{\sqrt{\log n}} - \limsup_{n \rightarrow \infty} \frac{\hat{h}_{n, \alpha, \lambda_{<1}}(\varepsilon)}{\sqrt{\log n}} > 0. \quad (100)$$

Applying Theorem 8, we have

$$\sup_{\mathbf{w} \in \mathcal{F}} \sup_{f_1, f_0 \in H_1(\mathbf{w}, \gamma)} \mathbb{E}[\inf_{\hat{\mathbf{w}} \in \hat{\mathcal{G}}_{\mathbf{z}}} \mathcal{E}_{\text{TV}}(\hat{\mathbf{w}}, \mathbf{w}) \mid f_1, f_0] \leq \frac{\varepsilon(1-p)}{2\gamma_n} + e^{-2(\gamma_n - h(\varepsilon))^2} \leq \frac{\varepsilon(1-p)}{2\gamma_n} + e^{-2(\gamma_n - \hat{h}_{n,\alpha,\lambda_{<1}}(\varepsilon))^2}, \quad (101)$$

for sufficiently large n . Consequently, combining (100), (10), (30), and the fact that $\lim_{n \rightarrow \infty} \gamma_n = \infty$, we obtain

$$r_{\mathcal{F}}^{(n)}(\hat{\mathcal{G}}_{\mathbf{z}}, \gamma_n) \leq \frac{1}{\log n} + \frac{\varepsilon(1-p)}{2\gamma_n} + e^{-2(\gamma_n - \hat{h}_{n,\alpha,\lambda_{<1}}(\varepsilon))^2} \xrightarrow{n \rightarrow \infty} 0. \quad (102)$$

Next, we prove parts 2 and 3 of Theorem 9. From (98), we have

$$\begin{aligned} \limsup_{n \rightarrow \infty} \frac{\hat{h}_{n,\alpha,\lambda_{<1}}(\varepsilon)}{\sqrt{\log n}} &\leq \limsup_{n \rightarrow \infty} \sqrt{\frac{0.5 \log \left(n \log n \cdot \left\lceil \frac{\log(n/\varepsilon)}{\log(\lambda_{<1}^{-1})} \right\rceil \right)}{\log n}} = \limsup_{n \rightarrow \infty} \sqrt{\frac{0.5 \log \left(\frac{n \cdot \log n \cdot \log(n/\varepsilon)}{\log(\lambda_{<1}^{-1})} \right)}{\log n}} \\ &= \limsup_{n \rightarrow \infty} \sqrt{\frac{0.5(\log n + \log(\log n) + \log(\log(n/\varepsilon)) - \log(\log(\lambda_{<1}^{-1})))}{\log n}} \\ &= \limsup_{n \rightarrow \infty} \sqrt{0.5 - \frac{\log(\log(\lambda_{<1}^{-1}))}{\log n}}. \end{aligned} \quad (103)$$

If $\lambda_{<1}$ is bounded away from 1, then it follows that

$$\limsup_{n \rightarrow \infty} \frac{\hat{h}_{n,\alpha,\lambda_{<1}}(\varepsilon)}{\sqrt{\log n}} \leq \limsup_{n \rightarrow \infty} \sqrt{0.5 - \frac{\log(\log(\lambda_{<1}^{-1}))}{\log n}} = \sqrt{0.5}. \quad (104)$$

Thus, if $\liminf_{n \rightarrow \infty} \gamma_n / \sqrt{\log n} > \sqrt{0.5}$, then $\gamma_n > \hat{h}_{n,\alpha,\lambda_{<1}}(\varepsilon) \geq h(\varepsilon)$ for all sufficiently large n , and $\hat{\mathcal{G}}_{\mathbf{z}}$ is locally consistent following (101)–(100). On the other hand, if $\lim_{n \rightarrow \infty} \lambda_{<1} = 1$, we have

$$\log(\lambda_{<1}^{-1}) \underset{n \rightarrow \infty}{\sim} 1 - \lambda_{<1}, \quad (105)$$

and therefore, if in addition $\lim_{n \rightarrow \infty} (1 - \lambda_{<1})n^\gamma > 0$ for some $0 < \gamma \leq 0.5$, we obtain

$$\begin{aligned} \limsup_{n \rightarrow \infty} \frac{\hat{h}_{n,\alpha,\lambda_{<1}}(\varepsilon)}{\sqrt{\log n}} &\leq \lim_{n \rightarrow \infty} \sqrt{0.5 - \lim_{n \rightarrow \infty} \frac{\log(\log(\lambda_{<1}^{-1}))}{\log n}} \\ &= \lim_{n \rightarrow \infty} \sqrt{0.5 - \frac{\log(1 - \lambda_{<1})}{\log n}} = \lim_{n \rightarrow \infty} \sqrt{0.5 - \frac{\log((1 - \lambda_{<1})n^\gamma) - \gamma \log n}{\log n}} \leq \sqrt{0.5 + \gamma}. \end{aligned} \quad (106)$$

Consequently, if $\liminf_{n \rightarrow \infty} \gamma_n / \sqrt{\log n} > \sqrt{0.5 + \gamma}$, then $\gamma_n > \hat{h}_{n,\alpha,\lambda_{<1}}(\varepsilon) \geq h(\varepsilon)$ for all sufficiently large n , and again $\hat{\mathcal{G}}_{\mathbf{z}}$ is locally consistent following (101)–(100).

Appendix J Proof of Theorem 10

Let $\{m_n\}$ be a sequence of integers, and for each index n consider a matrix $W \in \mathbb{R}^{n \times n}$ such that the corresponding graph G has $L_n = \lceil \frac{n}{m_n} \rceil$ connected components $\{\mathcal{C}_\ell\}_{\ell=1}^{L_n}$, where $|\mathcal{C}_1| = |\mathcal{C}_2| = \dots = |\mathcal{C}_{L_n-1}| = m_n$, and $|\mathcal{C}_{L_n}| = n - m_n(L_n - 1)$. That is, W can be permuted (symmetrically) into a block-diagonal form with L_n blocks, where the first $L_n - 1$ blocks are of size $m_n \times m_n$,

and the last block is of the appropriate size to match the dimensions of W . In addition, we take the values of W so that W_i is the uniform distribution over \mathcal{C}_ℓ for each $i \in \mathcal{C}_\ell$, $\ell = 1, \dots, L_n$. Specifically, $W_{i,j} = 1/|\mathcal{C}_\ell|$ for all $i, j \in \mathcal{C}_\ell$, and $W_{i,j} = 0$ otherwise. Clearly, W is nonnegative, symmetric, stochastic, and PSD, thereby satisfying Assumption 2. In this case, \mathcal{F} has only L_n distinct distributions, which are the uniform distributions over the connected components of G , i.e., $\mathcal{F} = \{\mathbb{1}_{\mathcal{C}_1}/m_n, \dots, \mathbb{1}_{\mathcal{C}_{L_n-1}}/m_n, \mathbb{1}_{\mathcal{C}_{L_n}}/(n - m_n(L_n - 1))\}$, where $\mathbb{1}_{\mathcal{C}_\ell}$ is the indicator vector over \mathcal{C}_ℓ . Continuing, let us define the hypothesis H'_0 as

$$H'_0 : f_1(x_i) = f_0(x_i) \quad \forall i = 1, \dots, n. \quad (107)$$

Notably, H'_0 implies that $s(x_i) = 0$ for all $i = 1, \dots, n$, and is therefore a subset of H_0 . Additionally, we define $H'_1(\ell)$, for $\ell = 1, \dots, L_n - 1$, as alternative hypotheses to H_0 (and H'_0), as

$$H'_1(\ell) : \begin{cases} f_0(x_i) = 0, & \forall i \in \mathcal{C}_\ell, \\ f_1(x_i) = f_0(x_i), & \forall i \notin \mathcal{C}_\ell. \end{cases} \quad (108)$$

Observe that under $H'_1(\ell)$, we have that $s(x_i) = 1 - p$ for all $i \in \mathcal{C}_\ell$, and hence

$$\langle \mathbb{1}_{\mathcal{C}_\ell}/m_n, \mathbf{s} \rangle = 1 - p = (1 - p)\sqrt{m_n}\|\mathbb{1}_{\mathcal{C}_\ell}/m_n\|_2. \quad (109)$$

Taking

$$m_n = \left\lceil \left(\frac{\gamma_n}{1 - p} \right)^2 \right\rceil, \quad (110)$$

guarantees that $\langle \mathbb{1}_{\mathcal{C}_\ell}/m_n, \mathbf{s} \rangle \geq \gamma_n\|\mathbb{1}_{\mathcal{C}_\ell}/m_n\|_2$. Therefore, each hypothesis $H'_1(\ell)$ is a subset of the alternative $H_1(\mathbb{1}_{\mathcal{C}_\ell}/m_n, \gamma_n)$, for $\ell = 1, \dots, L_n - 1$. Consequently, by our definitions of H'_0 and $\{H'_1(\ell)\}_{\ell=1}^{L_n-1}$, we have that

$$\begin{aligned} \tilde{R}^{(n)}(\gamma_n) &= \min_{Q_{\mathbf{z}}} \sup_{W' \in \mathcal{W}} R_{\mathcal{F}}^{(n)}(Q_{\mathbf{z}}, \gamma_n) \geq \min_{Q_{\mathbf{z}}} R_{\mathcal{F}}^{(n)}(Q_{\mathbf{z}}, \gamma_n) \\ &\geq \min_{Q_{\mathbf{z}}} \left\{ \sup_{f_1, f_0 \in H'_0} \Pr\{Q_{\mathbf{z}} = 1 \mid f_0, f_1\} + \max_{\ell=1, \dots, L_n-1} \sup_{f_1, f_0 \in H'_1(\ell)} \Pr\{Q_{\mathbf{z}} = 0 \mid f_0, f_1\} \right\}. \end{aligned} \quad (111)$$

Additionally, according to (110) and (45), we have

$$\liminf_{n \rightarrow \infty} \frac{m_n}{\log n} < \frac{1}{\log(p^{-1})}. \quad (112)$$

We now derive a lower bound on the right-hand side of (111) under the condition (112). Notice that under H'_0 , according to (2), the labels z_i are sampled independently from $(Z \mid X = x_i) \sim \text{Bernoulli}(p)$. On the other hand, under $H'_1(\ell)$, the labels z_i are always equal to 1 for all $i \in \mathcal{C}_\ell$, and are sampled independently from $\text{Bernoulli}(p)$ for all $i \notin \mathcal{C}_\ell$. Let $Q_{\mathbf{z}}^*$ be a test that outputs 1 if $[\mathbf{z}]_{\mathcal{C}_\ell} = \mathbf{1}$ for some $\ell \in \{1, \dots, L_n - 1\}$, and 0 otherwise, where $[\mathbf{z}]_{\Omega}$ is the restriction of the entries of \mathbf{z} to the index set Ω , and $\mathbf{1}$ is a corresponding vector of ones. Note that $\Pr\{Q_{\mathbf{z}}^* = 0 \mid H'_1(\ell)\} = 0$ for all $\ell = 1, \dots, L_n - 1$. In addition, we have

$$\Pr\{Q_{\mathbf{z}}^* = 1 \mid H'_0\} = 1 - (1 - p^{m_n})^{L_n-1} > 1 - \exp(-p^{m_n}(L_n - 1)), \quad (113)$$

where we used the inequality $\log(1 - x) < -x$ for $0 < x < 1$. Let us write

$$\log(p^{m_n}(L_n - 1)) = \log(L_n - 1) - m_n \log(p^{-1}) \geq \log(n - m_n) - \log(m_n) - m_n \log(p^{-1}), \quad (114)$$

where we used $L_n = \lceil \frac{n}{m_n} \rceil$. Combining (114) and (112), we obtain

$$\liminf_{n \rightarrow \infty} \frac{\log(p^{m_n}(L_n - 1))}{\log n} > \liminf_{n \rightarrow \infty} \frac{\log(n - m_n) - \log(m_n)}{\log n} - 1 = 0, \quad (115)$$

which implies that $\lim_{n \rightarrow \infty} p^{m_n}(L_n - 1) = \infty$, and therefore $\lim_{n \rightarrow \infty} \Pr\{Q_{\mathbf{z}}^* = 1 \mid H'_0\} = 1$.

Last, we prove that $Q_{\mathbf{z}}^*$ is a test which achieves the minimum in (111). If $Q_{\mathbf{z}}$ is any other test, then one of the following two statements must be true (or both).

1. $Q_{\mathbf{z}}$ outputs 0 for some \mathbf{z} satisfying $[\mathbf{z}]_{\mathcal{C}_\ell} = \mathbf{1}$ for some $\ell \in \{1, \dots, L_n - 1\}$.
2. $Q_{\mathbf{z}}$ outputs 1 for some \mathbf{z} satisfying $[\mathbf{z}]_{\mathcal{C}_\ell} \neq \mathbf{1}$ for all $\ell = 1, \dots, L_n - 1$.

If the first statement is true, then $\Pr\{Q_{\mathbf{z}} = 0 \mid H'_1(\ell)\} = 1$ for some $\ell \in \{1, \dots, L_n - 1\}$, and therefore the expression inside the minimization in (111) is lower bounded by 1 for the test $Q_{\mathbf{z}}$. The analogous expression for the test $Q_{\mathbf{z}}^*$ is upper bounded (with a strict inequality) by 1 according to (113), and is therefore always smaller than for $Q_{\mathbf{z}}$. On the other hand, if the second statement is true, then $Q_{\mathbf{z}}$ cannot be a test which achieves the minimum in (111), since there is no alternative $H'_1(\ell)$ for which $[\mathbf{z}]_{\mathcal{C}_\ell} \neq \mathbf{1}$ for all $\ell = 1, \dots, L_n - 1$. That is, the expression inside the minimization in (111) can always be made smaller for the test $Q_{\mathbf{z}}$ if we enforce that $Q_{\mathbf{z}} = 0$ for all \mathbf{z} that satisfy $[\mathbf{z}]_{\mathcal{C}_\ell} \neq \mathbf{1}$ for all $\ell = 1, \dots, L_n - 1$, while retaining all other aspects of $Q_{\mathbf{z}}$ unchanged.

Appendix K Proof of Proposition 12

If $K_{i,j} = 0$, then $D_{\text{KL}}(H_i \parallel K_i) = \sum_{i,j} H_{i,j} \log(H_{i,j}/K_{i,j})$ is defined through the limit $K_{i,j} \rightarrow 0$. Therefore, to keep the objective function finite, we must have $H_{i,j} = 0$. We know that there exists H that satisfies this property (that $H_{i,j} = 0$ if $K_{i,j} = 0$) and that is simultaneously symmetric and stochastic, due to the assumption in the theorem (that there exists d_1, \dots, d_n such that \widetilde{W} from (48) is symmetric and stochastic). Consequently, $H_{i,j} = 0$ for all indices i, j for which $K_{i,j} = 0$. Next, the Lagrangian function associated with (49) is given by

$$\mathcal{L}(H, \{\lambda_i\}_{i=1}^n, \{\mu_{i,j}\}_{i,j=1}^n) = \sum_{i,j} H_{i,j} \log\left(\frac{H_{i,j}}{K_{i,j}}\right) + \sum_{i=1}^n \lambda_i \left(\sum_{j=1}^n H_{i,j} - 1\right) + \sum_{i,j=1}^n \mu_{i,j} (H_{i,j} - H_{j,i}). \quad (116)$$

Taking the derivative of \mathcal{L} with respect to $H_{i,j}$ and equating to zero, gives

$$\log(H_{i,j}) = \log(K_{i,j}) - 1 - \lambda_i - \mu_{i,j} + \mu_{j,i}, \quad (117)$$

for all i, j for which $K_{i,j} \neq 0$. Applying the symmetry constraints $H_{i,j} = H_{j,i}$ to the above, and after some manipulation, we get that

$$\mu_{i,j} - \mu_{j,i} = (-\lambda_i + \lambda_j + \log(K_{i,j}) - \log(K_{j,i}))/2. \quad (118)$$

Substituting this back in (117), we have

$$\log(H_{i,j}) = -1 - (\lambda_i + \lambda_j)/2 + \log(\sqrt{K_{i,j}K_{j,i}}). \quad (119)$$

Taking the exponential of both hand sides of the above equation, and defining $d_i = \exp(-(\lambda_i + 1)/2)$, completes the proof.

Appendix L Analysis supporting the example in Section 6.1

We now approximate γ from (56) using (55). According to (55), and for sufficiently large n , we can write

$$\begin{aligned}\gamma &= \max_{1 \leq i \leq n} \sup_{t=1, \dots, \infty} \frac{\langle W_i^t, \mathbf{s} \rangle}{\|W_i^t\|} = \max_{1 \leq i \leq n} \sup_{t=1, \dots, \infty} \frac{\sum_{j=1}^n W_{i,j}^t s(\theta_j)}{\sqrt{\sum_{j=1}^n W_{i,j}^{2t}}} \\ &\approx \max_{\varphi \in [0, 2\pi)} \sup_{\tau > 0} \frac{\sum_{j=1}^n G_\tau(\varphi, \theta_j) s(\theta_j)}{\sqrt{\sum_{j=1}^n G_\tau^2(\varphi, \theta_j)}} = \max_{\varphi \in [0, 2\pi)} \sup_{\tau > 0} \frac{\frac{1}{n} \sum_{j=1}^n G_\tau(\varphi, \theta_j) s(\theta_j)}{\frac{1}{\sqrt{n}} \sqrt{\frac{1}{n} \sum_{j=1}^n G_\tau^2(\varphi, \theta_j)}}.\end{aligned}\quad (120)$$

Since G_τ and $s(\theta)$ are bounded, and $\theta_1, \dots, \theta_n$ are i.i.d, we have

$$\frac{1}{n} \sum_{j=1}^n G_\tau(\varphi, \theta_j) s(\theta_j) = \frac{1}{2\pi} \int_{-\pi}^{\pi} G_\tau(\varphi, \theta) s(\theta) d\theta + \mathcal{O}\left(\frac{1}{\sqrt{n}}\right), \quad (121)$$

$$\frac{1}{\sqrt{n}} \sqrt{\frac{1}{n} \sum_{j=1}^n G_\tau^2(\varphi, \theta_j)} = \frac{1}{\sqrt{n}} \sqrt{\frac{1}{2\pi} \int_{-\pi}^{\pi} G_\tau^2(\varphi, \theta) d\theta} + \mathcal{O}\left(\frac{1}{\sqrt{n}}\right). \quad (122)$$

Therefore, for sufficiently large n and sufficiently small σ , it follows that

$$\gamma \approx \max_{\varphi \in [0, 2\pi)} \sup_{\tau > 0} \frac{\frac{1}{2\pi} \int_{-\pi}^{\pi} G_\tau(\varphi, \theta) s(\theta) d\theta}{\frac{1}{\sqrt{n}} \sqrt{\frac{1}{2\pi} \int_{-\pi}^{\pi} G_\tau^2(\varphi, \theta) d\theta}} = \sup_{\tau > 0} \sqrt{\frac{n}{2\pi}} \frac{\int_{-\pi}^{\pi} G_\tau(0, \theta) s(\theta) d\theta}{\sqrt{\int_{-\pi}^{\pi} G_\tau^2(0, \theta) d\theta}}. \quad (123)$$

Next, using the expression for $s(\theta)$ from (53) we can write

$$\begin{aligned}\int_{-\pi}^{\pi} G_\tau(0, \theta) s(\theta) d\theta &= \int_{-\min\{\pi, 3\pi/2\omega\}}^{\min\{\pi, 3\pi/2\omega\}} e^{-\theta^2/\tau} 2p(1-p)b \cos(\omega\theta) d\theta \\ &= 2p(1-p)b \left(\int_{-\infty}^{\infty} e^{-\theta^2/\tau} \cos(\omega\theta) d\theta + E_1 \right) = 2p(1-p)b \left(\sqrt{\pi\tau} e^{-\omega^2\tau/4} + E_1 \right),\end{aligned}\quad (124)$$

where E_1 is an error term bounded by

$$\begin{aligned}|E_1| &= 2 \left| \int_{\min\{\pi, 3\pi/2\omega\}}^{\infty} e^{-\theta^2/\tau} \cos(\omega\theta) d\theta \right| \leq 2 \int_{\min\{\pi, 3\pi/2\omega\}}^{\infty} e^{-\theta^2/\tau} d\theta \\ &\leq 2 \int_{\min\{\pi, 3\pi/2\omega\}}^{\infty} \frac{\theta}{\tau} e^{-\theta^2/\tau} d\theta \leq e^{-(\min\{\pi, 3\pi/2\omega\})^2/\tau},\end{aligned}\quad (125)$$

for $\tau \leq \min\{\pi, 3\pi/2\omega\}$. Additionally,

$$\begin{aligned}\int_{-\pi}^{\pi} G_\tau^2(0, \theta) d\theta &= \int_{-\pi}^{\pi} e^{-2\theta^2/\tau} d\theta = \int_{-\infty}^{\infty} e^{-2\theta^2/\tau} d\theta + E_2 \\ &= \sqrt{\frac{\pi\tau}{2}} + E_2,\end{aligned}\quad (126)$$

where E_2 is an error term bounded by

$$|E_2| = 2 \int_{\pi}^{\infty} e^{-2\theta^2/\tau} d\theta \leq 2 \int_{\pi}^{\infty} \frac{\theta}{\tau} e^{-2\theta^2/\tau} d\theta \leq \frac{1}{2} e^{-2\pi^2/\tau}, \quad (127)$$

for $\tau \leq \pi$. By neglecting E_1 and E_2 (which will be justified shortly), we get

$$\gamma \approx (8/\pi)^{1/4} b \sqrt{np} (1-p) \sup_{\tau > 0} \left\{ \tau^{1/4} e^{-\omega^2 \tau / 4} \right\}, \quad (128)$$

and it is easy to verify that the supremum in the above expression is achieved at $\tau = 1/\omega^2$, hence

$$\gamma \approx (8/\pi e)^{1/4} b p (1-p) \sqrt{n/\omega}. \quad (129)$$

Note that the conditions $\tau \leq \min\{\pi, 3\pi/2\omega\}$ and $\tau \leq \pi$ (required for the bounds on E_1 and E_2) hold for $\tau = 1/\omega^2$, and one can verify that E_1 and E_2 are indeed negligible if ω is not too small.

References

- [1] Louigi Addario-Berry, Nicolas Broutin, Luc Devroye, Gábor Lugosi, et al. On combinatorial testing problems. *The Annals of Statistics*, 38(5):3063–3092, 2010.
- [2] Zeyuan Allen-Zhu, Yuanzhi Li, Rafael Oliveira, and Avi Wigderson. Much faster algorithms for matrix scaling. In *2017 IEEE 58th Annual Symposium on Foundations of Computer Science (FOCS)*, pages 890–901. IEEE, 2017.
- [3] Ery Arias-Castro, Emmanuel J Candes, and Arnaud Durand. Detection of an anomalous cluster in a network. *The Annals of Statistics*, pages 278–304, 2011.
- [4] Ery Arias-Castro, Emmanuel J Candès, Hannes Helgason, and Ofer Zeitouni. Searching for a trail of evidence in a maze. *The Annals of Statistics*, pages 1726–1757, 2008.
- [5] Joseph D Ayotte, Laura Medalie, Sharon L Qi, Lorraine C Backer, and Bernard T Nolan. Estimating the high-arsenic domestic-well population in the conterminous united states. *Environmental science & technology*, 51(21):12443–12454, 2017.
- [6] Tanya Barrett, Stephen E Wilhite, Pierre Ledoux, Carlos Evangelista, Irene F Kim, Maxim Tomashevsky, Kimberly A Marshall, Katherine H Phillippy, Patti M Sherman, Michelle Holko, et al. Ncbi geo: archive for functional genomics data sets—update. *Nucleic acids research*, 41(D1):D991–D995, 2012.
- [7] Etienne Becht, Leland McInnes, John Healy, Charles-Antoine Dutertre, Immanuel WH Kwok, Lai Guan Ng, Florent Gehring, and Evan W Newell. Dimensionality reduction for visualizing single-cell data using umap. *Nature biotechnology*, 37(1):38–44, 2019.
- [8] Tyrus Berry and Timothy Sauer. Consistent manifold representation for topological data analysis. *arXiv preprint arXiv:1606.02353*, 2016.
- [9] Lawrence D Brown, T Tony Cai, and Anirban DasGupta. Interval estimation for a binomial proportion. *Statistical science*, pages 101–117, 2001.
- [10] Jose Cadena, Feng Chen, and Anil Vullikanti. Near-optimal and practical algorithms for graph scan statistics. In *Proceedings of the 2017 SIAM International Conference on Data Mining*, pages 624–632. SIAM, 2017.
- [11] Jose Cadena, Feng Chen, and Anil Vullikanti. Near-optimal and practical algorithms for graph scan statistics with connectivity constraints. *ACM Transactions on Knowledge Discovery from Data (TKDD)*, 13(2):1–33, 2019.

- [12] Frédéric Cazáís and Alix Lhéritier. Beyond two-sample-tests: Localizing data discrepancies in high-dimensional spaces. In *2015 IEEE International Conference on Data Science and Advanced Analytics (DSAA)*, pages 1–10. IEEE, 2015.
- [13] Siheng Chen, Yaoqing Yang, Shi Zong, Aarti Singh, and Jelena Kovačević. Detecting localized categorical attributes on graphs. *IEEE Transactions on Signal Processing*, 65(10):2725–2740, 2017.
- [14] Xiuyuan Cheng and Alexander Cloninger. Classification logit two-sample testing by neural networks. *arXiv preprint arXiv:1909.11298*, 2019.
- [15] Robert Lorenz Chua, Soeren Lukassen, Saskia Trump, Bianca P Hennig, Daniel Wendisch, Fabian Pott, Olivia Debnath, Loreen Thürmann, Florian Kurth, Maria Theresa Völker, et al. Covid-19 severity correlates with airway epithelium–immune cell interactions identified by single-cell analysis. *Nature biotechnology*, 38(8):970–979, 2020.
- [16] Charles J Clopper and Egon S Pearson. The use of confidence or fiducial limits illustrated in the case of the binomial. *Biometrika*, 26(4):404–413, 1934.
- [17] Ronald R Coifman and Stéphane Lafon. Diffusion maps. *Applied and computational harmonic analysis*, 21(1):5–30, 2006.
- [18] Judit Csima and Biswa Nath Datta. The dad theorem for symmetric non-negative matrices. *Journal of Combinatorial Theory, Series A*, 12(1):147–152, 1972.
- [19] David C Dauphiné, Allan H Smith, Yan Yuan, John R Balmes, Michael N Bates, and Craig Steinmaus. Case-control study of arsenic in drinking water and lung cancer in california and nevada. *International journal of environmental research and public health*, 10(8):3310–3324, 2013.
- [20] Leslie A Desimone, Peter B McMahon, and Michael R Rosen. *Water Quality in Principal Aquifers of the United States, 1991-2010*. US Department of the Interior, US Geological Survey, 2014.
- [21] Luiz Duczmal, Martin Kulldorff, and Lan Huang. Evaluation of spatial scan statistics for irregularly shaped clusters. *Journal of Computational and Graphical Statistics*, 15(2):428–442, 2006.
- [22] Michael J Focazio. *A retrospective analysis on the occurrence of arsenic in ground-water resources of the United States and limitations in drinking-water-supply characterizations*, volume 99. US Department of the Interior, US Geological Survey, 2000.
- [23] PE Freeman, I Kim, and AB Lee. Local two-sample testing: a new tool for analysing high-dimensional astronomical data. *Monthly Notices of the Royal Astronomical Society*, 471(3):3273–3282, 2017.
- [24] Joseph Glaz and Narayanaswamy Balakrishnan. *Scan statistics and applications*. Springer Science & Business Media, 2012.
- [25] Zengyou He, Chaohua Sheng, Yan Liu, and Quan Zou. Instance-based classification through hypothesis testing. *arXiv preprint arXiv:1901.00560*, 2019.

- [26] Simon Hediger, Loris Michel, and Jeffrey Näf. On the use of random forest for two-sample testing. *arXiv preprint arXiv:1903.06287*, 2019.
- [27] Yosef Hochberg. A sharper bonferroni procedure for multiple tests of significance. *Biometrika*, 75(4):800–802, 1988.
- [28] Wassily Hoeffding. Probability inequalities for sums of bounded random variables. In *The Collected Works of Wassily Hoeffding*, pages 409–426. Springer, 1994.
- [29] Sture Holm. A simple sequentially rejective multiple test procedure. *Scandinavian journal of statistics*, pages 65–70, 1979.
- [30] Roger A Horn and Charles R Johnson. *Matrix analysis*. Cambridge university press, 2012.
- [31] Martin Idel. A review of matrix scaling and sinkhorn’s normal form for matrices and positive maps. *arXiv preprint arXiv:1609.06349*, 2016.
- [32] Ilmun Kim, Ann B Lee, Jing Lei, et al. Global and local two-sample tests via regression. *Electronic Journal of Statistics*, 13(2):5253–5305, 2019.
- [33] Philip A Knight. The sinkhorn–knopp algorithm: convergence and applications. *SIAM Journal on Matrix Analysis and Applications*, 30(1):261–275, 2008.
- [34] Martin Kulldorff. A spatial scan statistic. *Communications in Statistics-Theory and methods*, 26(6):1481–1496, 1997.
- [35] Martin Kulldorff, Richard Heffernan, Jessica Hartman, Renato Assunção, and Farzad Mostashari. A space–time permutation scan statistic for disease outbreak detection. *Plos med*, 2(3):e59, 2005.
- [36] Martin Kulldorff, Lan Huang, Linda Pickle, and Luiz Duczmal. An elliptic spatial scan statistic. *Statistics in medicine*, 25(22):3929–3943, 2006.
- [37] Martin Kulldorff and Neville Nagarwalla. Spatial disease clusters: detection and inference. *Statistics in medicine*, 14(8):799–810, 1995.
- [38] Boris Landa, Ronald R Coifman, and Yuval Kluger. Doubly-stochastic normalization of the gaussian kernel is robust to heteroskedastic noise. *arXiv preprint arXiv:2006.00402*, 2020.
- [39] David A Levin and Yuval Peres. *Markov chains and mixing times*, volume 107. American Mathematical Soc., 2017.
- [40] Evan Z Macosko, Anindita Basu, Rahul Satija, James Nemes, Karthik Shekhar, Melissa Goldman, Itay Tirosh, Allison R Bialas, Nolan Kamitaki, Emily M Martersteck, et al. Highly parallel genome-wide expression profiling of individual cells using nanoliter droplets. *Cell*, 161(5):1202–1214, 2015.
- [41] Markus Maier, Matthias Hein, and Ulrike Von Luxburg. Optimal construction of k-nearest-neighbor graphs for identifying noisy clusters. *Theoretical Computer Science*, 410(19):1749–1764, 2009.
- [42] Markus Maier, Ulrike V Luxburg, and Matthias Hein. Influence of graph construction on graph-based clustering measures. In *Advances in neural information processing systems*, pages 1025–1032, 2009.

- [43] Albert W Marshall, Ingram Olkin, and Barry C Arnold. *Inequalities: theory of majorization and its applications*, volume 143. Springer, 1979.
- [44] Nicholas F Marshall and Ronald R Coifman. Manifold learning with bi-stochastic kernels. *IMA Journal of Applied Mathematics*, 84(3):455–482, 2019.
- [45] Leland McInnes, John Healy, and James Melville. Umap: Uniform manifold approximation and projection for dimension reduction. *arXiv preprint arXiv:1802.03426*, 2018.
- [46] Loris Michel, Jeffrey Näf, and Nicolai Meinshausen. High probability lower bounds for the total variation distance. *arXiv preprint arXiv:2005.06006*, 2020.
- [47] Jing Qian, Venkatesh Saligrama, and Yuting Chen. Connected sub-graph detection. In *Artificial Intelligence and Statistics*, pages 796–804, 2014.
- [48] Moshe Sade-Feldman, Keren Yizhak, Stacey L Bjorgaard, John P Ray, Carl G de Boer, Russell W Jenkins, David J Lieb, Jonathan H Chen, Dennie T Frederick, Michal Barzily-Rokni, et al. Defining t cell states associated with response to checkpoint immunotherapy in melanoma. *Cell*, 175(4):998–1013, 2018.
- [49] James Sharpnack, Alessandro Rinaldo, and Aarti Singh. Detecting anomalous activity on networks with the graph fourier scan statistic. *IEEE Transactions on Signal Processing*, 64(2):364–379, 2015.
- [50] James Sharpnack, Aarti Singh, and Akshay Krishnamurthy. Detecting activations over graphs using spanning tree wavelet bases. In *Artificial Intelligence and Statistics*, pages 536–544, 2013.
- [51] James Sharpnack, Aarti Singh, and Alessandro Rinaldo. Changepoint detection over graphs with the spectral scan statistic. In *Artificial Intelligence and Statistics*, pages 545–553, 2013.
- [52] James L Sharpnack, Akshay Krishnamurthy, and Aarti Singh. Near-optimal anomaly detection in graphs using lovasz extended scan statistic. In *Advances in Neural Information Processing Systems*, pages 1959–1967, 2013.
- [53] Richard Sinkhorn. A relationship between arbitrary positive matrices and doubly stochastic matrices. *The annals of mathematical statistics*, 35(2):876–879, 1964.
- [54] Richard Sinkhorn and Paul Knopp. Concerning nonnegative matrices and doubly stochastic matrices. *Pacific Journal of Mathematics*, 21(2):343–348, 1967.
- [55] Craig Steinmaus, Meng Lu, Randall L Todd, and Allan H Smith. Probability estimates for the unique childhood leukemia cluster in fallon, nevada, and risks near other us military aviation facilities. *Environmental Health Perspectives*, 112(6):766–771, 2004.
- [56] Tim Stuart, Andrew Butler, Paul Hoffman, Christoph Hafemeister, Efthymia Papalexi, William M Mauck III, Yuhan Hao, Marlon Stoeckius, Peter Smibert, and Rahul Satija. Comprehensive integration of single-cell data. *Cell*, 177(7):1888–1902, 2019.
- [57] Fuchou Tang, Catalin Barbacioru, Yangzhou Wang, Ellen Nordman, Clarence Lee, Nanlan Xu, Xiaohui Wang, John Bodeau, Brian B Tuch, Asim Siddiqui, et al. mrna-seq whole-transcriptome analysis of a single cell. *Nature methods*, 6(5):377, 2009.
- [58] Stein Emil Vollset. Confidence intervals for a binomial proportion. *Statistics in medicine*, 12(9):809–824, 1993.

- [59] Guenther Walther and Andrew Perry. Calibrating the scan statistic: finite sample performance vs. asymptotics. *arXiv preprint arXiv:2008.06136*, 2020.
- [60] Caroline L Wormell and Sebastian Reich. Spectral convergence of diffusion maps: improved error bounds and an alternative normalisation. *arXiv preprint arXiv:2006.02037*, 2020.
- [61] Ron Zass and Amnon Shashua. Doubly stochastic normalization for spectral clustering. In *Advances in neural information processing systems*, pages 1569–1576, 2007.
- [62] Jun Zhao, Ariel Jaffe, Henry Li, Ofir Lindenbaum, Esen Sefik, Ruaidhri Jackson, Xiuyuan Cheng, Richard Flavell, and Yuval Kluger. Detection of differentially abundant cell subpopulations discriminates biological states in scrna-seq data. *bioRxiv*, page 711929, 2020.